

Developing a novel mechanistic model for four-phase oil-water-gas-sand stratified flow in a horizontal pipe.

MORADI, B.

2020

Copyright: the author and Robert Gordon University



Developing a Novel Mechanistic Model for Four-Phase Oil-Water-Gas-Sand Stratified Flow in a Horizontal Pipe

PhD Student:

Behshad Moradi

Supervisor Team:

Dr. Mamdud Hossain (Principal Supervisor)

Dr. Gbenga O.Oluyemi

School of Engineering
Sir Ian Wood Building
Riverside East
Robert Gordon University
Garthdee Road
Aberdeen AB10 7GJ
United Kingdom

Developing a Mechanistic Model for Four-Phase Oil-Water-Gas-Sand Stratified Flow in a Horizontal Pipe

Behshad Moradi

A thesis submitted in partial fulfilment of the requirements of the
Robert Gordon University for the degree of Doctor of Philosophy
(School of Engineering)

September 2020

To my parents for all they taught me,
To my wife Shiva, for her unconditional love and support and
To our son Shahrad for all the joy, he is giving us since he entered our lives.

It is not knowledge, but the act of learning, not possession but the act of getting there, which grants the greatest enjoyment.

Carl Friedrich Gauss (1777-1855)

Acknowledgements

Since I embarked on this research journey, I was continually being asked: “Why are you doing this?” Why someone in a satisfying full-time but demanding job and with a young family should even think about doing intense research?

It would be fair to say that I still do not know what the most fundamental reason was behind my decision to start this research. But what I do know is that despite countless hours spent in front of the computer, wrestling with the code or going through papers taking notes, the hours which I could and probably should spend with my family, thanks to this research, I have experienced the pleasure of “Knowing”. As Leonardo da Vinci said, the noblest pleasure is the joy of understanding. I cannot agree with him more as I certainly felt this pure pleasure on numerous occasions throughout this research.

I am immensely thankful to my wife and my son. They are my primary source of support and encouragement.

I am grateful for the support that I received from my supervisory team and in particular, my principal supervisor Dr. Mamdud Hossain. Our sessions to exchange ideas at the early phase of this research, which helped me to finalise the objectives, were invaluable.

I’m concluding this research, but I now have more questions than answers. The questions that didn’t occur to me when I started this journey. After these years, I now have a much better sense of appreciation for what I do know and what I do not know. Nicolaus Copernicus said, “To know that we know what we know, and to know that we do not know what we do not know, that is true knowledge”.

So next time, if I am being asked why I did the research, my answer would be “To know what I do not know”.

Behshad Moradi

March 2020

Abstract

Presence of sand and solid particles in untreated petroleum sometime is inevitable. Although many techniques have been developed to prevent sand particles from entering the pipeline, such as downhole gravel packs, these downhole sand control devices can cause significant production loss due to the risk of blockage. Transporting sand along with other flowing phases is the best way of managing produced sand. Pipelines should be designed in such a way that flowing phases keep the sand particles moving and formation of the stationary sand bed should be mitigated by understanding flow physics under realistic multiphase conditions. To better understand the behaviour of multiphase flow, this research was aimed to develop and verify a mechanistic model for the stratified four-phase gas-oil-water-sand flow in a horizontal pipe. This model takes into account some aspects of the existing multi-layer liquid-liquid and liquid-solid models. The entire stratified flow structure comprising of the stationary sand bed, moving sand bed, water, oil and gas layers are modelled by a system of 12 non-linear equations. An iterative numerical method has been developed to solve this system of non-linear equations. This solving method is using pressure balance in the moving phases as a criterion to converge to a solution that is physically possible. This model can also predict the flow structure by differentiating between fully suspended flow, stratified flow with moving and stationary beds and stratified flow with moving bed only, and then adjusting and solving the governing equations, accordingly. In the case of three phase water-oil-gas flow, the developed code was ran for two oil viscosity values of 1 (cP) and 100 (cP) where variation in the height of each layer versus total flow rate was studied. Comparison with three layer solid-liquid model was done by running the code while sand volumetric concentration was increased from 4% to 20% with 2% increment. Results of simulations compare well with the published data. The developed code was then employed to model the four phase horizontal stratified sand-water-oil-gas flow. Parametric study was performed to evaluate the impact of particle size, solid concentration, solid density, slurry velocity and oil velocity on holdup and pressure gradient. At constant solid concentration, increase in solid size up to certain threshold resulted in reduction in stationary sand bed height and increase in moving sand bed height, due to increase in particle surface and torque applied on each particle. Further increase in particle size resulted in accumulation of stagnated particles. To further study the effect of particle size, slurry and oil flow rates were increased whilst gas flow rate remained unchanged. This resulted in increase in both oil and water layer heights. Increase in particle size resulted in increase in pressure gradient. Effect of solid concentration was studied by gradually increasing the concentration whilst slurry, oil and gas flow rates remained unchanged. It was demonstrated that increase in solid concentration results in the sand build-up. Oil layer height showed downward trend while sand concentration increases and pressure gradient showed a linear increasing trend

whilst solid concentration increases. Effect of particle density was studied by increasing the density whilst other parameters including particle size remained unchanged. Density increase resulted in increase in total sand height and reduction in water layer height. Increase in slurry flow rate showed a linear relationship with water layer height and also resulted in increase in moving sand bed height while at the same time stationary sand bed height reduced. Increase in oil flow rate didn't show noticeable impact on sand bed height. As overall conclusion, the technique which was developed in this research to solve non-linear equations governing four phase stratified flow, proved to be reliable and resulted in satisfactory results. The mechanistic model, which is developed in this research along with solution algorithm can be used as a starting point to develop numerical models for flow regimes other than stratified. The code was developed in MATLAB software version "R2017b".

Table of Contents

Acknowledgements	v
Abstract	vi
Table of Contents	viii
List of Figures.....	x
List of Tables	xii
Nomenclature.....	xiii
Subscripts and Superscripts.....	xiv
Greek Letters.....	xv
Abbreviations	xvi
Chapter 1	1
1.1 What is Mechanistic Approach?	3
1.2 Four-Phase Flow in Oil and Gas.....	4
1.3 Research Objectives.....	7
1.4 Structure of This Report.....	8
Chapter 2.....	10
2.1 Experimental or Correlation Models.....	12
2.1.1 Durand (1) Model for Sand Hydraulic Transportation	12
2.1.2 Newitt <i>et al</i> (2) Model for Hydraulic Conveying of Solids	13
2.2 Semi-Theoretical Models	17
2.2.1 Liquid-Sand Model by Danielson (3).....	17
2.2.2 Incipient Velocity Model by Han and Hunt (4)	20
2.3 Mechanistic or Theoretical Models.....	23
2.3.1 Three-Layer Model by Doron and Barnea (5).....	23
2.3.2 Continuous Stratified Two Phase Model by Yang <i>et al.</i> (6).....	26
Chapter 3.....	29
3.1 Geometrical Parameters.....	30
3.2 Hydraulic Diameter.....	32
3.3 Mass Continuity	33
3.4 Sand and Droplet Distribution.....	34
3.5 Momentum Continuity.....	37
Chapter 4.....	41
4.1 Two-Guess Method.....	42

4.2	Code Formulation Adjustments	46
4.3	Code Verification- Comparison with Taitel et al (7) Model	47
4.4	Code Verification- Comparison with Doron and Barnea (5) Model.....	56
4.5	Statistical Analysis of Model Performance.....	62
Chapter 5.....		66
5.1	Effect of Particle Size on Flow Structure.....	68
5.2	Effect of Solid Concentration on Flow Structure	76
5.3	Effect of Solid Density	82
5.4	Effect of Slurry Velocity on Flow Structure	87
5.5	Effect of Oil Velocity on Flow Structure.....	93
Chapter 6.....		99
6.1	Proposal for Future Works.....	103
References:		106

List of Figures

Figure 1-1: Multiphase flow modelling evolution (8)	2
Figure 1-2: Illustration of a long subsea tieback	4
Figure 1-3: Multiphase flowline projects-completed and planned (9)	5
Figure 2-1: Definition of solid transport velocities (10)	11
Figure 2-2: Schematic drawing of Newitt et al flow loop (2)	14
Figure 2-3: Flow regime map for slurry flow (2).....	15
Figure 2-4: Flow regime map, showing transition velocities (2)	17
Figure 2-5: Sand holdup in two-phase flow. Model prediction against SINTEF data. Sand particle size 280 (μm), sand injection rate 2.2 (gm) (3).....	19
Figure 2-6: Pressure gradient in two-phase flow. Model prediction against SINTEF data (3)	20
Figure 2-7: Schematic diagram of the Han and Hun flow loop (4).....	21
Figure 2-8: Forces on single particle resting on a stationary horizontal surface (4)	21
Figure 2-9: Geometry of two-layer model (11)	24
Figure 2-10: Three layer model and forces acting on particles (12)	25
Figure 3-1: Structure of Stratified four-phase flow	29
Figure 3-2: Shear stress in Stratified four-phase flow	38
Figure 4-1 :Flow structures, recognised by the code	41
Figure 4-2: Flowchart showing loops for Two-Guess iterations	45
Figure 4-3: Liquid level for water-oil-air in horizontal pipes. Oil viscosity 1 cP.....	48
Figure 4-4: Water layer height vs Slurry velocity for water-oil-air in horizontal pipes.	49
Figure 4-5: Total liquid layer height vs Slurry velocity for water-oil-air in horizontal pipes.	49
Figure 4-6: Oil layer height vs Slurry velocity for water-oil-air in horizontal pipes.	50
Figure 4-7: Multi-layer height vs Slurry velocity for water-oil-air in horizontal pipes.	51
Figure 4-8: Liquid level for water-oil-air in horizontal pipes. Oil viscosity 100 cP.....	51
Figure 4-9: Water layer height vs Slurry velocity for water-oil-air in horizontal pipes.	52
Figure 4-10: Total liquid layer height vs Slurry velocity for water-oil-air in horizontal pipes.	53
Figure 4-11: Oil layer height vs Slurry velocity for water-oil-air in horizontal pipes.	53
Figure 4-12: Multilayer height vs Slurry velocity for water-oil-air in horizontal pipes.....	54
Figure 4-13: Effect of gas velocity on the liquid layer for water-oil-air in horizontal pipes.	55
Figure 4-14: Effect of gas velocity on water layer height for water-oil-air in horizontal pipes.	55
Figure 4-15: Effect of solid concentration on pressure gradient in water-Acetal flow in horizontal pipe (5).....	57
Figure 4-16: Pressure gradient vs slurry velocity for water-solid flow in horizontal pipe.....	58
Figure 4-17: Pressure gradient vs slurry velocity for water-solid flow in horizontal pipe.....	59
Figure 4-18: Pressure gradient vs slurry velocity for water-solid flow in horizontal pipe.....	60
Figure 4-19: Pressure gradient vs slurry velocity for water-solid flow in horizontal pipe.....	61
Figure 4-20: Effect of solid concentration on break point velocity for water-solid flow in horizontal pipe.....	61
Figure 5-1:Operating point with highest gas and liquid superficial velocities (\diamond) is plotted on Taitel et al. (7) flow regime map for three phase flow.....	68
Figure 5-2: Effect of particle size on stationary sand bed height-	68
Figure 5-3: Effect of particle size on moving sand bed height-	69
Figure 5-4: Effect of particle size on water, oil and gas layers-	70

Figure 5-5: Effect of particle size and flow rate on height of water layer-	71
Figure 5-6: Effect of particle size and flow rate on height of oil layer-	71
Figure 5-7: Effect of particle size and flow rate on height of moving bed layer-	72
Figure 5-8: Effect of particle size on height of stationary and moving bed layers-	73
Figure 5-9: Effect of particle size on total sand layer height -	74
Figure 5-10: Effect of particle size and flow rate on height of stationary bed layer -	75
Figure 5-11: Effect of particle size and flow rate on pressure loss -	75
Figure 5-12: Effect of solid concentration on sand layer height -	77
Figure 5-13: Effect of solid concentration on pressure loss -	78
Figure 5-14: Effect of solid concentration on oil layer height -	80
Figure 5-15: Effect of solid concentration on gas layer height -	81
Figure 5-16: Effect of solid density on stationary bed height -	83
Figure 5-17: Effect of solid density on moving bed height -	84
Figure 5-18: Effect of solid density on total sand bed height -	85
Figure 5-19: Effect of solid density on water layer height -	86
Figure 5-20: Effect of solid density on pressure loss -	86
Figure 5-21: Effect of slurry flow rate on water layer -	89
Figure 5-22: Effect of slurry flow rate on sand layer -	90
Figure 5-23: Effect of slurry flow rate on oil and gas layers -	91
Figure 5-24: Effect of slurry flow rate on pressure loss -	92
Figure 5-25: Effect of oil flow rate on water layer height -	94
Figure 5-26: Effect of oil flow rate on sand layer height -	95
Figure 5-27: Effect of oil flow rate on oil layer height -	96
Figure 5-28: Effect of oil flow rate on flowing areas -	97
Figure 5-29: Effect of oil flow rate on gas layer height -	97
Figure 5-30: Effect of oil flow rate on local velocities -	98

List of Tables

Table 4-1: Statistical parametrs- Two-Guess model vs. three phase Taitel et al. (7) model.....	63
Table 4-2: Statistical parametrs- Two-Guess model vs. experimental data in Doron and Barnea (5) work	64
Table 5-1: Flow loop setup Dabirian et al (13).....	66
Table 5-2: Physical properties of liquid and gas phases.....	66
Table 5-3: Modified superficial velocities	67
Table 5-4: Effect of solid concentration on flow structure- flow parameters.....	76
Table 5-5: Effect of solid density on flow structure- flow parameters.....	82
Table 5-6: Effect of slurry flow rate on flow structure- flow parameters	87
Table 5-7: Effect of oil flow rate on flow structure- flow parameters.....	93

Nomenclature

Parameter	Description	Unit
A	Area	m^2
C	Local concentration	-
C_D	Drag coefficient	-
C_L	Lift coefficient	-
D	Pipe diameter	m
D_i	Hydraulic diameter	m
d	Average size of sand particles	m
H, h	Layer height	m
M	Continuous friction force	N
N_{Fr}	Froude number	-
P	Pressure	N/m^2
S	Layer perimeter	m
Re	Reynolds number	-
N_{we}	Weber number	-
f, f_i	Fanning friction coefficient	-
F_B	Buoyance force acting on single particle	N
F_D	Drag force acting on single particle	N
F_L	Lift force acting on single particle	N
F_G	Gravitational force acting on single particle	N
g	Acceleration of gravity equal to 9.81	m/s^2
$i, dP/dx$	Pressure gradient	N/m^3
U	Velocity	m/s
U_{MB}	Moving bed velocity	m/s

Subscripts and Superscripts

Item	Description
<i>MB</i>	Moving sand bed
<i>O,o</i>	Oil
<i>G,g</i>	Gas
<i>S,s</i>	Sand
<i>SB</i>	Stationary sand bed
<i>I,i</i>	Inlet conditions
<i>W,w</i>	Water
<i>S.O</i>	Sand in oil
<i>S.W</i>	Sand in water
<i>O.G</i>	Oil in gas
<i>O.W</i>	Oil in water
<i>LD</i>	Limit Deposit
<i>p</i>	Particle
<i>rel.</i>	Relative parameter
<i>act.</i>	Actual parameter

Greek Letters

Symbol	Description	Unit
α	Volume fraction over the whole cross sectional area	-
θ	Wetted angle, measured from centre of pipe	degree
ρ	Density	kg/m^3
τ	Shear stress	$kg/m.s^2$
ϵ	Mean diffusion coefficient	-
ω	Sand terminal velocity	m/s
μ	Dynamic viscosity	Pa.s
σ	Surface tension	N/m^2
ν	Kinematic viscosity	c St
Γ	Mass transfer rate	$kg/m^3.s$
Δ	Difference	-
Ψ	Wick's dimensionless number	-
η	Statistical error parameter	-

Abbreviations

Abbreviation	Description
<i>CFD</i>	Computational Fluid Dynamic
<i>MIC</i>	Microbially Induced Corrosion
<i>PMMA</i>	Polymethylmethacrylate
<i>VOF</i>	Volume of Fluid

Chapter 1

Introduction

Multiphase flow where more than one form of medium exists in the flow regime is one of the most dominant forms of flow in nature. Although outlining a definitive description for multiphase seems to be difficult, flow is considered as multiphase when each flowing medium is not soluble in other mediums or phases. For example solution of salt and water or brine is considered as one phase or medium but the flow of salt particles in oil is considered as two phase (solid/liquid) because salt is not soluble in oil. Phases or mediums can be different forms of the same substance; for example, a flowing mixture of steam and water bubbles in steam power plants is seen as two phase gas/liquid flow.

Multiphase flow accounts for almost more than half of flows which are produced and present in modern industries (14). From transporting crops (wheat, maize, soya, etc.) using airflow, to power generation and internal combustion engines, to pipelines handling untreated hydrocarbon, all these and many other cases represent the application of multiphase flow in industrial scales. This type of flow also represents one of the most complex phenomena in fluid mechanics in terms of modelling and simulation. Complexity arises because of the presence of individual phases and the way that those phases interact with one another.

Presence of solid particles; as a phase; and studying how solid phase is transported by other moving phases, e.g. gas and/or liquid, is one of the most challenging subjects in the multiphase study. This type of multiphase flow has very wide applications from sediment movement in geology studies (15), to moving rocks and sand particles in river beds (16) and in pharmaceutical industries where some drugs such as inhalers should be transported in powder forms by gas or liquid medium (17) to chemical and energy industries where moving gas through fluidised beds are playing a pivotal role on any modern petrochemical and refinery complex (18).

Numerous models have been developed in the last century to study two phase (gas-liquid), and three phase (liquid-liquid-gas) flows. Concept behind early models was empirical and correlation approach where aim was to carry out set of experiments to observe multiphase flow behaviour and then develop set of correlation methods based on experimental results and expand those to other pipe sizes and operating scenarios, e.g. Lockhart and Martinelli (19) , Flanigan (20) and Beggs and Brill (21)

models. All these empirical models were essentially correlative models based on some data gathered in the lab or from the fields and that was the inherent weakness of these models. Using these models for conditions other than original lab or field datasets led to inaccurate results (8). For example, Durand (1) developed a model based on a dataset containing 310 tests using sand particles ranging from 2 (μm) to 25 (μm) diameter, with sand volumetric concentration ranging from 0.002 to 0.23 and pipe diameter ranging from 0.0375 (m) to 0.7 (m). Using Durand (1) model for any sand particle larger than 25 (μm) resulted in inaccurate results and that encouraged other researchers such as Wasp *et al* (22), Newitt *et al* (2) and Wicks (23) to come up with modified versions of Durand (1) model to overcome these limitations.

By introducing computers, petroleum engineers and operating companies started to model entire pipelines from the reservoir up to processing facilities to calculate pressure drop and liquid holdup. But then available models proved to be inefficient because all the models were based on empirical approaches. Most of the empirical models were based on this assumption that liquid holdup is a function of flow rate or superficial velocity only. But it was revealed that other parameters such as inclination angle have a direct and significant impact on liquid holdup (24). Another problem with empirical models was that most of these models either ignored flow patterns effect in their correlation, e.g. Dukler *et al.* (25) and Eaton *et al.* (26) or inadequately modelled it, e.g. Guzhov *et al.* (27).

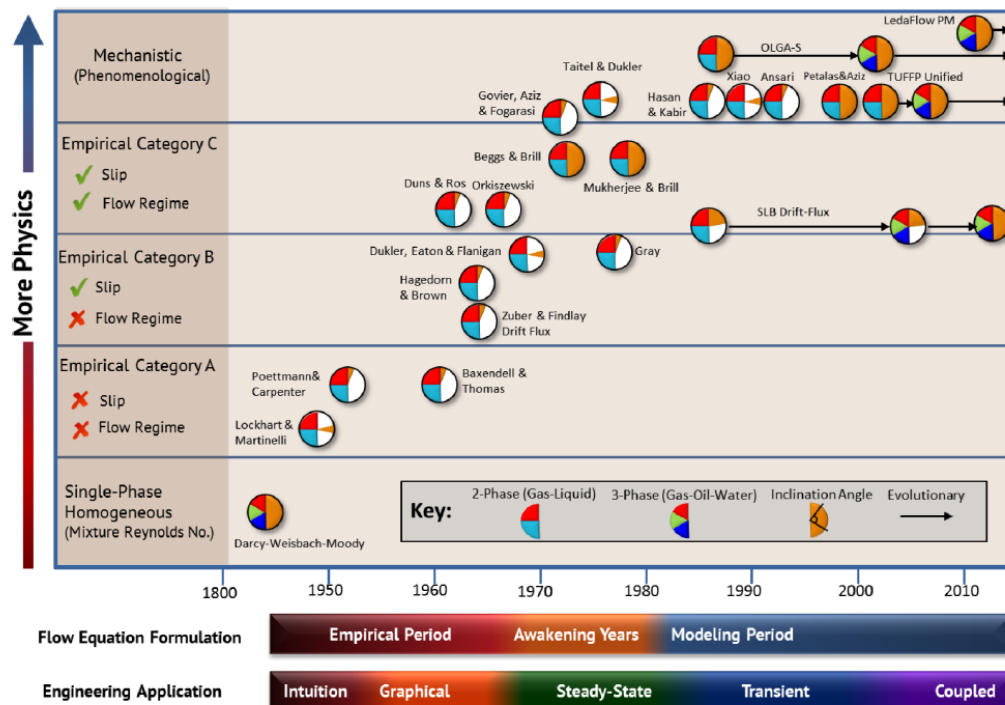


Figure 1-1: Multiphase flow modelling evolution (8)

Shippen and Bailey (8) published an article in 2012 to study the evolution of multiphase flow models, from the early 1900s to present days. Figure 1-1 was presented in their article, showing the most widely used models and how these models evolved in the last century to adopt more fundamental physics. The label on the horizontal axis of Figure 1-1 which classifies evolution period into "Empirical", "Awakening" and "Modelling ", was first introduced by Brill and Arirachakaran (28) in their 1992 paper.

It became clear that a basic approach with more emphasis on physics of flow is necessary to explain the behaviour of multiphase flow. Therefore oil and gas companies and research institutes started to invest in new R&D programmes to develop more accurate models based on basic physics of flow including mass and momentum equations. These models took into account the effect of flow patterns and came up with a more accurate prediction for flow transition. One of the first models of this kind was developed and introduced by Taitel and Dukler (24) for Two-Phase flow in their 1976 paper. And this is how "Mechanistic" models were introduced.

1.1 What is Mechanistic Approach?

Taitel who in his 1976 paper with Dukler (24), first introduced "Mechanistic" approach, describes the approach as follow (29):

"The term "Mechanistic Modelling " was adopted for modelling where the physical phenomenon is approximated by taking into consideration the most important processes, neglect other less important effects that can complicate the problem but do not add considerably to accuracy of the solution. "Mechanistic Modelling " should be sufficiently close to the natural phenomenon as the flow pattern involved should not be overlooked."

Unlike conventional numerical methods used in Computational Fluid Dynamics (CFD) that directly solve Navier-Stocks equations to predict the behaviour of fluids, Mechanistic model is based on a more simplified approach. In Multiphase medium, more than one fluid phase exists and, more often than not, the whole flow regime is in turbulent condition. This makes it very difficult if not impossible for even direct numerical methods to model the entire system (30). Especially in oil and gas industries, application of CFD to model multiphase flow has been limited to some finite boundary and special cases, such as modelling internals of multiphase separators.

Modelling an entire multiphase flowline from wellhead to slug catchers using CFD techniques needs enormous computing memory which makes

this approach impractical. Hence applying some methods to simplify the modelling process was inevitable, and this was one of the main drivers behind developing “Mechanistic” methods. Mechanistic models still employ some level of correlation and empiricism in their formulation. Although core concept is to formulate and solve the momentum and mass continuity equations, in order to couple the equations to form a system of equations, closure terms used, e.g., wall-liquid and interface shear terms, are mainly based on empirical equations. Nevertheless, Mechanistic models are considered to be the most robust models to study the behaviour of multiphase flow (31).

1.2 Four-Phase Flow in Oil and Gas

One of the industries which has been investing considerably in R&D programs for multiphase flow modelling is Oil and Gas. Understanding the behaviour of multiphase flow is essential because the entire flow system in upstream oil and gas is multiphase in its real form. From the reservoir to wellbore, in the pipeline and even in production systems and beyond.

It is almost inevitable that multiphase crude oil would be transported for some distance by the pipeline before reaching to a processing facility. Particularly in the offshore application as illustrated in figure 1-2, if untreated production can be transported for more distance either by using multiphase pipeline or using subsea processing facilities, it can result in massive cost saving by mitigating the need to install offshore platforms.

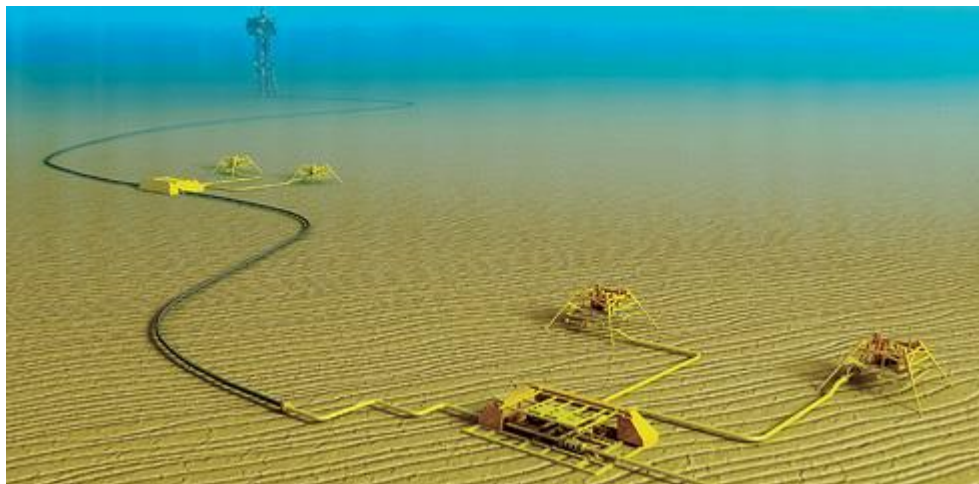


Figure 1-2: Illustration of a long subsea tieback

Particularly in recent years, offshore development activities have been focused on deep and ultra-deep reservoirs, where production fluid should travel longer distances to reach either offshore or onshore processing facilities. Developments in two-phase liquid-gas and three-phase liquid-

liquid-gas models resulted in some “state-of-the-art” commercial software which can be used for a broad range of operating scenarios. The most widely used software are OLGA Steady-State Model (OLGAS) (32) , Tulsa University Fluid Flow Projects (TUFFP) (33) and LedaFlow Point Model (Leda-PM) (34). All these software are classified as Mechanistic models (Figure 1-1), but using a different set of equations to describe the physics governing the flow.

For example, OLGA which is based on the three-phase concept, solves three mass continuity equations and two momentum equations but TUFFP which is mainly used for horizontal-near horizontal configurations, uses semi-correlative models which were developed by Barnea (35,36). Despite some underlying limitations that all these state-of-the-art models have, oil and gas companies have now managed to tap into multiphase reservoirs which had been considered as technically impossible before (Figure 1-3). Multiphase pipelines now can transport untreated production fluid across longer distances, thanks to these software with functionality to predict the behaviour of multiphase flow.



Figure 1-3: Multiphase flowline projects-completed and planned (9)

One of the limitations which is common between all these software is that the presence of the 4th phase cannot be included. This is also the limitation of almost all the correlation models. Liquid-solid flow has been subject to extensive research in recent decades, which resulted in many comprehensive models such as Durand (1) and Thomas (37) models.

Untreated production fluid is a four-phase fluid, it consists of oil, produced water, associated gas, and solid mainly in the form of sand particles. Presence of sand in the mainstream will increase the erosion rate. Also, if sand stagnates and forms a stationary bed, it will pose additional corrosion risk due to Microbially Induced Corrosion (MIC). Therefore multiphase pipeline systems should be designed in such a way that keeps the sand moving. In addition to these, moving or stationary sand beds will also affect the pipe friction factor, and consequently affects the flow regime transition mechanism (31).

Although the intention of the earlier installations was to stop the sand from entering the pipeline by means of downhole sand control devices, such as gravel packs, slotted liners, and other methods which have been proven to be the cause of significant production reduction and to require continuous intervention (38). Rather than installing sand monitoring devices on the pipelines and performing regular pigging operations which are costly and pose operational risks, the preferred method is to allow sand particles to enter the pipeline but then be transported along with other phases in some managed ways.

In order to achieve this, developing reliable models to predict Minimum Transport Velocity (MTV) or Critical Velocity (CV) is crucial. MTV is the velocity below which, sand will not be transported by the carrier fluid and form a stationary bed on the bottom of the pipe. Although there are different definitions for MTV, including velocity to keep the particles fully suspended or velocity that keeps the particles moving even when particles are forming a moving sand bed (39), importance is to keep the sand particles moving. One of the main responsibilities of any flow assurance engineer is to make sure velocity is always higher than Critical Velocity, to mitigate the formation of the stationary sand bed.

It is surprising to know that until now only a few research studies have been done to study multiphase flow as four-phase system of Oil-Water-Gas-Sand to calculate the MTV. This subject was highlighted by many renowned researchers such as Professor James Brill (University of Tulsa) (28) and Professor Geoff Hewitt (Imperial College, University of London) (40) as an area which needs further studies. While other modelling techniques to simulate single-phase and two-phase flow regimes have been developed in recent decades, understanding the physics governing the four-phase flow still poses great challenges to researchers.

Extensive literature survey suggests that no model has ever been developed for four-phase liquid-liquid-gas-solid, which is the dominant flow in petroleum and process industries. Only a few experimental data on four-phase solid-liquid-liquid-gas flow could be found in open

publications. One of the reasons could be because of the complex test setup needed to model four-phase flow in an experimental environment which makes the test expensive. Four-phase test facility generally needs more components compared to two phase or even three phase test flow loop. Introducing the solid phase means a multiphase separator should be installed in the test loop in order to separate oil, gas and slurry. And in order to control the solid concentration in the flow, a slurry preparation loop should be included in the flow loop which adds to the complexity of the test setup. Details of a three phase sand-water-air can be found in Ibarra and Ram (41) work. It is worth mentioning that their experimental setup does not include oil phase. To add oil phase, another mixing and separation loop should be added to their flow loop.

It seems essential and prudent to develop a numerical model based on governing physics that can predict the behaviour of four-phase flow. The model needs to be verified against limited experimental data available and should be able to calculate the liquid holdup and pressure loss, which are the most important parameters for designing a multiphase pipeline. The goal of developing a model for four-phase flow drives the objectives of this research.

1.3 Research Objectives

The aim of this research is to develop and solve a set of equations which describe the physics governing stratified horizontal four-phase flow using a Mechanistic approach. This hopefully will help to better understand the behaviour of four-phase sand-water-oil-gas flow. The key flow parameters which will be studied in this research are holdup in the form of physical height of each phase and pressure loss.

Stratified flow regime has been chosen for the study. There are three main reasons for this choice. Firstly, stratified flow structure allows the model formulation to be simplified. Stratified flow has separated layers which reduces the number of non-linear equations to represent the momentum continuity. Secondly, three-layer solid transport model by Doron and Barnea (5) which is used in the formulation of this research is based on distinctive solid and liquid layers which can only be found in stratified flow regime. And third reason is the central role that stratified flow is playing in flow regime map. Even though no flow regime map could be found for four-phase, as suggested by Taitel and Dukler (24), Barnea (42) and Xia *et al* (43), stratified flow is the most dominant flow regime in horizontal and near-horizontal pipe.

The pipe inclination angle is considered to be zero in order to negate the change in gravitational forces. This is to simplify the formulation. Four

phases are flowing in a pipe with a circular cross section. Hence flow structure is geometrically symmetrical around the vertical axis.

The aim of this research is to develop a mechanistic model for four-phase stratified flow in order to improve flow assurance prediction capability. Specific objectives of this research can be summarised as follow:

- To develop a set of governing equations for four-phase stratified flow in a layered arrangement.
- To investigate closure relationship between flow governing equations including mass and momentum continuity.
- To develop a solution algorithm which can be used without any priori.
- To develop an algorithm for detecting different solid phase configurations in stratified flow including layered and fully dispersed solid phase.
- To develop a computer code accordingly to verify the four-phase stratified model using available experimental data on two and three phase flow.
- To perform a comprehensive parametrical study on effects of physical properties on flow characteristics. Physical parameters consist of particle size, density and concentration and velocity of water and oil phases.

1.4 Structure of This Report

Following chapter 1 which is the introduction, chapter 2 contains the result of the literature review. In chapter 2 some of the most important and widely used models for sand transport in either two or three phase flow are described.

Chapter 3 is dedicated to the formulation of the four-phase flow model which is subject of this research. In chapter 3, the geometry of the stratified four-phase flow is explained and geometrical parameters which define phase holdup are defined. Mass continuity equations for each phase are laid out in chapter 3 along with momentum continuity equations which will be solved to calculate pressure loss for entire flow structure.

Chapter 4 describes the solution algorithm which is used to solve the equations developed in chapter 3 . This chapter also explains how code will adjust itself to differentiate between three-layer solid model and fully dispersed flow. Chapter 4 contains results of verification of the code against three phase liquid-liquid-gas and two phase liquid-solid models, developed by other researchers.

Chapter 5 contains simulation results for four-phase solid-water-oil-gas stratified flow. Code was ran for five different scenarios to study the effect of several parameters on four-phase stratified flow structure. Results are being analysed and discussed in chapter 5.

Chapter 6 contains conclusion and proposal for future works.

Chapter 2

Literature Review

In order to study some of the most important sand transport models in a harmonised way, first, it is necessary to explain some of the basic concepts which were used and referenced in all these models. In a single phase carrier flow, sand particles can be seen in several different flow patterns and researchers used a variety of different terminologies to identify these patterns. As suggested by Vocaldo and Charles (44), Goedde (45) and Parzonka *et al* (46) , all different flow patterns can be classed in one of the following main forms:

- Stationary Layer where sand particles have no movement and are forming a highly concentrated sand bed at the bottom of the pipe.
- Moving Bed Layer where sand particles are moving at the vicinity of a stationary bed or pipe wall. Mechanism of particle movement can be classed as either drag move or rolling move. As observed by Ramadan *et al* (47) in inclined pipes, rolling is the most dominant movement mechanism. But it is also subject to particle shape because non-spherical sand particles need higher liquid velocity to roll. Therefore non-spherical particles have a tendency to drag move rather than rolling move (48).
- Suspended Layer where particles are fully suspended in the carrier flow. This form was then sub-divided by Doron and Barnea (49) into homogenous and heterogeneous forms. The homogenous suspension is where particles are distributed fairly evenly in the liquid form and the heterogeneous suspension is where the concentration of particles near the bottom of the pipe is higher than the rest of the mixture. The velocity of the carrier flow is the governing factor in defining homogenous and heterogeneous forms. When carrier velocity is high enough, lifting forces acting on each particle is considerably higher than gravitational forces. Hence particle is lifted with a tendency to move towards the centre of the pipe where velocity is maximum. This results in the formation of homogenous mixture as defined by Doron and Barnea (49). By reduction in carrier flow velocity, the gap between the magnitude of lifting forces and gravitational forces starts to close and particles tend to move towards the bottom of the pipe whilst are still moving with the carrier flow. This results in heterogeneous mixture formation. For the purpose of this research, both homogenous and heterogeneous mixtures are classed as suspended flow.

Existence of flow regimes above and transition from one form to another is governed by carrier flow velocity. Hence these velocity thresholds have been named by researchers in order to differentiate between different flow regimes.

Figure 2-1 from Soepyan *et al.* (10) depicts definition of these velocities.

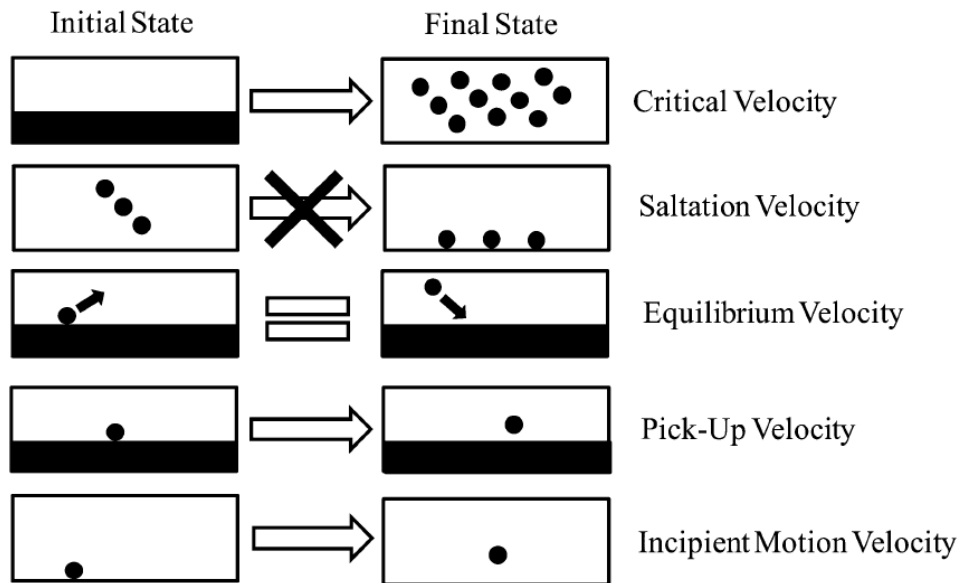


Figure 2-1: Definition of solid transport velocities (10)

Velocities in Figure 2-1 are defined based on changing the mixture form from initial state to final state. Critical velocity as defined by Oroskar and Turian (50) is the velocity which changes the flow regime from stationary bed to fully suspended. Therefore when the carrier flow velocity is equal to critical velocity, all particles are fully suspended. Equilibrium velocity as defined by Gruesbeck *et al.* (51) is when the rate of particle entrance into the carrier medium is equal to the settling rate. Velocity at which particle is picked up by carrier flow from the stationary sand bed is defined as Pick-Up velocity by Rabinovich and Kalman (52). Incipient motion velocity has a similar definition as Pick-up velocity except for the initial location of the particle should be at bottom of the pipe instead of stationary sand bed (52). Grass and Ayoub (53) defined Saltation velocity as the velocity where although particles have the tendency to settle, do not settle and continue to move with carrier flow. Below saltation velocity, moving sand layer starts to form.

Given the different mixture forms and different mechanisms for initiation of particle movement, numerous models were developed by researchers throughout the years to predict these velocities and to calculate the

pressure loss as the main parameter in studying slurry flow. Based on their approach, these models can be categorised as follow:

2.1 Experimental or Correlation Models

Early attempts to understand behaviours of slurry flow were focused on experimental (empirical) studies. The aim of these studies was to carry out a set of experiments to observe multiphase flow behaviour and then develop a set of correlation formulas based on experimental results and subsequently expand those to other pipe sizes and operating scenarios.

Most notable models in this category are developed by Durand (1), Newitt et al (2), Zandi and Govatos (54) and Turian and Yuan (55). Duran (1) and Zandi and Govatos (54) models restricted their applicability to one or two flow patterns but some other researchers such as Newitt *et al.* (2) and Turian and Yuan (55) claimed that their models could be used for all flow patterns in liquid-solid mixture.

2.1.1 Durand (1) Model for Sand Hydraulic Transportation

Durand (1) performed 310 tests to develop data bank for sand transport in the water stream. He used sand particles ranging from 2 (μm) to 25 (μm) diameter, with sand volumetric concentration ranging from 0.002 to 0.23 and pipe diameter ranging from 0.0375 (m) to 0.7 (m). He defined "Limit Deposit Velocity" as threshold velocity where sand particles start to settle and boundaries between flow with and without sand bed can be identified. Referring to Figure 2.1, "Saltation Velocity" as defined by Grass and Ayoub (53) is the nearest term to "Limit Deposit Velocity", defined by Durand (1).

Using experimental results, Durand (1) proposed correlation equation below to predict Limit Deposit Velocity. Durand (1) formula was one of the earliest attempts to understand hydraulic transportation of sand particles.

$$V_C = F_L \cdot \sqrt{2 \cdot g \cdot D \left(\frac{\rho_s}{\rho_l} - 1 \right)} \quad (2.1)$$

Where V_C is Limit Deposit Velocity and F_L is a function of sand volumetric concentration C_v and particle diameter. F_L is described in the form of a curve by Durand (1). Other researchers such as Wasp *et al.* (22)

modified the Equation (2.1) to extend the coverage of the formula for more particle diameters by taking into account mean diameter.

Durand (1,56) proposed the correlation presented in Equation (2.2) below for the calculation of pressure gradient in slurry flow:

$$\frac{i - i_w}{C \cdot i_w} = 121 \cdot \left[g \cdot \frac{D}{V^2} \left(\frac{\rho_s}{\rho_w} - 1 \right) \cdot \frac{W}{\sqrt{g \cdot d \left(\frac{\rho_s}{\rho_w} - 1 \right)}} \right]^{\frac{3}{2}} \quad (2.2)$$

Where i is the pressure gradient of slurry flow and i_w is pressure gradient when only water is flowing in the pipe. C , V and W are volumetric slurry concentration, mean slurry velocity and terminal falling velocity of a particle in water, respectively.

Durand (1) only used particles with the same density and different sizes in his experiment. Hence although Equations (2.1) and (2.2) are referring to solid density ρ_s , in reality, these equations result in considerable errors when used for particles whose densities differ from original experiments.

Another limitation of Durand (1,56) correlation is its sensitivity to particle diameter. Because he used closely-graded particles in his experiment, proposed equations do not have enough accuracy when used for mixed particles with varying diameters. This limitation encouraged other researchers such as Wasp *et al* (22), Newitt *et al* (2) and Wicks (23) to modify Durand (1,56) formulations in order to overcome these limitations.

Despite its limitations, Durand (1) model and its modified versions has been used widely in the oil and gas industry. One of the reasons for its popularity among pipeline and flow assurance engineers was because Durand (1) model was developed using low sand volumetric concentrations which is closer to actual sand loading in a hydrocarbon flow line. There were other models which were developed using much higher slurry loading which were predominately applicable to mining and powder industries.

2.1.2 Newitt *et al* (2) Model for Hydraulic Conveying of Solids

Newitt *et al.* (2) conducted a series of experiments in 1955, using a variety of different type of solids which were conveyed by water. Unlike Duran (1) experiments which all were conducted by particles with the

same density, Newitt *et al.* (2) used different particle material to build their data bank. Setup of the flow loop is shown in Figure 2-2:

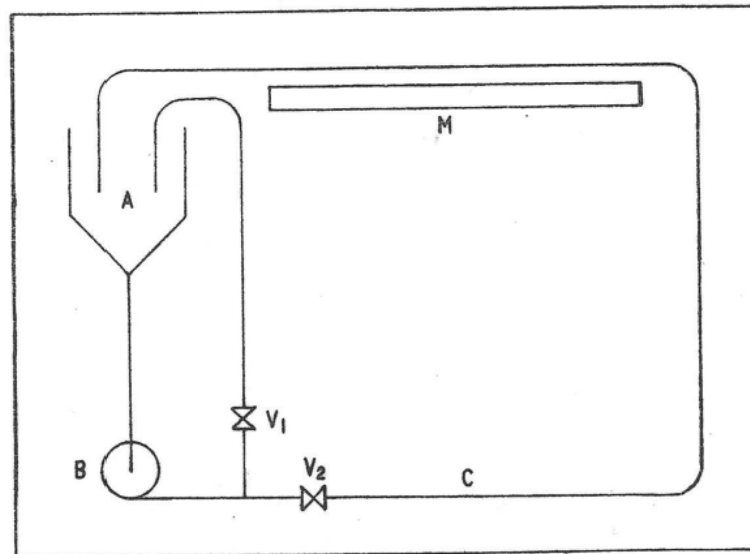


Figure 2-2: Schematic drawing of Newitt et al flow loop (2)

Tank A holds the slurry mixture and is connected to a centrifugal pump B. The pump is pushing the slurry mixture into plastic pipe loop C. Valves V1 and V2 will be used as flow throttling devices to control the flowrate. A mirror M is installed in the observation section to aid with the visual inspection of the flow regime.

Newitt *et al* (2) managed to achieve maximum velocity of 1.8 m/s in observation section. By varying the velocity from zero to 1.8 m/s, the following flow regimes were observed:

- a) Fully suspended flow where all particles are suspended
- b) Suspended particles with a moving layer at the bottom of the pipe
- c) Suspended particles with a moving layer over the stationary layer
- d) Stationary layer where only small quantities of particles were suspended
- e) Stationary layer with no suspended particle in the liquid phase

Figure 2-3 is Newitt *et al.* (2) attempt to plot the flow regime map using slurry velocity and sand concentration.

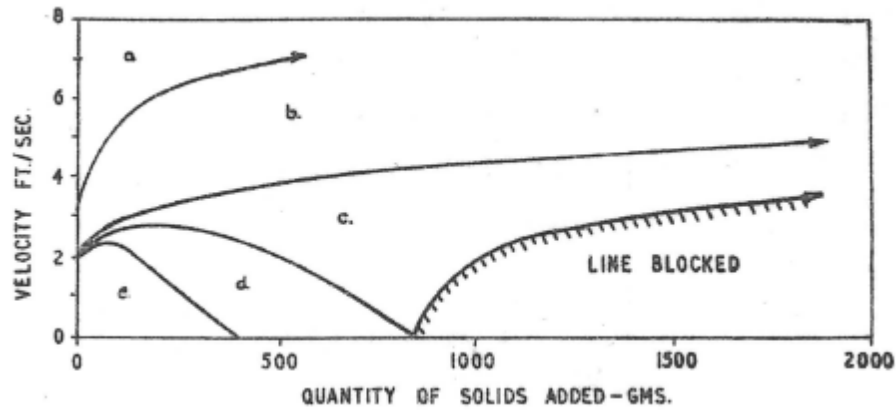


Figure 2-3: Flow regime map for slurry flow (2)

Newitt *et al.* (2) observed that different particles with different specific gravity all exhibit flow regime very similar to that shown in Figure 2-3. Particle which was used in this experiment were Perspex, Coal, Sand, Gravel and Manganese Dioxide.

The basis for their approach was to build a data bank of pressure drop versus velocity and slurry concentration and then try to find a correlation between these parameters, considering physical properties of solid and carrier medium. In other words, Newitt *et al.* (2) were trying to improve the pressure gradient model which was developed by Durand (1). By installing 10 pressure transducers at 3 (m) intervals they could measure the pressure loss across the entire straight length of the flow loop.

Newitt *et al.* (2) assumed that correlation between pressure gradient and flow parameters can be expressed in the following form which has striking similarity with Durand (1,56) model in Equation (2.2):

$$\frac{i - i_w}{C \cdot i_w} = M \cdot \left(\frac{\rho_s}{\rho_w} - 1 \right) \quad (2.3)$$

Where i is the pressure gradient of slurry flow, i_w is pressure gradient when only water is flowing in the pipe and C is volumetric slurry concentration.

Parameter M in Equation (2.3), is one of the following terms depends on flow regime:

$$M = 66. \frac{g \cdot D}{V^2} \quad \text{Flow with saltation and sliding bed} \quad (2.4)$$

$$M = 1100. \frac{g \cdot D}{V^2} \cdot \frac{W}{V} \quad \text{Heterogeneous flow} \quad (2.5)$$

Where V ($\frac{ft}{sec}$) is mean slurry velocity and W is the terminal falling velocity of a particle in water which can be calculated from equations below:

$$W = k_1 \cdot \left(\frac{\rho_s}{\rho_w} - 1 \right) \cdot d^2 \quad d < 130 \mu m \quad (2.6)$$

$$W = k_2 \cdot \sqrt{\left(\frac{\rho_s}{\rho_w} - 1 \right)} \cdot d \quad d > 130 \mu m \quad (2.7)$$

By equating M terms expressed in Equations (2.4) and (2.5), transition velocity from saltation to heterogonous flow V_B will be calculated from the equation below which is independent of pipe diameter:

$$V_B = 17. W \quad (2.8)$$

Another transition velocity is from heterogonous to homogenous flow regime V_H , which Newitt *et al.* (2) proposed using the below equation:

$$V_H = (1800 \cdot g \cdot D \cdot W)^{\frac{1}{3}} \quad (2.9)$$

They attempted to show these transitional velocities on a flow regime map for slurry flow in 1 inch and 6 inch pipes as shown in Figure 2-4. V_C which is shown in Figure 2-4, is critical velocity defined by Durand (1) in Equation 2.1, below which stationary sand bed exists. Froude Number $\frac{V}{\sqrt{g \cdot D}}$ which is playing a fundamental role in Newitt *et al.* (2) and Durand (1) models, have been used by other researchers such as Bonnington and Bain (57), Shook (58) and Babcock (59) to develop their correlation models.

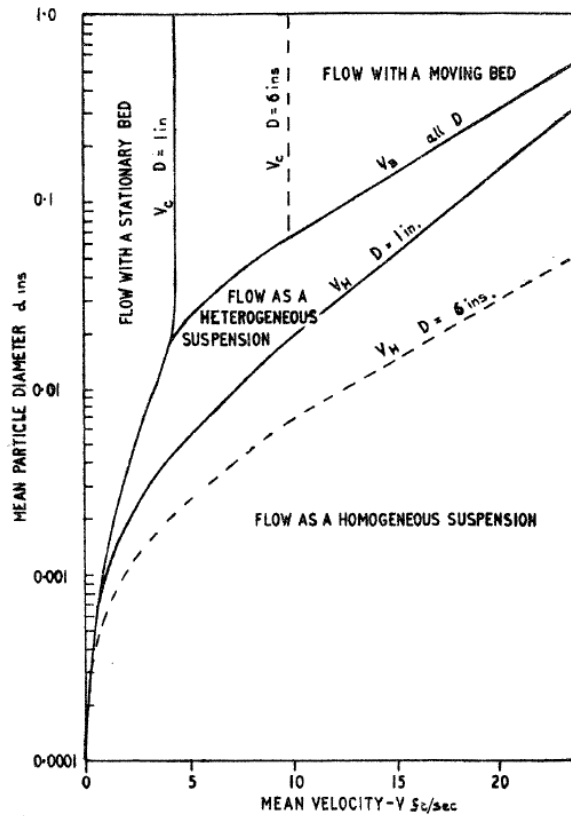


Figure 2-4: Flow regime map, showing transition velocities (2)

2.2 Semi-Theoretical Models

To overcome the inherent limitation of Correlation models, researchers started to develop models by employing more fundamental equations to describe the governing physics. But unlike Mechanistic models, the Semi-Theoretical models are still using some parameters in their formulations which were developed using a correlation approach. To name some of the most notable models in this category, reference can be made to Oroskar and Turian (50), Danielson (3), Thomas (60) and Han and Hunt (4) models.

2.2.1 Liquid-Sand Model by Danielson (3)

Danielson (3) assumed that in liquid-solid flow, there is slip velocity between sand particles and carrier liquid which remains constant over a range of mixture velocities. Experimental observations by some researchers showed that sand particles and carrier flow are travelling with different velocities, but the trade-off between the complexity of the

model and accuracy of the model as a result of the inclusion of slip velocity was subject of debates between researchers.

By taking into account volumetric flow rate of water Q_w and sand Q_s and sand holdup H_s , slip velocity can be expressed by the equation below:

$$U_{slip} = U_w - U_s = \frac{Q_w}{A \cdot (1 - H_s)} - \frac{Q_s}{A \cdot H_s} \quad (2.10)$$

Using experimental results gathered in SINTEF STRONG JIP programme (61,62), Danielson (3) developed a correlation model for Critical Velocity U_c . Definition of Critical Velocity is illustrated in figure 2-1.

$$U_c^2 \cdot C_D = \frac{4}{3} \cdot g \cdot D \cdot \left(\frac{\rho_s}{\rho_w} - 1 \right) \quad (2.11)$$

$$C_D = f(Re^{-n}) \quad (2.12)$$

For $n = \frac{1}{5}$ in Equation (2.12) and rewriting Reynolds number in Equation (2.12), Critical Velocity can be derived from the equation below.

$$U_c = K \cdot v^{-\frac{1}{9}} \cdot d^{\frac{1}{9}} \cdot \left(g \cdot D \cdot \left(\frac{\rho_s}{\rho_w} - 1 \right) \right)^{\frac{5}{9}} \quad (2.13)$$

K is an experimental constant which if it equates to 0.23, this equation provides a good fit to data gathered in SINTEF STRONG JIP programme (61,62). Equation (2.13) is very similar to Critical Velocity correlation proposed by Stevenson *et al* (48) and Salama (63). Both Salama (63) and Stevenson *et al.* (48) used the same SINTEF experimental data to develop their models, but they used different correlation constants for curve-fitting.

One of the major constrains of Danielson (3) correlation for Critical Velocity is that Equation (2.13) does not show any dependency on sand concentration. It was proved by many researchers such as Durand (1,56), Newitt *et al.* (2), Hill *et al.* (39) and many others that sand concentration plays a key role in defining threshold velocities as depicted in figure 2-1.

By replacing U_{slip} in Equation (2.10) with U_c and rewriting it for the sand holdup H_s , following quadratic equation was derived which Critical Velocity and volumetric flowrates are the constants. This equation can then be solved to give the sand holdup.

$$U_c \cdot H_s^2 + \left(\frac{Q_w}{A} + \frac{Q_s}{A} - U_c \right) \cdot H_s - \frac{Q_s}{A} = 0 \quad (2.14)$$

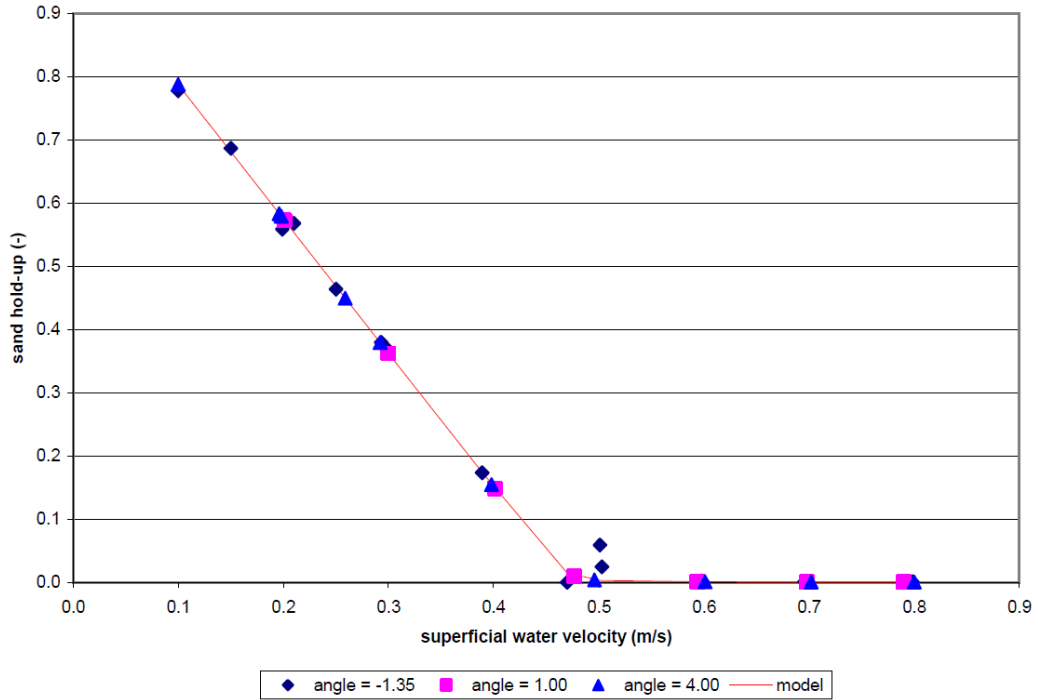


Figure 2-5: Sand holdup in two-phase flow. Model prediction against SINTEF data. Sand particle size 280 (μm), sand injection rate 2.2 ($\frac{\text{g}}{\text{m}}$) (3)

Figure 2-5 shows the results of Equation (2.14) and its perfect fit on SINTEF STRONG JIP programme data set (61,62) for different inclination angles. As it can be seen in Figure 2-5, inclination angle shows no effect on Critical Velocity which is also shown in Equation (2.14).

Using SINTEF STRONG JIP programme data (61,62) which also included pressure gradient, Danielson (3) developed following correlation equation for pressure gradient:

$$\frac{dP}{dx} = f \cdot \rho \cdot \frac{U_L^2}{(2 \cdot D)} \quad (2.15)$$

At first glance Equation (2.15) seems similar to the standard friction based pressure gradient equation. But in order to achieve a good fit to SINTEF STRONG JIP programme data (61,62), the following modifications were proposed by Danielson (3).

$$f = 0.0055 \cdot \left\{ 1 + \left(\frac{(\pi - \theta)}{\pi} \cdot \frac{(\varepsilon \cdot D_i^{-1})}{50} + \sin \delta \cdot \frac{(\varepsilon \cdot D_i^{-1})}{40} + \frac{10^6}{Re} \right)^{\frac{1}{3}} \right\} \quad (2.16)$$

$$D_i = \pi \cdot \frac{(1 - H_S) \cdot D}{(\theta + \sin \theta)} \quad (2.17)$$

Where ε is pipe roughness and θ is the wetted angle, measured from the centre of the pipe. Figure 2-6 illustrates pressure gradient vs. superficial slurry velocity showing calculated values using equation (2.15) and experimental data from STRONG JIP programme (61,62). As explained by Danielson (3), slope of pressure gradient curve changes from negative to positive around U_c due to formation of moving dunes.

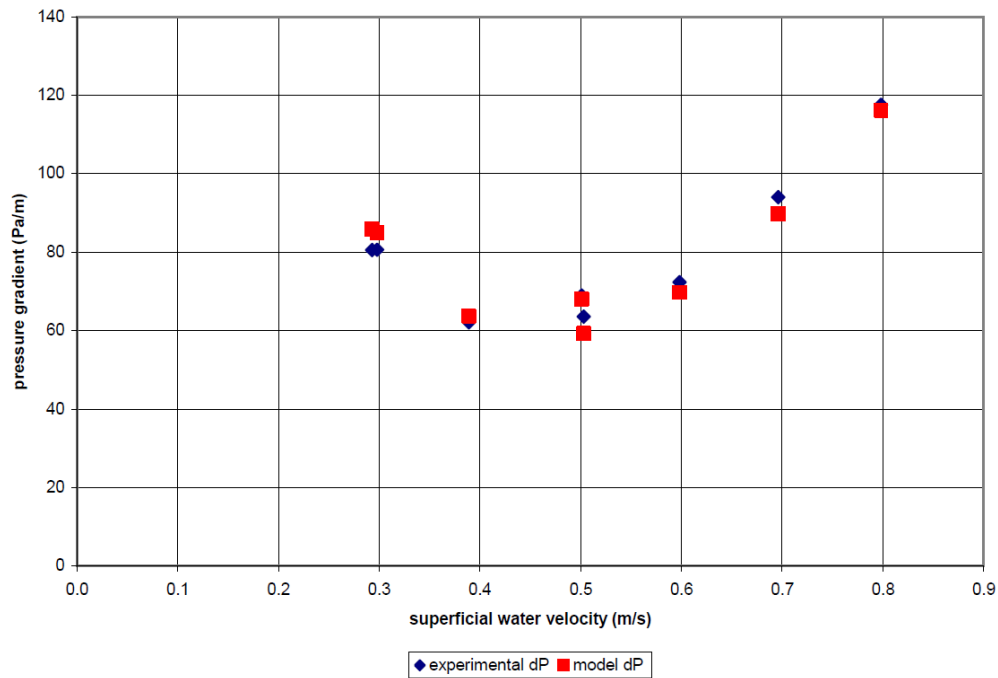


Figure 2-6: Pressure gradient in two-phase flow. Model prediction against SINTEF data (3)

2.2.2 Incipient Velocity Model by Han and Hunt (4)

Han and Hunt (4) conducted series of experiments using PMMA (Polymethylmethacrylate) particles, aluminum particles and steel balls in order to investigate the incipient velocity when a single particle starts its motion.

They conducted the experiment using two types of surfaces. In the first experiment, particles start to move from a smooth perspex surface. They then repeated the experiment with an ice-water freezing surface. Flow loop setup is shown in Figure 2-7. Unlike Danielson (3) who assumed slip velocity between particles and carrier liquid, Han and Hun (4) model assumes that particles are traveling with the same velocity as carrier flow. They used water as carrier flow and in order to measure the carrier flow velocity, they introduced 20 μm tracer particles with the same density as water.

Heat sink at the bottom of the viewing chamber was used to form an ice-freeze surface using liquid nitrogen. Viewing chamber was equipped with

a laser for illumination and high speed video camera attached to a microscope. For each type of particles, by increasing the flow rate of water and subsequently increasing the velocity in the viewing chamber, it was observed that particles started to move and eventually lifted by carrier flow in higher flowrate. Han and Hunt (4) observed that particle size is the major contributing factor for defining incipient velocity where bigger particles need much higher water velocity to lift from their original position and then transported by carrier fluid.

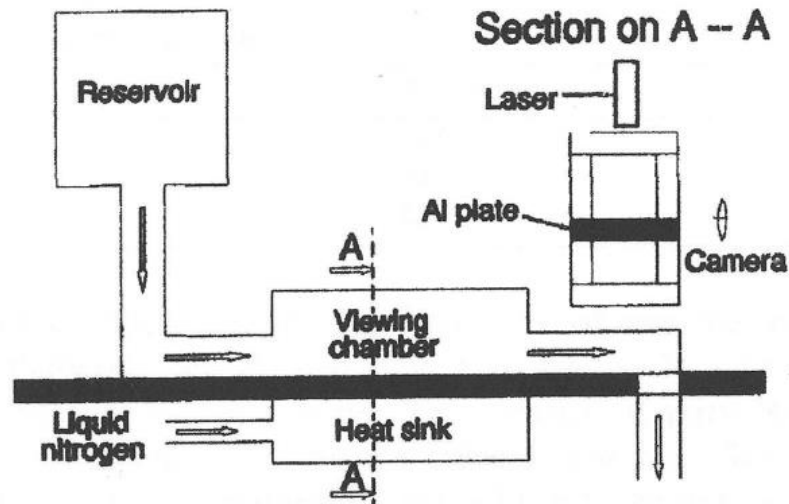


Figure 2-7: Schematic diagram of the Han and Hun flow loop (4)

The governing motion mechanism in Han and Hunt (4) experiment was observed as rolling rather than drag or lift. The reason could be because they used particles with a spherical shape. They used Doron and Barnea (5) approach for calculating driving torque on a single particle. In order to develop the formulation, Han and Hunt (4) assumed that a single particle is either a "truncated sphere" resting on a smooth interface (particle "a" in Figure 2-8) or resting on another particle with the same radius (particle "b" in Figure 2-8).

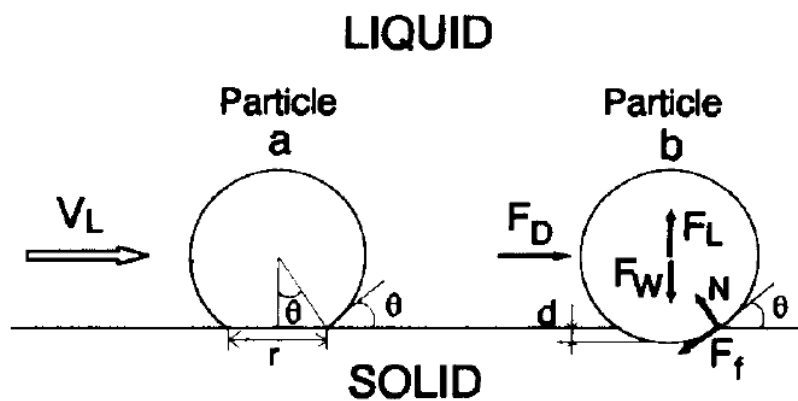


Figure 2-8: Forces on single particle resting on a stationary horizontal surface (4)

V_L is the liquid velocity, θ is contact angle with surface or particle underneath and F_i is an acting force on the particle. These variables are being calculated using the following equations:

$$F_W \text{ (Gravity Force)} = \frac{4}{3} \cdot \pi \cdot (\rho_p - \rho_l) \cdot a^3 \cdot g \quad (2.18)$$

$$F_L \text{ (Lift Force)} = 6.46 \cdot \mu \cdot a^2 \cdot \left(\frac{S}{v}\right)^{0.5} \cdot u_p \quad (2.19)$$

$$F_f \text{ (Friction Force)} = f \cdot N \quad (2.20)$$

$$F_D \text{ (Drag Force)} = 6\pi \cdot \mu \cdot V_L \cdot a \cdot \epsilon \quad (2.21)$$

$$\epsilon = \frac{5}{12} \cdot \ln\left(\frac{a}{h}\right) \quad (2.22)$$

Where a is particle radius and h is the distance from the interface. When the particle is completely detached from the surface and traveling with liquid, ϵ is equal to 1.

f is friction factor which can be calculated using method developed by Televantos *et al* (64).

By writing the force balance on a particle:

$$F_L + F_D \cdot \left(\frac{1 - f \cdot \tan \theta}{f + \tan \theta}\right) = F_W \quad (2.23)$$

Where

$$\tan \theta = \frac{r}{\sqrt{(a^2 - r^2)}} \quad (2.24)$$

As suggested by Doron *et al* (11), value of $\tan \theta$ varies between 0.35 and 0.75, depends on type of the flow and shape of the particle. Particle will be lifted from the surface when gravity force F_W is smaller than summation of other forces on left hand side of the Equation (2.23). By replacing the F_L , F_D and F_W in Equation (2.23) by Equations (2.18), (2.19) and (2.21), critical velocity can be defined as follow:

$$V_c = \frac{2}{9\mu} \cdot \frac{a^2}{\epsilon} \cdot (\rho_p - \rho_l) \cdot g \cdot \left(\frac{f + \tan \theta}{1 - f \cdot \tan \theta}\right) \quad (2.25)$$

The advantage of Han and Hunt (4) model is its simplicity and increased reliance on fundamental physics, compared to other Semi-Mechanistic models. Simplicity of the model is partly due to the fact that it does not recognise pressure loss, which can be seen as a shortfall for this model.

2.3 Mechanistic or Theoretical Models

Mechanistic models are closer to fundamental physics governing multi-phase flow. By limiting the use of correlation or experimental terms in their formulation, these models have broader applicability in terms of particle diameter, pipe geometry and densities. Majority of the available mechanistic models were developed and validated by experimental data on low solid concentration flow(10).

Models in this category analyse the forces acting on solid particles in a moving liquid or gas media. Forces considered are Lift Force F_L , Drag Force F_D , Friction Force F_F , Gravity Force F_W , Plastic Force F_p , Turbulence Force F_T , Eddy Fluctuation Force F_E and force acting by weight of particles on top F_N . Not all the mechanistic models take into account all these forces but most comprehensive models such as Doron and Barnea (5), Yang et al (6), Rabinovich and Kalman (52,65), Wu and Chou (66) and Ramadan *et al* (67) utilise most of these loads in their formulations.

In this chapter, two of the most comprehensive mechanistic models which have been used greatly in this research are reviewed.

2.3.1 Three-Layer Model by Doron and Barnea (5)

The central concept of multi-layer models is to consider the entire multi-phase flow structure in distinctive and separate layers. To explain multi-layer concept, imagine a slurry flow consists of liquid and solid where solid particles have tendency to settle, flowing in a horizontal pipe. At high velocities, the particles are almost fully suspended in the liquid phase because magnitude of turbulence forces acting on each particle is greater than gravitational force. Hence particles are fully suspended. In this research and for ease of referencing this flow regime is classed as "Fully Suspended", however some researches classified this even further in other categories such as "Homogeneous" and "Heterogeneous" (68,69).

By reducing mean velocity of slurry flow, the gap between gravitational forces and turbulent forces narrows to a stage where particles start to settle at the bottom of the pipe, forming a "Moving" layer. By further reduction of velocity, particles at the bottom of the moving layer become stagnated, forming a "Stationary" layer while particles at the top of the layer and in immediate vicinity of liquid layer are still moving (11). These distinctive layers of "Stationary", "Moving" and "Suspended" in solid-liquid slurry flow were observed and reported by many researchers (11,69,70).

Doron *et al* (11) first introduced their two-layer model in 1987 to explain the behaviour of flowing slurry mixture. This model consisted of a layer of heterogeneous mixture of liquid-particles and a moving bed layer of particles, as shown in Figure 2-9. When mixture velocity is high enough to create turbulence and cause particles to suspend in the liquid phase, then heterogeneous phase occupies the whole pipe area. But when mixture velocity drops below a certain threshold known as "Suspending Velocity", then particles will fall to bottom of the pipe because turbulence and buoyancy forces cannot overcome the gravitational force.

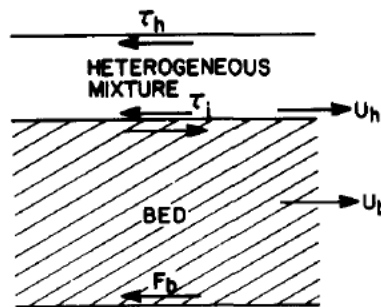


Figure 2-9: Geometry of two-layer model (11)

In this case, a packed layer of particles is formed at the pipe bottom. Force balance equations for these two layers were then developed to take into account the pressure gradient caused by shear friction forces (11).

The critical assumption in this research was that bed layer is either moving when shear stress on top of the layer caused by liquid phase is greater than friction force between particles and pipe wall, or stationary when friction force between solid particles is greater than shear force. Although this assumption was seen as valid but then further studies by Doron and Barnea (5,49,71) showed that this assumption is not entirely accurate because experimental investigations proved that sand bed layer itself in Figure 2.9 consists of two distinct regions namely "Moving Bed Layer" and "Stationary Bed Layer".

As confirmed by experiment (5), moving and stationary layers can coexist, but the two layer assumption in Doron *et al.* (11) model did not consider this because in this model sand layer is either moving or stationary. Although Doron *et al.* (11) two layer model proved to be accurate when mixture velocity is higher than "Suspending Velocity", but it could not accurately predict the formation of stationary bed when velocity drops below "Deposit Velocity". This led to the development of the three-layer model by Doron and Barnea (5).

"Deposit Velocity" or as defined by Doron and Barnea (5) "Minimum Moving Bed Velocity" is the minimum velocity for which particles can continue to move. If slurry velocity drops below this value, then the stationary layer will start to form.

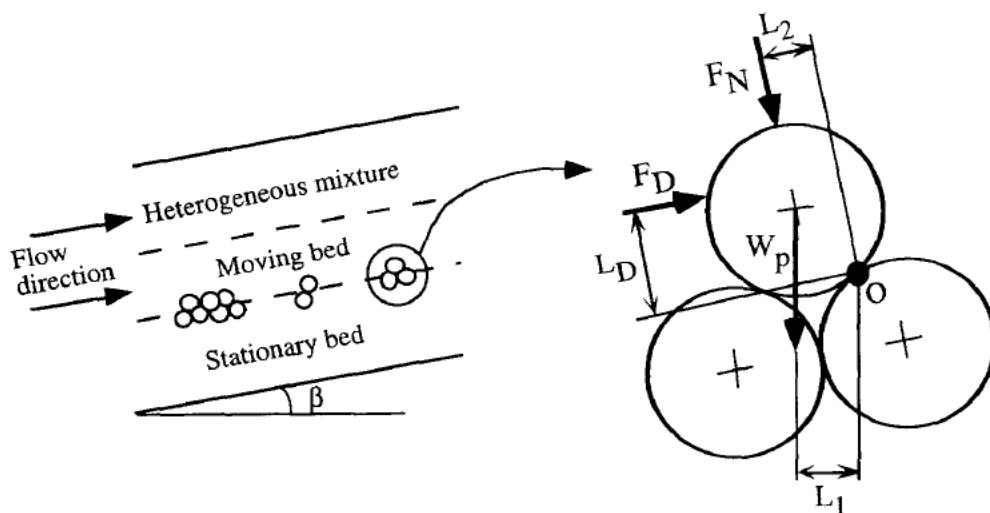


Figure 2-10: Three layer model and forces acting on particles (12)

Introducing the minimum moving bed velocity or " U_{bc} " in three layer model is the fundamental improvement from the previous two layer model. Method to calculate " U_{bc} " is based on required torque to rotate the upper particle shown in Figure 2.10 with point "O" as the centre of rotation.

Hence it is obvious to see that " U_{bc} " will be a function of particle diameter, drag coefficient, and gravitational force. Details of the calculation method can be found in (5).

Because moving bed layer was added to the flow geometry, force balance equations in two layer model needed to be revised to take into account this new layer. Stationary bed exists only if shear forces imposed by moving bed are smaller than dry friction forces between sand particles and the pipe wall. Methods to calculate the dry friction force are mathematically complex due to the gravitational effect of moving bed on the Columbic friction force and also sand volumetric concentration in the stationary bed. Further details can be found in (5,49,71).

In “Three-Layer” model, the entire flow regime has been explained by six unknowns, i.e. velocity of the moving bed layer (U_{bc}), the velocity of the heterogeneous or liquid layer, heights of the moving and stationary beds, pressure gradient and sand concentration in the liquid phase.

Six equations which are representing these unknowns are momentum equation for moving sand bed layer, momentum equation for liquid layer, minimum moving bed velocity equation, two mass continuity equations for liquid and sand and sand distribution concentration in the liquid phase. Details of these equations and solution method have been described in (5).

2.3.2 Continuous Stratified Two Phase Model by Yang *et al.* (6)

In 2006, Yang *et al.* (6) introduced the first two-phase liquid/sand model based on continuous average equation concept. This model and subsequent three-phase flow model by Yang *et al.* (31) were developed using extensive experimental research conducted by Dahl *et al.* (61,62,72) at Multiphase Flow Laboratory at SINTEF Petroleum Research Facilities in Norway.

Yang *et al.* (6,31) claimed that their one-dimensional and isothermal model is the first and only continuous model that fully coupled the dynamic of carrier fluid with sand particle dynamic across the whole flow area. In order to develop the closure equations, they used the closure terms which were introduced by Doron *et al.* (5,12,71) multi-layer models. They have used their model using “Volume Averaging” technique, which although it is much closer to Navier-Stokes equations for “Numerically-Exact” solution of single phase flow, it still uses a considerable amount of correlation terms in its formulation.

They assumed sand bed and two mixture layers in the flow: liquid layer mixed with traveling sand particles and gas layer mixed with liquid droplets. The model consists of two momentum conservation equations for moving layers and four mass conservation equations for sand, liquid, gas and droplet fields. They assumed that there will be no sand particles in the gas stream and no gas bubbles in the liquid field. The former assumption is backed by Dahl *et al.* (61,62,72) experiments and the latter assumption is valid for stratified flow.

Mass and momentum conservation equations were written in a generic form, which could then be applied to all the present fields by changing the indexes.

Mass conservation equation:

$$\frac{\partial}{\partial t} \alpha_k \cdot \rho_k + \frac{\partial}{\partial x} \alpha_k \cdot \rho_k \cdot u_k = \sum_{i \neq k} \Gamma_{k,i} + \Gamma_{k,exit} \quad (2.26)$$

Momentum conservation equation:

$$\begin{aligned} \frac{\partial}{\partial t} \alpha_k \cdot \rho_k \cdot u_k + \frac{\partial}{\partial x} \alpha_k \cdot \rho_k \cdot u_k \cdot u_k = & - \frac{\partial}{\partial x} \alpha_k \cdot P_k - \alpha_k \cdot \rho_k \cdot g \cdot \sin \theta \\ + \sum_{i \neq k} u_{k,i} \cdot \Gamma_{k,i} + \sum_{i \neq k} M_{k,i}^P + \sum_{i \neq k} M_{k,i}^i + M_k^W + & u_{k,exit} \cdot \Gamma_{k,exit} \end{aligned} \quad (2.27)$$

Where $\Gamma_{k,i}$ is mass transfer from field k to field i and $u_{k,i}$ is the velocity at interface layer between field k and field i . $M_{k,i}^i$ is the interfacial friction force between two fields, $M_{k,i}^P$ is pressure variation force at the interface layer and M_k^W is friction force between layer k and wall (73).

To simplify the numerical solution process, Yang *et al.* (6,31) introduced the multi-mixture layer approach. In this approach, a mixture of liquid-sand particles and gas-liquid droplets are considered as two continuous layers which are governed by their momentum continuity equations. The benefit of this approach is that now three individual momentum equations for sand, liquid and gas can be replaced with two equations for multi-mixture fields.

Physical properties of the mixture fields (liquid layer mixed with sand particles and gas layer mixed with liquid droplets) are written in volume-averaged forms.

$$\rho_{ck} = \frac{\sum_{k \in ck} \alpha_k \cdot \rho_k}{\alpha_{ck}} \quad (2.28)$$

$$u_{ck} = \frac{\sum_{k \in ck} \alpha_k \cdot \rho_k \cdot u_k}{\alpha_{ck} \cdot \rho_{ck}} \quad (2.29)$$

$$\alpha_k = \sum_{k \in ck} \alpha_k \quad (2.30)$$

Even though Yang *et al.* (6) comprehensively used Doron *et al.* models (5,11,12,71) for development of closure terms, by introducing multi-mixture approach they removed the concept of moving sand bed which is fundamental in Doron and Barnea (5) model. Moving sand bed is

modelled as part of mixture sand-liquid layer, and the stationary sand bed can be formed or eroded dynamically in Yang *et al.* (6,31) models.

Multi-mixture approach can only be seen as a simplifying step if all the phases in mixture-layer are travelling at the same speed, i.e. no slip velocity between suspended and carrier phases. In reality, there will be slip velocity between suspended and carrier phases, but considering it in moving layers increases the complexity of equations and does not significantly improve the accuracy of the results. Therefore neither Yang *et al.* (6) nor Doron and Barnea (5) models take the slip velocity into account. In their 2007 model, Yang *et al.* (31) tried to introduce slip velocity by using drift-flux model which was first introduced by Nicklin (74) and used by Danielson (3) in his semi-theoretical sand transport model, but results didn't demonstrate massive improvement compared to the previous model where slip velocity wasn't considered. It can be argued that in stratified flow regime where velocities are lower than other flow regimes, all moving phases are travelling in almost equal velocity. Hence slip velocity between dispersed and carrier phases can be neglected.

Yang *et al.* (6,31) used droplet entrainment and deposition model by Pan and Hanratty (75) to calculate droplet concentration in gas flow. Even though deposition coefficient in Pan and Hanratty (75) model was modified using data obtained in SINTEF as shown in Equation (2.31) below.

$$C_{deposition} = 10^{-3} \cdot \frac{g \cdot \rho_l \cdot d_{droplrt}^2}{\mu_g} \quad (2.31)$$

Another simplifying assumption in Yang *et al.* (6,31) models is neglecting shear stresses between suspended phase and wall. The effect of dispersed phase was considered in the density of mixture layer as shown in Equation (2.27), but the viscosity of the mixture wasn't modified based on dispersed phase as suggested by Gillies *et al.* (76).

Yang *et al.* (6,31) works are of particular interest to this research because these models refer to only available experimental data on sand transport in three-phase flow (61,62,72), which will be used to validate and verify the four-phase model developed in this research.

Chapter 3

Model Development and Formulation

Inspired by Doron and Barnea (5) model, proposed four-phase flow consists of five layers, namely Stationary Sand bed (*SB*), Moving Sand bed (*MB*), Water layer (*W*), Oil layer (*O*) and Gas layer (*G*). These five abbreviations are used as subscript throughout this research to show parameters related to each layer.

Figure 3.1 depicts the flow structure, showing the geometrical parameters which are used in the formulation and subsequently in the computer code.

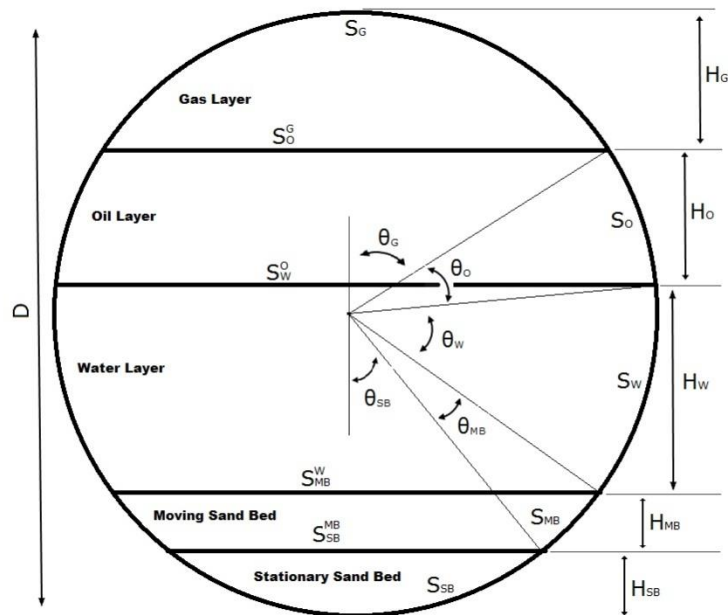


Figure 3-1: Structure of Stratified four-phase flow

In the studies done by Lee *et al.* (77) for three-phase water/oil/air flow, stratified and wavy stratified flow regimes were observed, where phases were separated based on their densities. By adding sand to three-phase water/oil/gas flow and while flow regime is stratified or semi-stratified

where phases are segregated, sand particles tend to settle at the bottom of the pipe.

This behaviour of sand particles has been observed by numerous researchers such as Televantos *et al.* (64), Hsu *et al.* (78) and Doron *et al.* (11), just to name some. Although most of these studies were performed on two-phase liquid/solid flow, it can be assumed with some level of certainty that sand particles in four-phase stratified flow will be settled at the bottom of the pipe as shown in figure 3.1.

Presence of stationary and moving bed layers very much depends on the velocity of slurry flow. In high flow rate cases where the velocity of the water layer is high enough, sand particles will be fully suspended in the water layer. It is worth noting that as long as water and oil are flowing in segregated layers, sand particles will only be in contact with water and will not be mixing with the oil. This is based on the assumption that sand particles are water wet and will only be transported by the water layer. Extensive experiments were done by Yang *et al.* (31) at SINTEF petroleum research facilities in Norway on three phase sand/liquid/gas also showed that sand particles never crossed water layer to enter the gas phase.

Consideration of oil wet sand particles does not change the number of equations in the current model because the flow regime is assumed to be stratified with the fully segregated layers. Hence there is no coupling term between oil and water mass continuity equations. The only impact will be on physical properties of the oil layer where effective physical properties should be calculated using sand concentration in the oil layer ($C_{s,o}$) as shown in equations below:

$$\rho_{s,o} = C_{s,o} \cdot \rho_s + (1 - C_{s,o}) \cdot \rho_o \quad (3.1)$$

$$\mu_{s,o} = C_{s,o} \cdot \mu_s + (1 - C_{s,o}) \cdot \mu_o \quad (3.2)$$

3.1 Geometrical Parameters

In Figure 3.1, H_i represents the height of the layer and subscript i is one of these indexes: stationary sand bed or sand phase (SB), moving sand bed layer (MB), water layer or water phase (W), oil layer or oil phase (O), gas layer or gas phase (G). Each of these layers has interfaces with pipe wall and with at least another layer. Middle layers, i.e., moving sand bed, water, and oil, each has interfaces with two layers.

To identify these interfaces, S_i^k represents the perimeter of the interface between field k and i , where field k is always on top of the field i e.g. S_{MB}^W is perimeter of the interface between the water layer and moving sand bed layer.

S_i is perimeter of the interface between field i and pipe wall. Subscripts k and i can be one of the five indexes for each layer, shown in figure 3.1.

A_i is the cross sectional area for layer i and A is the pipe cross sectional area. All geometrical parameters in Figure 3.1 can be expressed by H_i , using equations below:

$$A_{SB} = \frac{1}{2} \cdot \left(\frac{D}{2}\right)^2 \cdot \left\{ 2 \cdot \cos^{-1} \left[1 - \frac{2 \cdot H_{SB}}{D} \right] - \sin \left[2 \cdot \cos^{-1} \left[1 - \frac{2 \cdot H_{SB}}{D} \right] \right] \right\} \quad (3.3)$$

$$A_{MB} = \frac{1}{2} \cdot \left(\frac{D}{2}\right)^2 \cdot \left\{ 2 \cdot \cos^{-1} \left[1 - \frac{2 \cdot (H_{SB} + H_{MB})}{D} \right] - \sin \left[2 \cdot \cos^{-1} \left[1 - \frac{2 \cdot (H_{SB} + H_{MB})}{D} \right] \right] \right\} - A_{SB} \quad (3.4)$$

$$A_W = \frac{1}{2} \cdot \left(\frac{D}{2}\right)^2 \cdot \left\{ 2 \cdot \cos^{-1} \left[1 - \frac{2 \cdot (H_{SB} + H_{MB} + H_W)}{D} \right] - \sin \left[2 \cdot \cos^{-1} \left[1 - \frac{2 \cdot (H_{SB} + H_{MB} + H_W)}{D} \right] \right] \right\} - (A_{SB} + A_{MB}) \quad (3.5)$$

$$A_O = \frac{1}{2} \cdot \left(\frac{D}{2}\right)^2 \cdot \left\{ 2 \cdot \cos^{-1} \left[1 - \frac{2 \cdot (H_{SB} + H_{MB} + H_W + H_O)}{D} \right] - \sin \left[2 \cdot \cos^{-1} \left[1 - \frac{2 \cdot (H_{SB} + H_{MB} + H_W + H_O)}{D} \right] \right] \right\} - (A_{SB} + A_{MB} + A_W) \quad (3.6)$$

$$A_G = \frac{\pi \cdot D^2}{4} - (A_{SB} + A_{MB} + A_W + A_O) \quad (3.7)$$

$$S_{SB} = D \cdot \cos^{-1} \left[1 - \frac{2 \cdot H_{SB}}{D} \right] \quad (3.8)$$

$$S_{MB} = D \cdot \left\{ \cos^{-1} \left[1 - \frac{2 \cdot (H_{SB} + H_{MB})}{D} \right] - \cos^{-1} \left[1 - \frac{2 \cdot H_{SB}}{D} \right] \right\} \quad (3.9)$$

$$S_W = D \cdot \left\{ \cos^{-1} \left[1 - \frac{2 \cdot (H_{SB} + H_{MB} + H_W)}{D} \right] - \cos^{-1} \left[1 - \frac{2 \cdot (H_{SB} + H_{MB})}{D} \right] \right\} \quad (3.10)$$

$$S_O = D \cdot \left\{ \cos^{-1} \left[1 - \frac{2 \cdot (H_{SB} + H_{MB} + H_W + H_O)}{D} \right] - \cos^{-1} \left[1 - \frac{2 \cdot (H_{SB} + H_{MB} + H_W)}{D} \right] \right\} \quad (3.11)$$

$$S_G = \pi \cdot D - (S_{SB} + S_{MB} + S_W + S_O) \quad (3.12)$$

$$S_{SB}^{MB} = D \cdot \sin(\cos^{-1} \left[1 - \frac{2 \cdot H_{SB}}{D} \right]) \quad (3.13)$$

$$S_{MB}^W = D \cdot \sin(\cos^{-1} \left[1 - \frac{2 \cdot (H_{SB} + H_{MB})}{D} \right]) \quad (3.14)$$

$$S_W^O = D \cdot \sin(\cos^{-1} \left[1 - \frac{2 \cdot (H_{SB} + H_{MB} + H_W)}{D} \right]) \quad (3.15)$$

$$S_O^G = D \cdot \sin(\cos^{-1} \left[1 - \frac{2 \cdot (H_{SB} + H_{MB} + H_W + H_O)}{D} \right]) \quad (3.16)$$

All these geometrical parameters including A_i , S_i^k and S_i will be used throughout this chapter to calculate the hydraulic diameter, shear stress and pressure gradient for each layer. Models presented in (7,12,31) all used wetted angle parameter (θ) in their formulations, but in this study, the use of wetted angle was avoided. The reason is that in calculation loops if the wetted angle becomes greater than $\frac{\pi}{2}$ then its trigonometric values change sign and controlling it adds another layer of check, in the code.

3.2 Hydraulic Diameter

Another difference between formulations in this study and Taitel *et al.* model (7) is the way that hydraulic diameters were calculated. In Taitel *et al.* model (7), interface perimeters were not included in the hydraulic diameter calculation of oil and water layers. In Taitel *et al.* model (7) hydraulic diameters for oil and water layers were calculated, using equations below:

$$D_G = \frac{4 \cdot A_G}{S_G} \quad (3.17)$$

$$D_O = \frac{4 \cdot A_O}{S_O} \quad (3.18)$$

In these equations, only the interface perimeter between layer and pipe wall was considered. But when oil and water layers are thin, hydraulic diameter equations above can result in high values which in turn results in inaccurate Reynold number for oil and water layers Re_i .

In this study, the modifications which were proposed by some other researchers such as Andritsos and Hanratty (79), Kowalski (80) and Khor *et al* (81) were used. Their approaches take into account the interface perimeters between the layers to calculate hydraulic diameters. In this study interface perimeter between two flowing layers was included in the hydraulic diameter calculation of top layer, as shown in Equations (3.19-3.21) below:

$$D_G = \frac{4 \cdot A_G}{(S_G + S_O^G)} \quad (3.19)$$

$$D_O = \frac{4 \cdot A_O}{(S_O + S_W^O)} \quad (3.20)$$

$$D_W = \frac{4 \cdot A_W}{(S_W + S_{MB}^W)} \quad (3.21)$$

3.3 Mass Continuity

Four mass continuity equations represent each flowing phase. For sand which is only transported in water and moving bed layers:

$$U_W \cdot C_{S,W} \cdot A_W + U_{MB} \cdot C_{S,MB} \cdot A_{MB} = U_I \cdot C_{S,I} \cdot A \quad (3.22)$$

Where U_I and $C_{S,I}$ refer to slurry flow velocity and sand concentration at the inlet.

It is assumed that water and oil layers are fully segregated. Therefore water is only present in the moving bed layer and water layer.

$$U_W \cdot (1 - C_{S,W}) \cdot A_W + U_{MB} \cdot (1 - C_{S,MB}) \cdot A_{MB} = U_I \cdot C_{W,I} \cdot A \quad (3.23)$$

Where " $C_{W,I}$ " is volumetric fraction of water at inlet slurry flow.

Oil is present in the gas layer in the form of oil droplets and in the segregated oil layer.

$$U_O \cdot A_O + U_G \cdot C_{O,G} \cdot A_G = U_I \cdot C_{O,I} \cdot A$$

(3.24)

And for the gas layer, by taking into account the oil droplets:

$$U_G \cdot (1 - C_{O,G}) \cdot A_G = U_I \cdot C_{G,I} \cdot A \quad (3.25)$$

Where $C_{O,G}$ is volumetric concentration of oil droplets in the gas layer and $C_{G,I}$ and $C_{O,I}$ are volumetric fractions of gas and oil at the inlet.

Mass continuity equations of sand and water are coupled because of $C_{S,W}$. This reflects the fact that sand particles are water wetted and are transported by water only. The assumption that sand particles are only water wetted has been made to help with the verification of the formulation and results in this study. Due to the lack of actual four-phase gas/liquid/liquid/solid experimental data in open publications, it was decided to verify the code in two steps.

First step is to check the code outputs against available experimental data for three phase liquid/liquid/gas flow in Taitel *et al.* (7) studies. The second step is to introduce solid phase and use experimental data found in Doron and Barnea (5,71) and Al-Labadidi *et al* (82) studies for liquid/solid flow. In all these experiments, aqueous mixture with water-wetted sand particles was used.

It is also assumed that there is no slip velocity between carrying flow and carried particles. This means that sand particles in the water layer are traveling at the same velocity as water. Same applies to oil droplets in the gas layer. This assumption has been verified by Doron and Barnea (5).

3.4 Sand and Droplet Distribution

If $C_{S,W}$ and $C_{O,G}$ values in Equations (3.23) and (3.25) are greater than zero; it means that water and gas layers are transporting sand particles and oil droplets respectively. Solution process starts with the assumption that sand particles and oil droplets are both present in water and gas layers.

In this research, it was assumed that if the sand layer exists and the water layer is transporting sand particles, then sand distribution in the water layer is heterogeneous (76). The highest concentration is always near the sand layer, and the lowest concentration at the water-oil interface reduces in a non-linear form.

As suggested by Gillies *et al* (76) and Doron *et al.* (11), sand distribution in water layer when sand bed exists is governed by diffusion equation bellow:

$$\epsilon \frac{d^2C}{dy^2} + \omega \frac{dC}{dy} = 0 \quad (3.26)$$

Where ϵ is mean diffusion coefficient and ω is settling velocity for a cluster of sand particles as defined by Taylor (83) and are calculated as follow:

$$\epsilon = 0.052 \cdot U_W \cdot \frac{D}{2} \sqrt{\frac{f_{MB}^W}{2}} \quad (3.27)$$

$$\omega = \omega_0 \cdot (1 - C_{S,W})^m \quad (3.28)$$

f_{MB}^W in Equation (3.27) is friction factor between the water layer and moving bed layer which calculation method is shown in Section 3.5.

ω is calculated using Richardson and Zaki (18) method. Numerical calculation of ω proved to be a challenge because of the very unstable nature of Equations (3.29) to (3.32). The calculation method is explained in chapter 4.

$$\omega_0 = \sqrt{\frac{4}{3} \cdot \frac{(\frac{\rho_S}{\rho_W} - 1) \cdot d \cdot g}{C_D}} \quad (3.29)$$

$$C_D = \begin{cases} 18.5 \cdot Re_p^{-0.6} & 0.1 < Re_p < 500 \\ 0.44 & 500 < Re_p < 2 * 10^5 \end{cases} \quad (3.30)$$

$$m = \begin{cases} 4.45 \cdot Re_W^{-0.1} & 1 < Re_W < 500 \\ 2.39 & 500 < Re_W \end{cases} \quad (3.31)$$

$$\omega = \omega_0 \cdot (1 - C_{S,W})^m \quad (3.32)$$

C_D is drag coefficient for single sand particle and is a function of particle Reynolds number. m is a dimensionless parameter introduced by Richardson and Zaki (18) and is a function of water Reynolds number.

By reviewing Equations (3.26) and (3.32), it is evident that $C_{S,W}$ and ω are non-linear functions of each other. Integrating Equation (3.26)

between H_{MB} and H_W results in mean particle concentration in the water layer.

When sand particles are fully suspended in the water, H_{MB} and H_{SB} equate to zero in Equations (3.3) to (3.16). In this case, sand distribution in the water layer is considered to be homogenous, and is calculated as follow:

$$C_{S,W} = C_0 \int_0^{H_W} \exp\left(-\frac{\omega \cdot y}{\epsilon}\right) dy \quad (3.33)$$

C_0 is the concentration at the bottom of the pipe and is calculated using the equation below, described by Thomas (37).

$$C_0 = \frac{\pi}{2} \cdot C_{S,I} \int_{-\frac{\pi}{2}}^{\frac{\pi}{2}} \exp\left(-\frac{\omega \cdot D}{2\epsilon} \cdot \sin x\right) \cdot \cos^2 x \, dx \quad (3.34)$$

In chapter 4, how code switches between a fully suspended homogenous mixture and heterogeneous mixture to calculate sand concentration in the water layer is described.

In the case of homogenous suspension, sand concentration in the water layer has an impact on the viscosity of the slurry mixture. Code also calculates effective viscosity using Gillies *et al.* (76) method, in the equation below. When stationary and moving beds are detected, i.e. heterogeneous mixture, code only uses the viscosity of water in the calculation.

$$\frac{\mu_{W.effective}}{\mu_W} = 1 + 2.5 \cdot C + 10 \cdot C^2 + 0.0019 \cdot \exp(20 \cdot C) \quad (3.35)$$

Where C is sand concentration in water layer as detailed in Equation (3.33).

The concentration of oil droplet in the gas layer is considered as an average value with no vertical distribution, unlike sand particles. The model developed by Pan and Hanartty (75) is employed to calculate the oil droplet concentration in the gas layer, using Equations (3.36) to (3.40).

$$C_{O,G} = 3 \cdot 10^{-6} \cdot \frac{U_G^2 \cdot (\rho_G \cdot \rho_O)^{0.5}}{\sigma} \cdot \frac{W_l - W_{l,c}}{\pi \cdot D} \cdot \frac{S_O^G}{A} \quad (3.36)$$

$$W_l = C_{O,I} \cdot \rho_O \cdot U_O \cdot A \quad (3.37)$$

$$W_{l.c} = \frac{\pi \cdot D \cdot Re_{o.critical} \cdot \mu_o}{4} \quad (3.38)$$

$$Re_{o.critical} = 7.3(\log_{10}\varphi)^3 + 44.2 \cdot (\log_{10}\varphi)^2 - 263(\log_{10}\varphi) + 439 \quad (3.39)$$

$$\varphi = \frac{\mu_o}{\mu_g} \cdot \sqrt{\frac{\rho_g}{\rho_o}} \quad (3.40)$$

3.5 Momentum Continuity

Momentum equations are written for each layer, using the approach detailed in Doron *et al.* (11).

Shear stresses applying on each layer are depicted in Figure 3.2. Shear stress τ_i^k is the acting force between two moving layers where layer k is moving on top of layer i . Shear stress between the moving layer and wetted pipe wall perimeter is shown as τ_i .

One dimensional force balance for gas, oil and water layers are:

Gas layer:

$$A_G \cdot \frac{dP}{dx} = -\tau_G \cdot S_G - \tau_O^G \cdot S_O^G \quad (3.41)$$

Oil layer:

$$A_O \cdot \frac{dP}{dx} = -\tau_O \cdot S_O - \tau_W^O \cdot S_W^O + \tau_O^G \cdot S_O^G \quad (3.42)$$

Water layer:

$$A_W \cdot \frac{dP}{dx} = -\tau_W \cdot S_W - \tau_{MB}^W \cdot S_{MB}^W + \tau_W^O \cdot S_W^O \quad (3.43)$$

Because of dry friction factor of sand particles, friction forces between the moving sand bed, stationary sand bed, and pipe wall should also be included in the momentum equations (5). This will add an additional term to the right hand side of the pressure loss equation for moving bed.

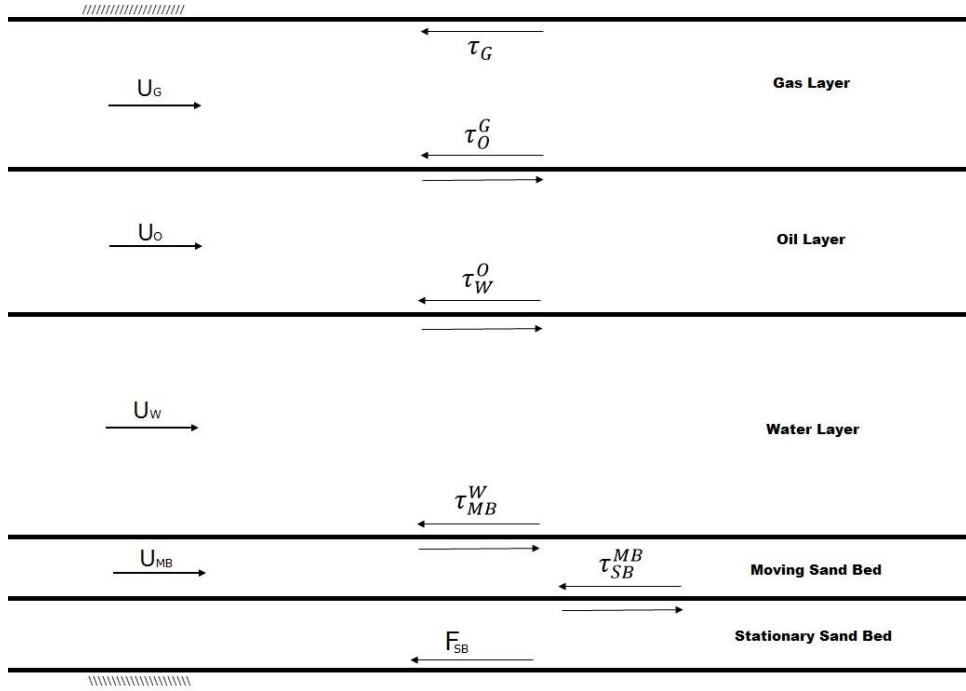


Figure 3-2: Shear stress in Stratified four-phase flow

Considering friction forces between moving and stationary beds, force balance equation for moving bed layer is:

$$A_{MB} \cdot \frac{dP}{dx} = -\tau_{SB}^{MB} \cdot S_{SB}^{MB} + \tau_{MB}^W \cdot S_{MB}^W - \tau_{MB} \cdot S_{MB} - F_{friction.MB} \quad (3.44)$$

$F_{friction.MB}$ in Equation (3.44) is the summation of dry friction forces between the moving bed layer and stationary layer and the friction between sand particles in the moving bed layer and pipe wall.

Unlike moving layers, the force balance equation for the stationary bed is not an equilibrium equation. For a stationary bed to exist, the summation of all the driving forces applying to this layer because of moving bed shall be less than dry friction forces applying on its surrounding perimeter.

$$A_{SB} \cdot \frac{dP}{dx} + \tau_{SB}^{MB} \cdot S_{SB}^{MB} + F_{friction.MB.SB} \leq F_{SB} \quad (3.45)$$

F_{SB} as shown in Figure 3-2 is the opposing force which prevents the stationary bed from moving, and as long as its magnitude is greater than driving forces, stationary bed exists (5). The developed code checks Equation (3.45) in every calculation loop to establish if the stationary bed exists.

The developed code calculates these forces i.e. F_{SB} , $F_{friction.MB.SB}$ and $F_{friction.MB}$, using the method described in (5,11,12). Tangent of internal friction is considered 0.6 as suggested by Bagnold (84) and dry dynamic coefficient η is considered "0.3" as suggested by Doron *et al.* (11).

For water, oil and gas layers, shear stress between the moving layer and pipe wall is calculated as follow:

$$\tau_i = \frac{1}{2} \cdot \rho_{i.effective} \cdot f_i \cdot U_i^2 \quad (3.46)$$

$\rho_{i.effective}$ in Equation (3.46) is effective density, taking into account the densities of particles and carrying medium. Hence for gas and water layers because those may carry oil droplets and sand particles respectively, densities will be corrected as follow:

$$\rho_{G.effective} = C_{O.G} \cdot \rho_O + (1 - C_{O.G}) \cdot \rho_G \quad (3.47)$$

$$\rho_{W.effective} = C_{S.W} \cdot \rho_S + (1 - C_{S.W}) \cdot \rho_W \quad (3.48)$$

Because oil layer does not carry sand particles, its density does not need correction.

f_i in Equation (3.46) is the friction coefficient and is calculated as follow (24):

$$f_i = \begin{cases} 16 \cdot Re_i^{-1} & Re_i \leq 2000 \\ 0.046 \cdot Re_i^{-0.2} & Re_i > 2000 \end{cases} \quad (3.49)$$

Re_i is the Reynolds number for the water, oil, or gas layer and is calculated using hydraulic diameter, as described in Section 3.2.

Shear stress at interfaces between gas, oil and water layers τ_i^k is calculated slightly differently from Equation (3.46). Code uses the approach detailed in Doron *et al.* (11) to calculate the interface friction factor.

Interface shear stresses are:

$$\tau_o^G = \frac{1}{2} \cdot \rho_G \cdot f_o^G \cdot |U_G - U_o| \cdot (U_G - U_o) \quad (3.50)$$

$$\tau_W^O = \frac{1}{2} \cdot \rho_O \cdot f_W^O \cdot |U_O - U_W| \cdot (U_O - U_W) \quad (3.51)$$

Interface friction factor f_i^k for gas, oil, and water layers is calculated using Taitel *et al.* (7) model which is the largest of 0.014 and value computed using Equation 3.49.

Sand in moving sand bed increases the effective roughness at the interface with the water layer. Therefore, rather than using Equation (3.49) Televantos *et al.* (64) equation is used to calculate friction factor at water-sand moving bed interface f_{MB}^W as shown below. This is a non-linear equation which is calculated iteratively in the code.

$$\frac{1}{\sqrt{2 \cdot f_{MB}^W}} = -0.86 \cdot \ln \left[\frac{\left[d / \left(4 \cdot \frac{A_W}{S_W + S_{MB}^W} \right) \right]}{3.7} + \frac{2.51}{Re_W \cdot \sqrt{2 \cdot f_{MB}^W}} \right] \quad (3.52)$$

Water Reynolds number Re_W is calculated, using effective density for water layer and hydraulic diameter as detailed in Section 3.2.

Chapter 4

Solving Algorithm and Code Verification

Equations which are presented in chapter 3 demonstrate that, given stationary and moving sand beds exist, entire flow regime can be defined by 12 unknowns. These unknowns are five geometrical variables $H_{SB}, H_{MB}, H_W, H_O, H_G$, two concentration variables $C_{S,W}, C_{O,G}$, four velocity variables U_{MB}, U_W, U_O, U_G and pressure gradient $\frac{dP}{dx}$. If water layer velocity is high enough, all sand particles are dispersed in the water layer, and consequently, equations and variables which are representing moving and stationary sand beds will be removed from the entire formulation. If water layer is below critical velocity where sand particles tend to settle and form sand layers, the number of equations and unknowns should be adjusted accordingly to reflect the existence of one or both sand layers (49). Hence it is evident that the proposed solution method should be able to differentiate between these scenarios and alter the number of equations and variables accordingly.

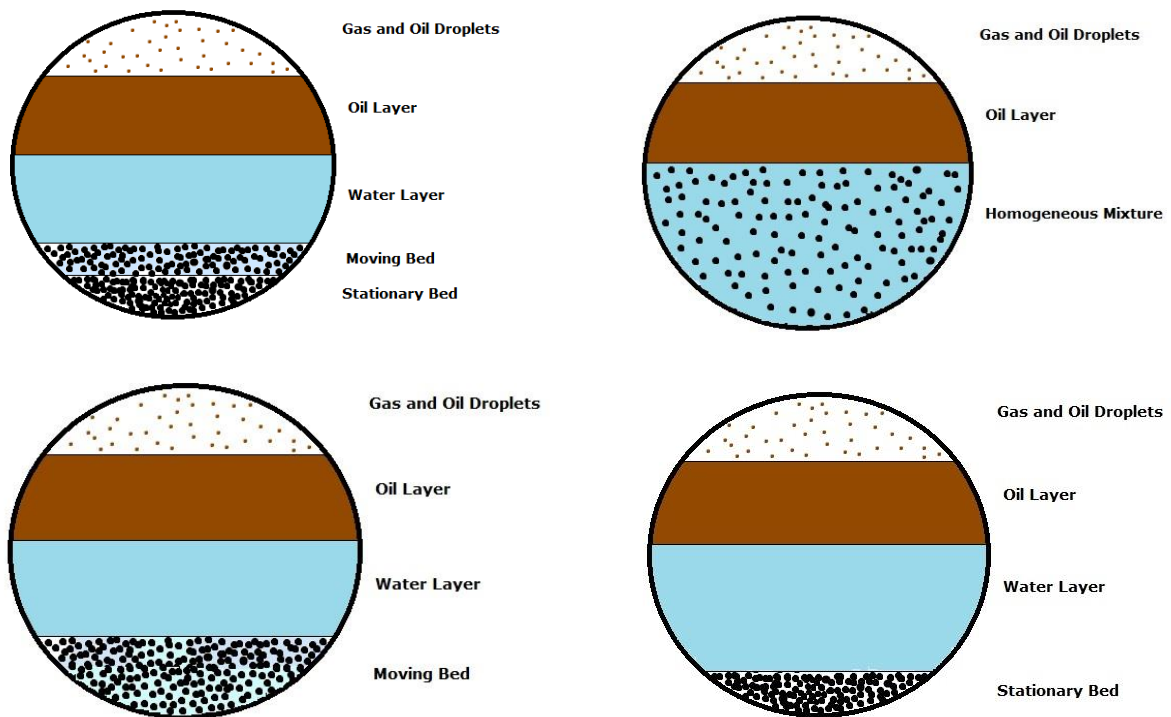


Figure 4-1 :Flow structures, recognised by the code

Figure 4-1 is a summary of all the flow structures that code is designed to recognise. Solution process starts with the assumption that all five layers, namely stationary sand bed, moving sand bed, water layer, oil layer, and gas layer exist. Built-in checks in the code detect whether the stationary sand bed is stable or not. And if it is not stable, then it moves to flow with moving sand bed and so on.

As claimed by Doron *et al.* (11), for three layer solid-liquid model when moving bed exist, no initial guess or priori can be estimated to start the solution process. Therefore all the five non-linear equations in their model had to be solved simultaneously. Employing this approach to solve all 12 non-linear equations for four-phase flow has proven to be mathematically challenging. For example, equations representing friction factors f_i and sand concentration distribution in the water layer $C_{s,W}$ are non-linear some of the parameters in these equations such as ω in concentration equation, are again non-linear variables of other flow parameters such as Reynolds number Re_i .

In this research, an iterative method was developed to solve these equations by guessing two of the variables to start the solution process. Main concept behind this solution method is that the flow regime is stable, and results are acceptable only if the pressure gradient for moving layers are equal i.e. $\frac{dP}{dx}\Big|_{MB} = \frac{dP}{dx}\Big|_W = \frac{dP}{dx}\Big|_O = \frac{dP}{dx}\Big|_G$

The main advantage of this iterative method is that the system of non-linear equations does not need to be solved simultaneously. Equations can be calculated individually using guessed variables and physical concept of equivalent pressure loss in all flowing phases will be applied as guardian in order to converge to a solution set which is feasible from a physics perspective. A shortcoming of this method is that there is a trade-off between the accuracy of the results and running time. Because it is not an exact solution method, calculated pressure losses are not exactly equal and there is always a difference between pressure loss values for the layers which solution converged to. In order to minimise the difference, iteration shall be done in much smaller increment which consequently results in the longer run.

4.1 Two-Guess Method

Iteration process starts by assuming that the sand layer is formed at the bottom of the pipe. Minimum height of the sand bed is assumed to be equal to three particles (4,11).

$$H_{S.minimum} = 3 \cdot d_p \quad (4.1)$$

Moving bed layer only exists if at least two particles on top of the sand bed are moving. This is based on the sand concentration of 0.52 in moving bed for cubic packing particles (5).

$$C_{S,MB} = 0.52 \Rightarrow H_{MB,minimum} = 2 \cdot d_p \quad (4.2)$$

These assumptions set the variation boundaries for H_{MB}, H_{SB} as follow:

$$2. d_p \leq H_{MB} < (0.9D - d_p) \quad (4.3)$$

$$3. d_p \leq (H_{SB} + H_{MB}) < 0.9D \quad (4.4)$$

Probability of having a sand bed with a height of $0.9D$ seems to be slim, but for the purpose of capturing all possible scenarios, the upper limit of sand height is set to $0.9D$. This limit will have an impact on running time and can be relaxed to more realistic values such as $0.6D$ if needed.

By knowing the variations of H_{MB} and $H_{SB} + H_{MB}$, solution process can start by guessing both of these variables at their minimum values and calculating all other variables, using equations detailed in chapter 3. Iteration steps continue by increasing the sand height by d_p and then repeat the solution process. Calculation steps are shown in Figure 4-2. Calculated values in each iterative loop will be stored in a data file for post processing. These data will be used later to identify the physically possible solution.

$$\text{Output of the internal loop} = \text{Maximum of} \left\{ \begin{array}{l} \left| \left(\frac{dp}{dx} \right)_O - \left(\frac{dp}{dx} \right)_W \right| \\ \left| \left(\frac{dp}{dx} \right)_O - \left(\frac{dp}{dx} \right)_G \right| \\ \left| \left(\frac{dp}{dx} \right)_W - \left(\frac{dp}{dx} \right)_G \right| \\ \left| \left(\frac{dp}{dx} \right)_{MB} - \left(\frac{dp}{dx} \right)_G \right| \\ \left| \left(\frac{dp}{dx} \right)_{MB} - \left(\frac{dp}{dx} \right)_W \right| \\ \left| \left(\frac{dp}{dx} \right)_{MB} - \left(\frac{dp}{dx} \right)_O \right| \end{array} \right. \quad (4.5)$$

Figure 4-2 depicts two iteration loops. First or internal loop calculates all the variables for an assumed value of H_{MB} , considering total sand bed height $H_{SB} + H_{MB}$ is given. Loop is being repeated until termination criterion is met. Pressure gradient equations detailed in Chapter 3; Equations (3.41) to (3.45); are all calculated and pressure gradient

values for each phase is stored in a matrix form. After completion of the first loop and before moving to second or external loop which controls total sand bed height, the developed code evaluates calculated data by comparing pressure gradients for all phases to pick the case where the difference between pressure gradients for two phases is maximum. This will be stored as the outcome of the internal loop and the code then moves to the external loop to increase the sand bed height and repeat the process.

Overall sand bed height will be increased by d_p increment until it reaches $0.9D$. At this stage, iteration process terminates, and code evaluate the results to find the most probable combination of sand, water, oil and gas heights. This evaluation will be done by minimising the output of internal loops, which means finding the minimum value for maximum pressure gradients.

By using this iterative method, the problem of having multiple solutions which occurs by solving the equations by the direct numerical method will be avoided. Taitel *et al* (7) and Taitel and Barnea (85) discussed in great length the issue of having multiple solutions for the system of non-linear equations. Multiple solutions can be seen as physically possible at first glance but Taitel and Barnea (85) concluded that the only solution with the thinnest liquid layer is stable. Because "Two-Guess" method converges to a solution with equal pressure gradient in all layers, it does not encounter the multiple solution issue.

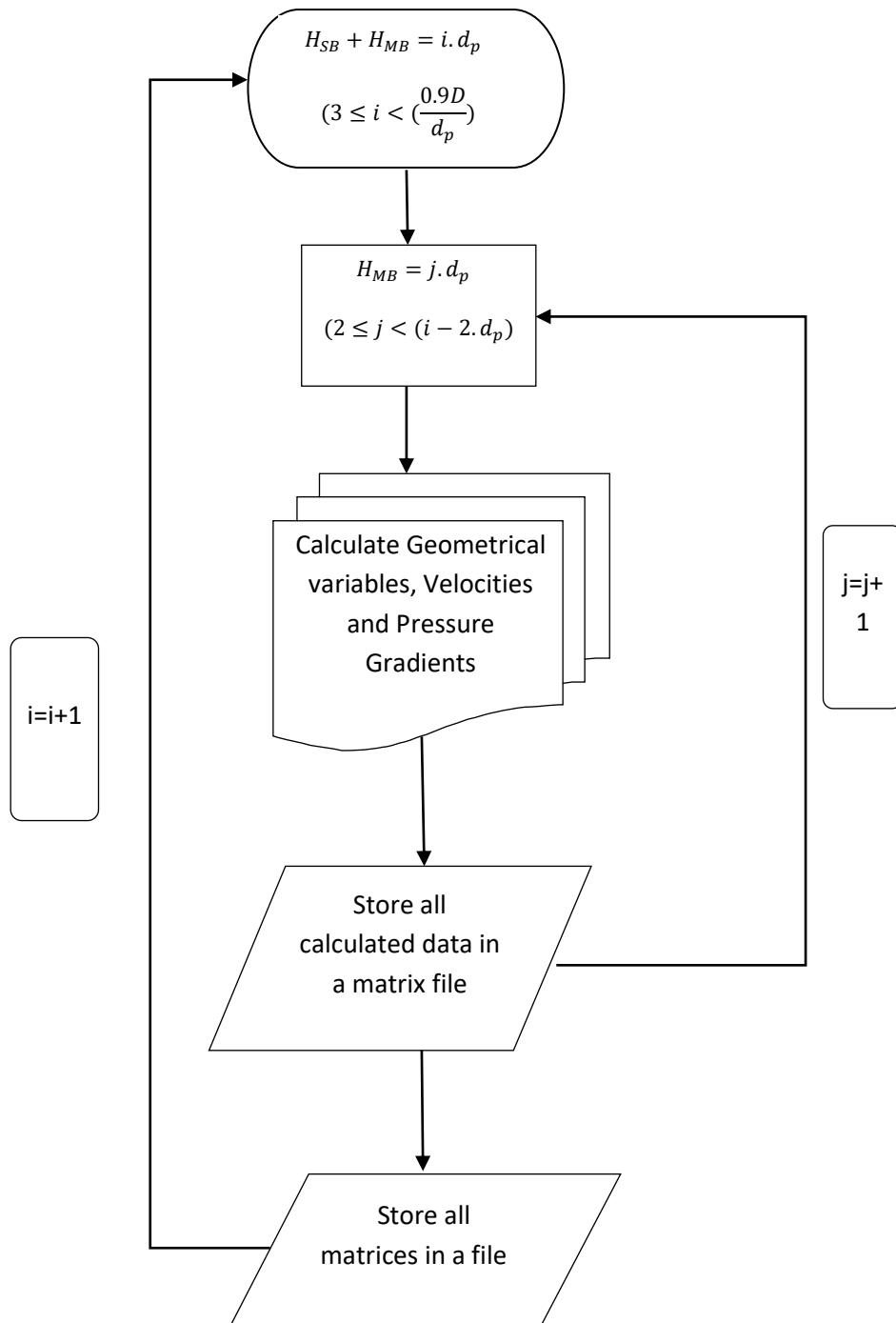


Figure 4-2: Flowchart showing loops for Two-Guess iterations

4.2 Code Formulation Adjustments

The code has been developed with the intention to detect the existence or absence of stationary and moving sand beds and adjust the formulation and solution process accordingly. This approach necessitates several criteria and checks to be incorporated in the code, which are explained in this section.

The formulations detailed in chapter 3 are only applicable when the flow regime is stratified. Therefore, the developed code should check the flow regime in every step to make sure it remains stratified. Despite the fact that stratified flow is the most critical flow regime for sand transport purpose (86) and even though several criteria for flow regime detection in two phase liquid/gas flow were developed, no flow regime detection criteria for four-phase flow could be found in publications. In the absence of such criteria, Taitel *et al.* (7) stratified transition condition for three layer liquid/liquid/gas flow is used in this research to check the stability of stratified flow.

$$U_G - U_O > \left(1 - \frac{H_W + H_O}{D}\right) \cdot \sqrt{\frac{(\rho_O - \rho_G) \cdot g \cdot A_G}{\rho_G \cdot S_O^G}} \quad (4.6)$$

Although Equation (4.6) does not take into account the heights of water and sand layers, as argued by Barnea (87) the velocity difference between gas and adjacent phase, i.e. oil layer, will determine the stability of stratified flow, regardless of other flowing layers beneath the oil layer. Comprehensive investigations on two and three phase flows show that transition of stratified flow to other flow regimes will start by wave formation at top of the oil layer (43,88,89). It is governed by the Kelvin-Helmholtz instability theory which is influenced by velocity difference between oil layer and adjacent relatively high velocity gas layer. Therefore, it is acceptable to assume that Equation (4.6) can adequately predict the stability of four-phase flow. Effect of water and sand layers can indirectly be seen in the height of the oil layer which determines the oil layer velocity.

The developed code also checks the calculated velocities for each moving layer in every iteration to single out any negative velocity. If calculated velocity is negative, the system of equations which is governing the flow regime is not acceptable from the physics perspective. Hence equations should be adjusted to reflect the physically possible flow structure.

Existence of stationary sand bed layer is also checked in every iteration, using Equation (3.45). If Equation (3.45) is not satisfied, then the

developed code assumes that $H_{SB} = 0$ and either entire sand bed is moving i.e. $H_S = H_{MB}$ or sand particles are fully suspended in water layer i.e. $H_{SB} = H_{MB} = 0$. In both cases, equations will be adjusted accordingly and the iteration process will be repeated for new set of equations. Code will be using minimum moving bed velocity criteria in Equation (4.7) which was introduced by Doron and Barnea (5) in order to define whether moving bed exists or particles are fully suspended in the water layer.

$$U_{MB.Minimum} = \sqrt{\frac{0.779 \cdot (\rho_S - \rho_W) \cdot g \cdot d_p \cdot \left[C_{MB} \cdot \frac{H_{MB}}{d_p} + (1 - C_{MB}) \right]}{\rho_W \cdot C_D}} \quad (4.7)$$

If U_{MB} calculated by the code is higher than $U_{MB.Minimum}$ but less than U_I which is inlet superficial velocity of slurry flow, then moving bed exists and code should adjust the equations to include H_{MB} in the formulations. Otherwise, all the particles are fully suspended in the water layer, and flow structure geometry will be adjusted to $H_{SB} = H_{MB} = 0$.

As described in Section 3.4, sand particles will only be transported by the water layer. Therefore in the case of fully suspended flow, density and viscosity of the water layer will be averaged to take into account sand particles. In these circumstances, the slurry mixture will be considered to be homogeneous with constant sand concentration throughout the slurry layer (11). Flow structure geometry which is depicted in figure 3.1 will be adjusted to show three layers, i.e. slurry, oil, and gas. Governing equations are very similar to Taitel *et al.* (7) stratified three phase flow model, with this difference that physical properties of water layer in Taitel *et al.* (7) model should be replaced with averaged density and viscosity to take into account sand presence.

4.3 Code Verification- Comparison with Taitel et al (7) Model

Concept of "Two-Guess" method, which is detailed in Section 4.1, is needed to be verified. Due to unavailability of experimental data for four-phase flow in open publications, it was decided to validate the accuracy of "Two-Guess" method against available experimental data for two and three phase flow.

To start, Taitel *et al.* (7) model for stratified three phase horizontal flow was selected. Flow structure consists of two immiscible liquids and gas layer, flowing in a horizontal pipe. Given liquid phases are water and oil,

they didn't consider any oil droplet in the gas phase in their model formulation. Therefore to match their model, code was modified to remove the sand phase and oil droplet from the equations. Taitel *et al.* (7) conducted a series of experiments with water, oil, and air in 5 cm pipe diameter. Properties of water and air were taken from standard tables at room temperature and atmospheric pressure with water viscosity set at 1 (cP). They used oil with 800 (kg/m^3) density and two viscosity values as 1 (cP) and 100 (cP).

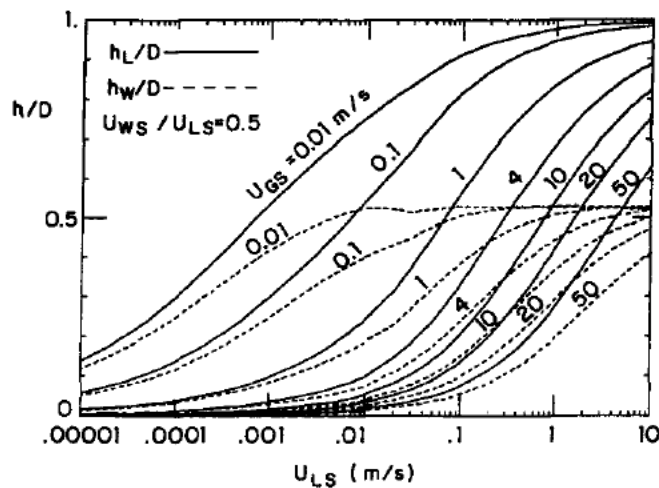


Figure 4-3: Liquid level for water-oil-air in horizontal pipes. Oil viscosity 1 cP. Water flow rate ratio 50% (7)

Figure 4-3 which is taken from Taitel *et al.* (7) work, depicts the total liquid level $\frac{h}{D} = \frac{h_W + h_O}{D}$ against total superficial liquid flow rate of $U_{LS} = U_{WS} + U_{OS}$ for equal water and oil flow rate. Water and oil viscosities are equal in Figure 4-3 results. Dotted lines are the height of the water layer, and solid lines show the total liquid level height.

Using physical properties in Taitel *et al.* (7) work, the developed code was ran for a series of slurry liquid velocities and constant gas velocity. Figure 4.4 shows the height of the water layer vs. liquid slurry velocity. It can be seen that for constant gas velocity, water layer height will increase by increasing slurry velocity.

Increasing trend of $\frac{H_W}{D}$ in Figure 4-4 is very similar to Figure 4-3 from Taitel *et al.* (7) work. Water layer height increases noticeably to 0.48 at the slurry velocity of 0.01 (m/s). It then reduces slightly when liquid velocity increases to 0.1 (m/s). Code was terminated for slurry velocities beyond 0.1 (m/s) because stratified flow requirement could not be met.

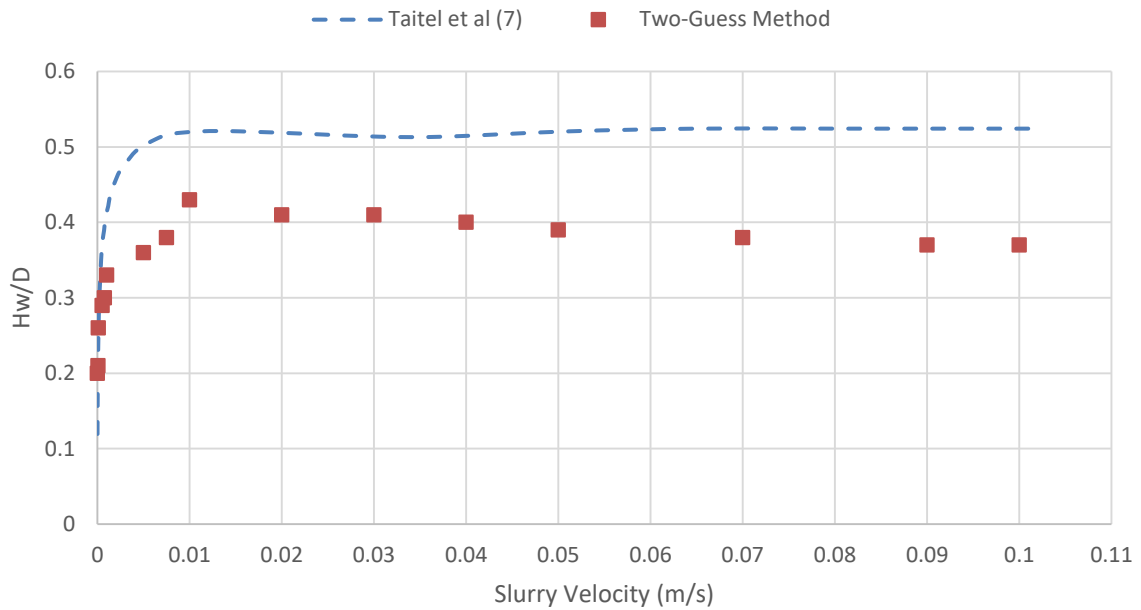


Figure 4-4: Water layer height vs Slurry velocity for water-oil-air in horizontal pipes.

$$\mu_o = 1 \text{ (cP)}, \mu_w = 100 \text{ (cP)}, U_G = 0.01 \left(\frac{m}{s}\right), Q_w = Q_o$$

Figure 4-5 is the total liquid layer height $\frac{H_L}{D} = \frac{H_W}{D} + \frac{H_O}{D}$ for the same criteria which figure 4-4 is representing.

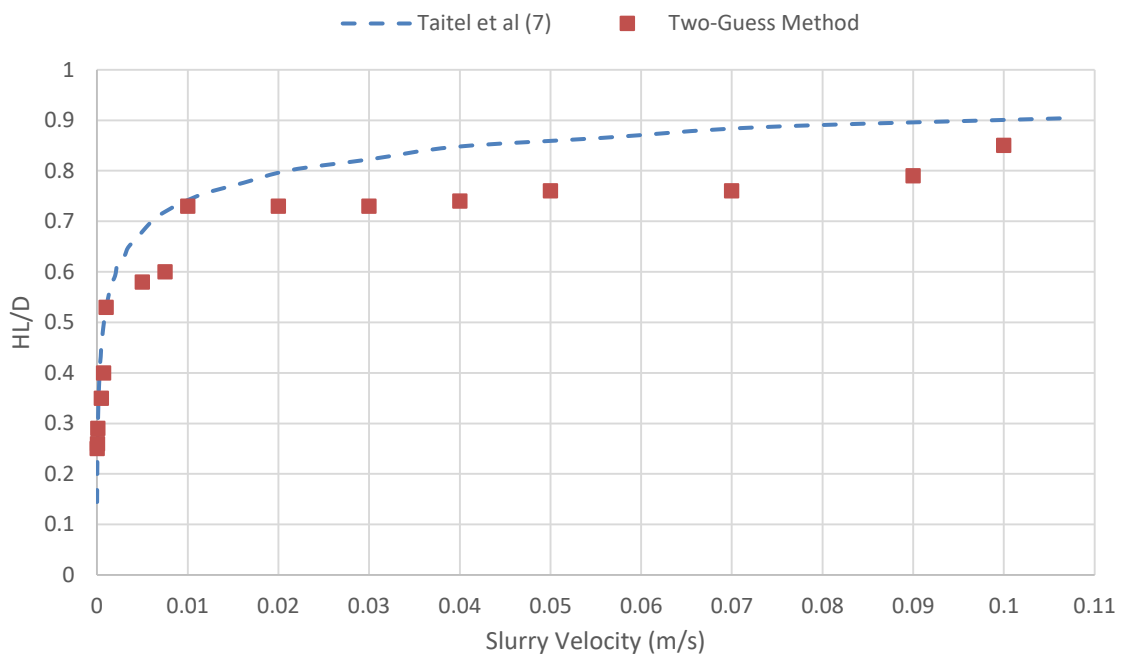


Figure 4-5: Total liquid layer height vs Slurry velocity for water-oil-air in horizontal pipes.

$$\mu_o = 1 \text{ (cP)}, \mu_w = 100 \text{ (cP)}, U_G = 0.01 \left(\frac{m}{s}\right), Q_w = Q_o$$

The total liquid height can reach up to 80% of the internal diameter of the pipe by increasing the slurry flowrate. Results in Figure 4-5 are

comparable with Figure 4-3 from Taitel *et al.* (7) work. By increasing the slurry flow rate to approach 0.1 (m/s), stratified flow regime becomes unstable, and this could be the reason for variations at the right hand side of the curve. Even though Taitel *et al.* (7) plotted the curves in Figure 4-3 for slurry velocity up to 10 (m/s), code results are showing that stratified flow regime exhibits signs of instability when velocity increases beyond 0.04 (m/s).

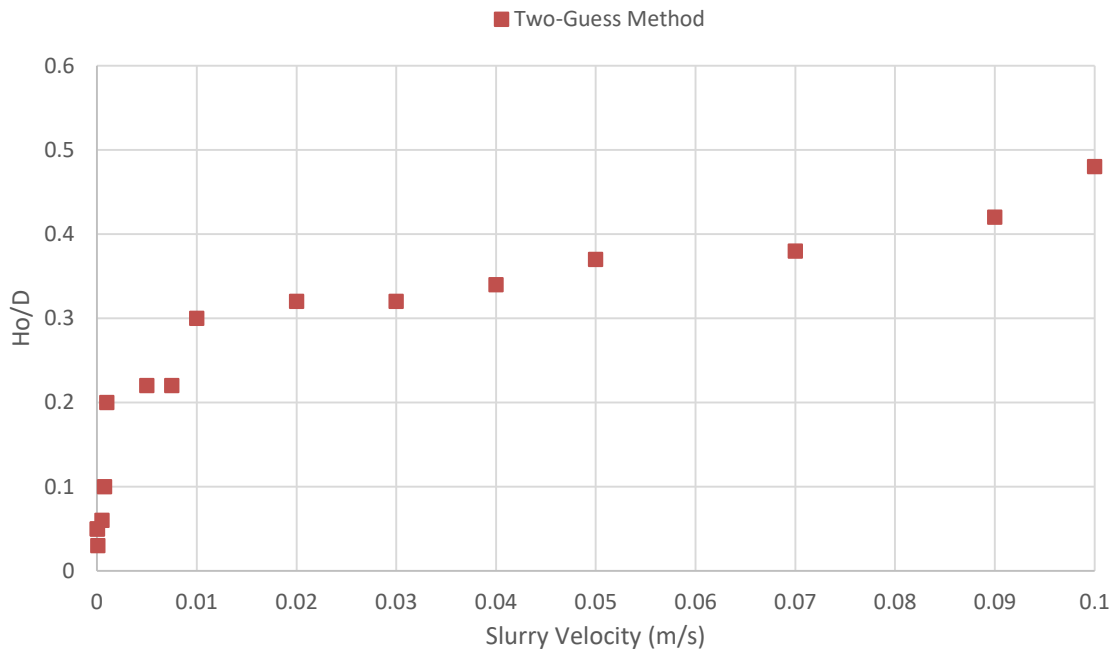


Figure 4-6: Oil layer height vs Slurry velocity for water-oil-air in horizontal pipes.

$$\mu_o = 1 \text{ (cP)}, \mu_w = 100 \text{ (cP)}, U_G = 0.01 \left(\frac{m}{s}\right), Q_w = Q_o$$

Figure 4-6 exhibits the variation of oil layer with slurry velocity. Even though water and oil have same volumetric flow rate $Q_w = Q_o$, the holdup of oil is less than water at each velocity. This is because oil flows quicker than water layer due to its vicinity with fast flowing gas layer. The lower viscosity of oil compare to water also plays a role here. In momentum equations which are detailed in chapter 3, the friction coefficient is a direct function of viscosity. Therefore, oil layer with much lower viscosity than water should have bigger interface surfaces with adjacent layers in order to have pressure loss equal to water layer. This means thickness of the oil layer should reduce so both interface surfaces with gas and water layers can increase.

Figure 4-7 shows the variation of all three layers (water, oil, and gas) with slurry velocity. Unlike Figure 4-3 which is plotted for slurry velocities up to 10 (m/s), in Figure 4-7 slurry velocity is limited to 0.04 (m/s) because code calculation shows that condition for stability of stratified flow in Equation (4.6) cannot be entirely satisfied for higher velocities. It

is noticeable that when slurry liquid velocity is higher than 0.015 (m/s), the height of the layers changes slightly with velocity. The gradient of the line for slurry velocities between 0.015 (m/s) and 0.04 (m/s) is low for all three layers. Taitel *et al.* (7) reported that flow is still stratified, but they didn't elaborate whether it is stratified smooth or stratified wavy. A low gradient of the height difference can be a sign that stratified flow is still in stable condition but is approaching transition boundary with other flow regimes. This can suggest that flow is more likely to be stratified wavy for velocities higher than 0.015 (m/s). It was also observed by Açıkgöz *et al.* (90) that stratified flow is difficult to maintain in a horizontal three phase flow.

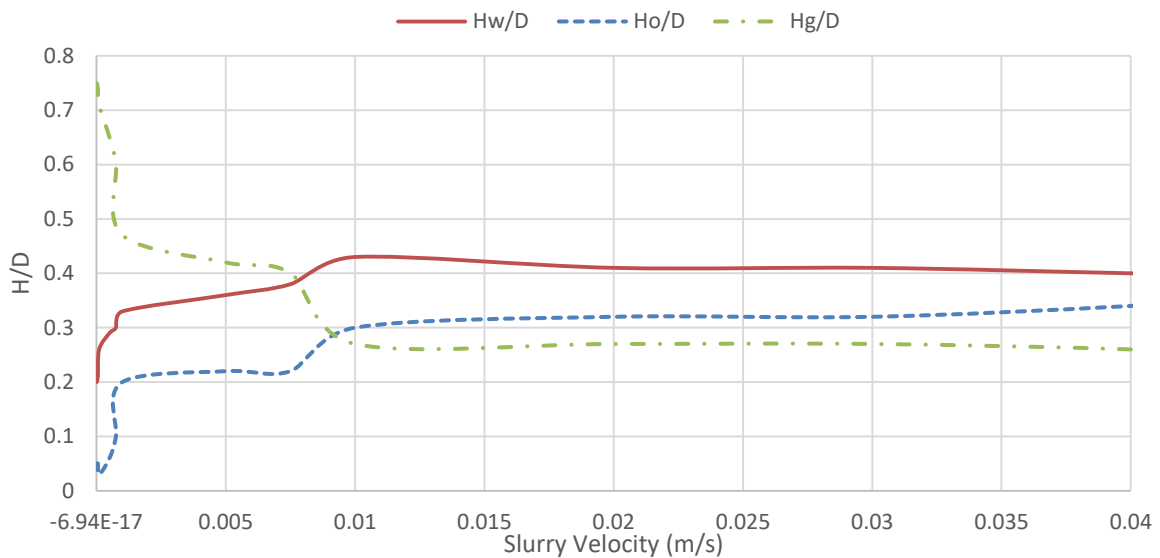


Figure 4-7: Multi-layer height vs Slurry velocity for water-oil-air in horizontal pipes.

$$\mu_o = 1 \text{ (cP)}, \mu_w = 100 \text{ (cP)}, U_G = 0.01 \left(\frac{m}{s}\right), Q_w = Q_o$$

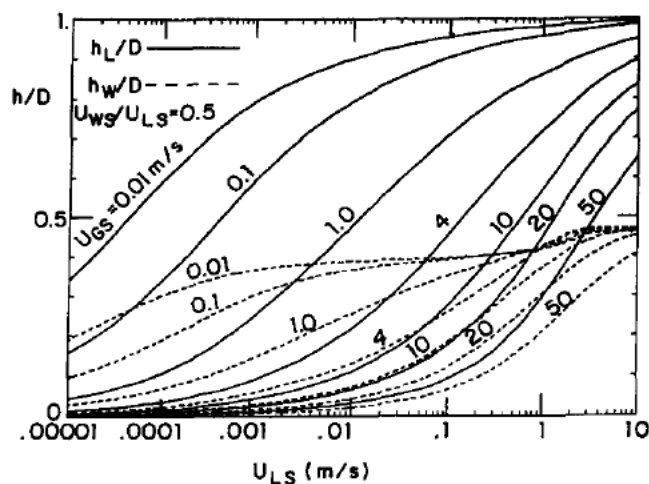


Figure 4-8: Liquid level for water-oil-air in horizontal pipes. Oil viscosity 100 cP. Water flow rate ratio 50% (7)

Since the developed code showed comparable results for low viscosity oil in Figure 4-3, in the next step it has been used to simulate the Taitel *et al.* (7) work for high oil viscosity as demonstrated in Figure 4-8. The developed code was ran with the same viscosity for both oil and water at 100 (cP). Gas velocity for this run was set at 1.0 (m/s). Figure 4-9 shows the height of the water layer. Compared to Figure 4-4, water holdup reduces in this case which is expected because gas velocity is 100 times higher. This increases the local velocity of oil and water, resulted in less water holdup. Variation of water layer height with slurry velocity differs from Figure 4-4 and shows a continuous rise. The developed code shows more stable stratified flow regime in this run, which can be seen as a result of increased oil viscosity. Higher oil viscosity creates a more stable flowing layer that needs higher velocity differences to be disturbed.

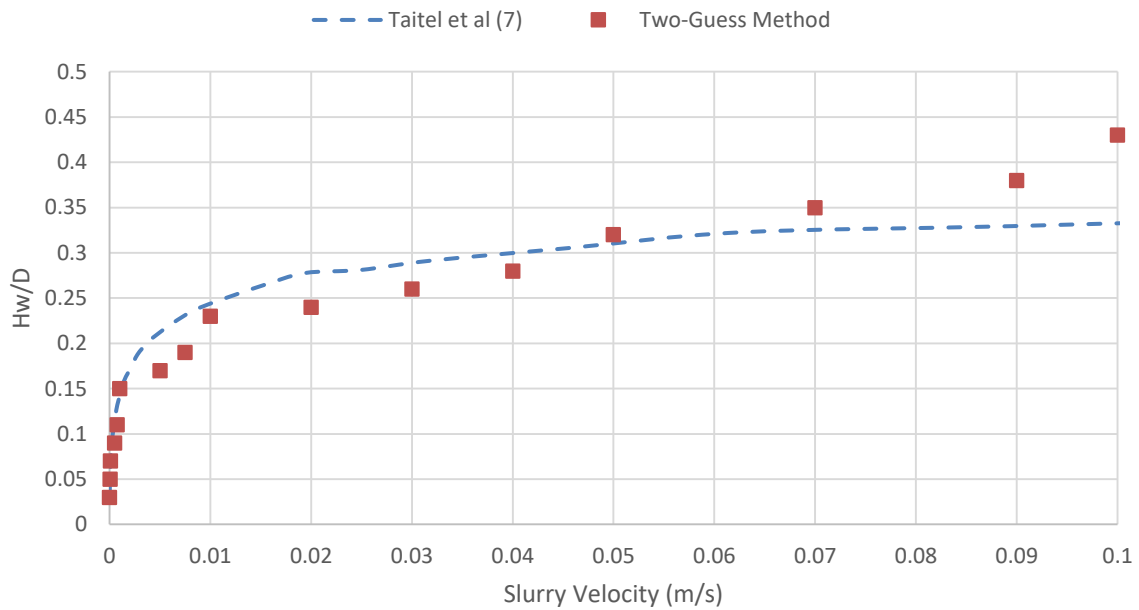


Figure 4-9: Water layer height vs Slurry velocity for water-oil-air in horizontal pipes.

$$\mu_o = 100 \text{ (cP)}, \mu_w = 100 \text{ (cP)}, U_G = 1.0 \left(\frac{m}{s}\right), Q_w = Q_o$$

Figure 4-10 shows total liquid layer vs. slurry velocity. Compared to Figure 4-5 where liquid occupied up to 80% of the pipe diameter, in this case, total liquid height could only reach 60% of the diameter. Higher gas flow velocity could be the reason for the less liquid holdup. Increase in gas velocity directly impacts the oil layer and causes it to flow quicker. Quick flowing oil layer then increases the water layer velocity at the interface layer. Hence whole flow structure moves quicker which in turn results in less holdup for liquid phases.

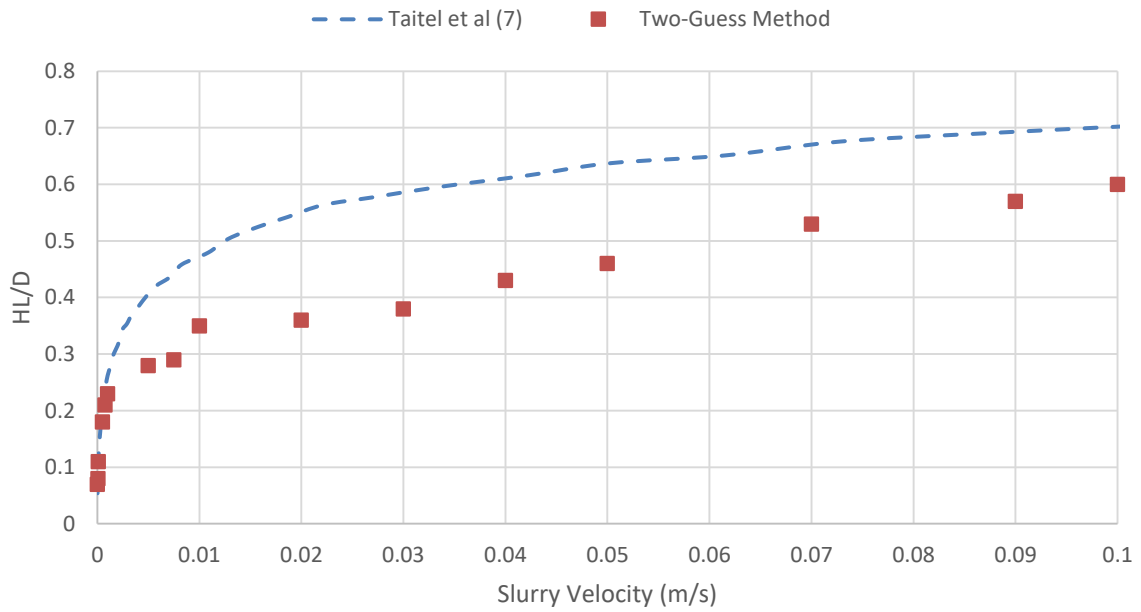


Figure 4-10: Total liquid layer height vs Slurry velocity for water-oil-air in horizontal pipes.

$$\mu_o = 100 \text{ (cP)}, \mu_w = 100 \text{ (cP)}, U_G = 1.0 \left(\frac{m}{s}\right), Q_W = Q_O$$

Variation of oil layer height vs. slurry velocity is depicted in Figure 4-11. Trend is same as water layer height in Figure 4-9 but shows less holdup for the oil layer compared to water for the reason explained before. Even though higher oil viscosity should result in height layer increase, higher gas velocity has a counter effect and reduces the holdup.

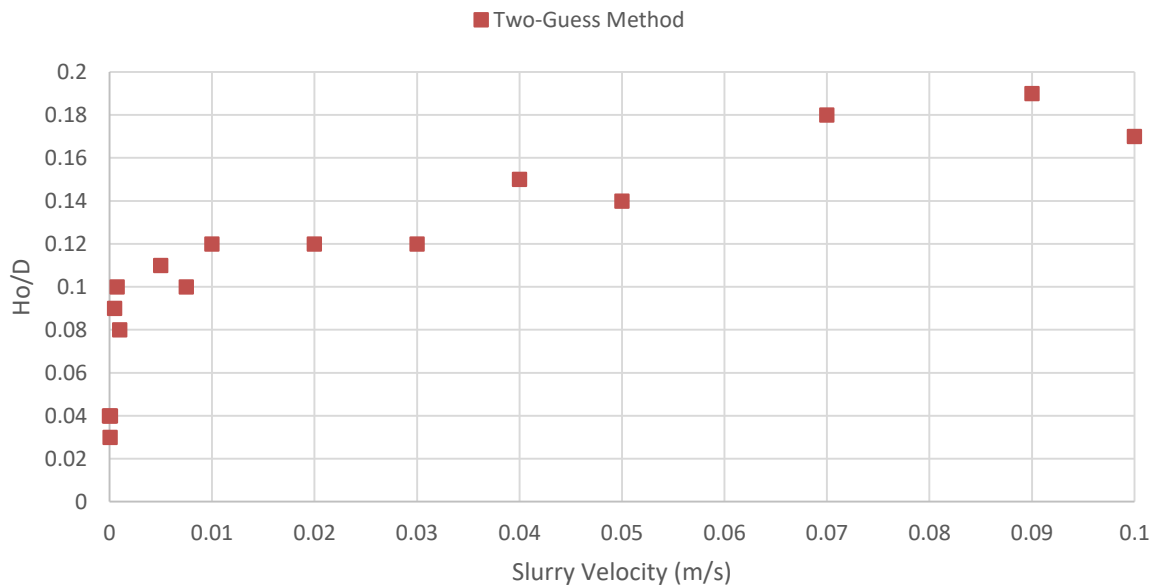


Figure 4-11: Oil layer height vs Slurry velocity for water-oil-air in horizontal pipes.

$$\mu_o = 100 \text{ (cP)}, \mu_w = 100 \text{ (cP)}, U_G = 1.0 \left(\frac{m}{s}\right), Q_W = Q_O$$

Figure 4-12 shows variation in the height of all three phases vs. slurry velocity. Whilst liquid phases occupy more volume in the pipe; the gas flowing area starts to squeeze. This causes local gas velocity to increase which in turn creates waves on the surface of the oil layer due to interfacial shear. If surface waves start to grow, the stratified flow regime becomes unstable and will transfer to other flow regimes such as intermittent or annular.

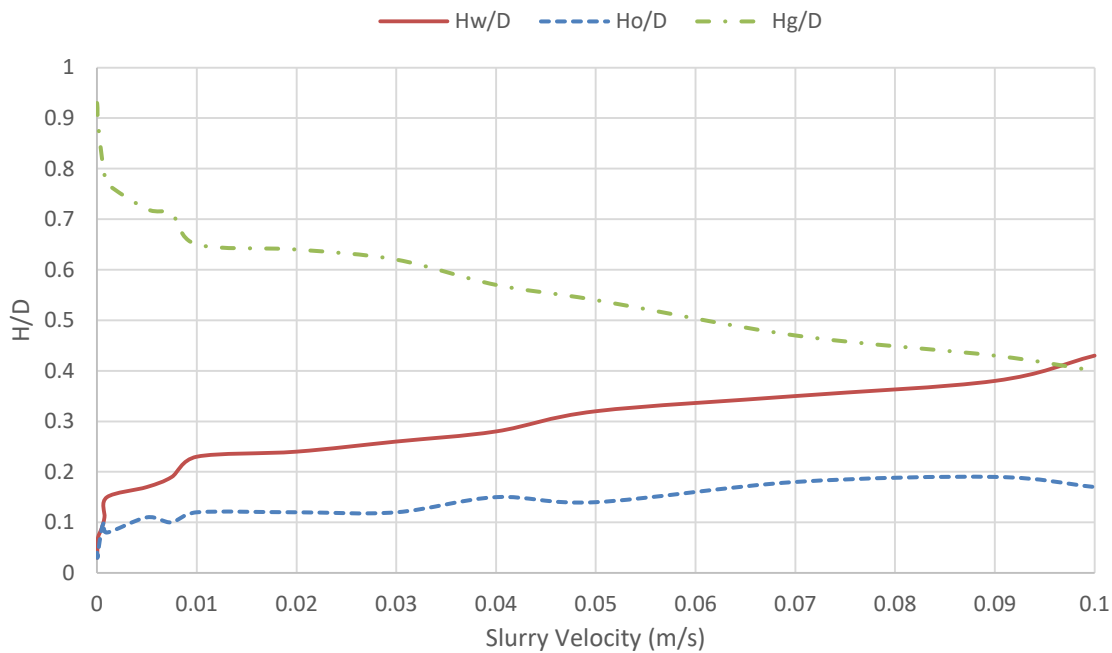


Figure 4-12: Multilayer height vs Slurry velocity for water-oil-air in horizontal pipes.

$$\mu_o = 100 \text{ (cP)}, \mu_w = 100 \text{ (cP)}, U_G = 1.0 \left(\frac{m}{s}\right), Q_w = Q_o$$

Code results suggest that stratified flow is stable up to 0.1 (m/s) slurry velocity. Results of the program for two different operating scenarios showed proper alignment with Taitel *et al.* (7) work. Figures 4-13 to 4-14 show the effect of gas velocity on the height of liquid and water layers. As expected, by increasing gas velocity, liquid holdup and subsequently height of liquid layer will decrease.

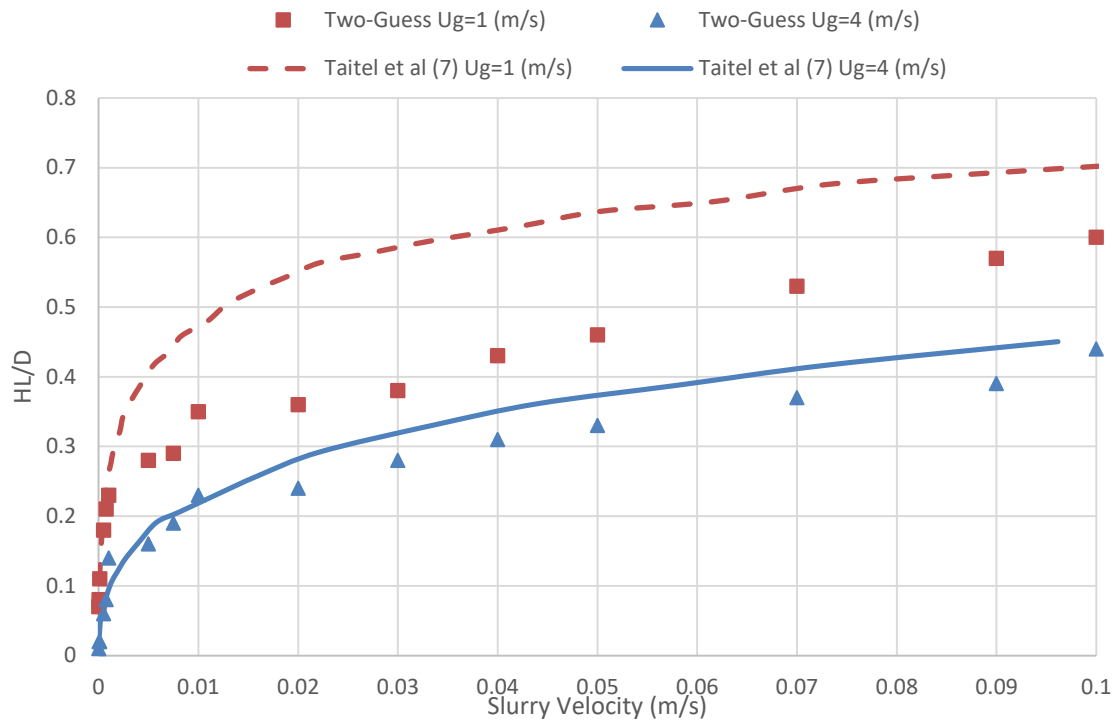


Figure 4-13: Effect of gas velocity on the liquid layer for water-oil-air in horizontal pipes.

$$\mu_o = 100 \text{ (cP)}, \mu_w = 100 \text{ (cP)}, U_G = 1.0 \text{ \& \; } 4.0 \left(\frac{m}{s}\right), Q_w = Q_o$$

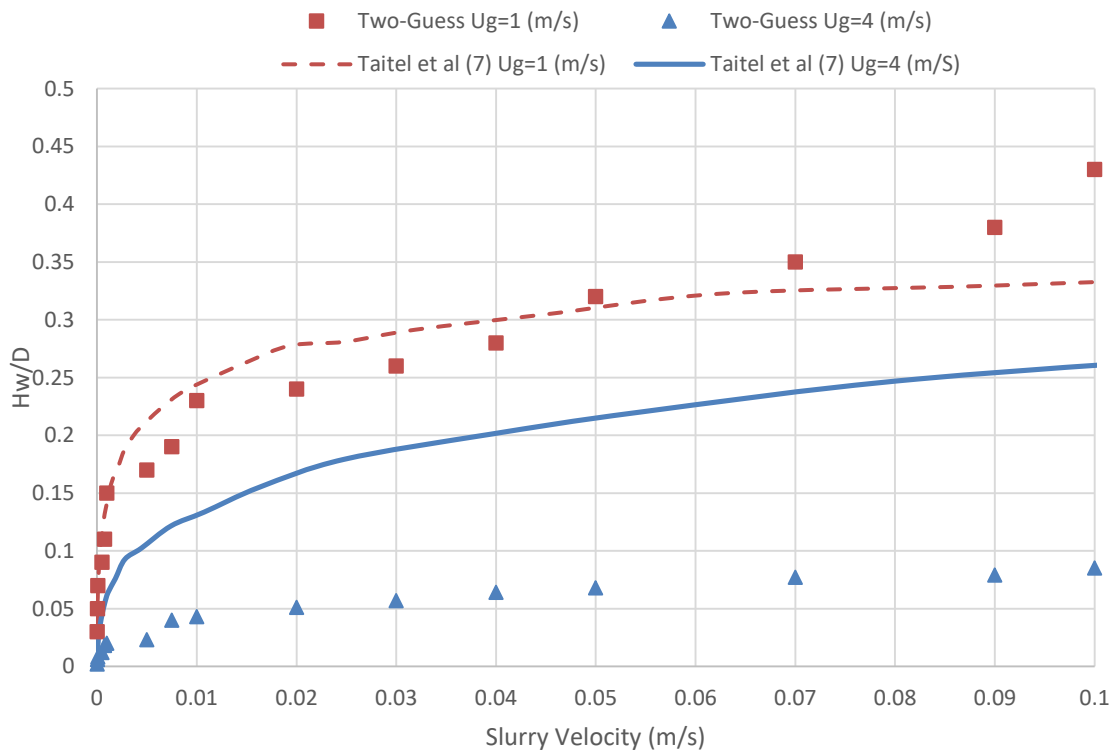


Figure 4-14: Effect of gas velocity on water layer height for water-oil-air in horizontal pipes.

$$\mu_o = 100 \text{ (cP)}, \mu_w = 100 \text{ (cP)}, U_G = 1.0 \text{ \& \; } 4.0 \left(\frac{m}{s}\right), Q_w = Q_o$$

Increasing gas velocity from 1 (m/s) to 4 (m/s), reduces in-situ water layer height considerably. When gas velocity is high enough, an increase in slurry flow rate does not increase the water height as much as it does in lower gas velocity. This effect can be noticed in figure 4-14, where gradients of water layer height curves for different gas velocities differ significantly.

Results for three phase water/oil/gas stratified system which were presented in this chapter shows very good agreement with the Taitel *et al.* (7) work. Statistical performance of the code versus Taitel *et al.* (7) model is studied in Section 4.5 of this report. In the next step, code is tested against available experimental results for liquid-solid flow.

4.4 Code Verification- Comparison with Doron and Barnea (5) Model

In this stage, the developed code was put to the test against experimental data, which were obtained by Doron and Barnea (5). Their three-layer model which was explained in Section 2.3.1 has been verified by the results of comprehensive experiments on two phase water-solid flow in horizontal pipe arrangement. In order to verify their three-layer model, Doron and Barnea (5) performed series of experiments using a mixture of water and "Acetal" particles with a density of $1240 \frac{kg}{m^3}$ and diameter of 3 (mm), flowing in a pipe with 50 (mm) internal diameter. The primary purpose of their experiment was to determine the limit deposit velocity U_{LD} where a stationary bed starts to disappear. Therefore most of the findings were presented against U_{LD} .

As the intention of the developed code in this research is to calculate pressure gradient and heights for each layer for four-phase flow, code had to be modified extensively in order to calculate the " U_{LD} " whilst solution core, which is based on "Two-Guess" approach, remained the same. It was a necessary attempt to verify the solution algorithm when solid particles exist in the flow.

Another challenge in utilising Doron and Barnea (5) experimental data to validate the code was that they didn't quite describe in their research whether the flow is stratified or in other forms. This is of particular importance because code is formulated based on the stratified flow regime. As their focus was to study the formation and disappearance of stationary solid bed, it was assumed that this transition from stationary bed to moving or fully suspended flow is very likely to happen in low local velocities which subsequently justifies the existence of stratified flow.

Oil and gas phases had to be removed from the formulation because Doron and Barnea (5) work was for two phase liquid-solid. Even though by eliminating oil and gas phases, momentum and mass continuity equations could be solved directly, "Two-Guess" method was employed to solve the system of non-linear equations.

Figure 4-15 from Doron and Barnea (5) work shows the effect of solid concentration on pressure gradient.

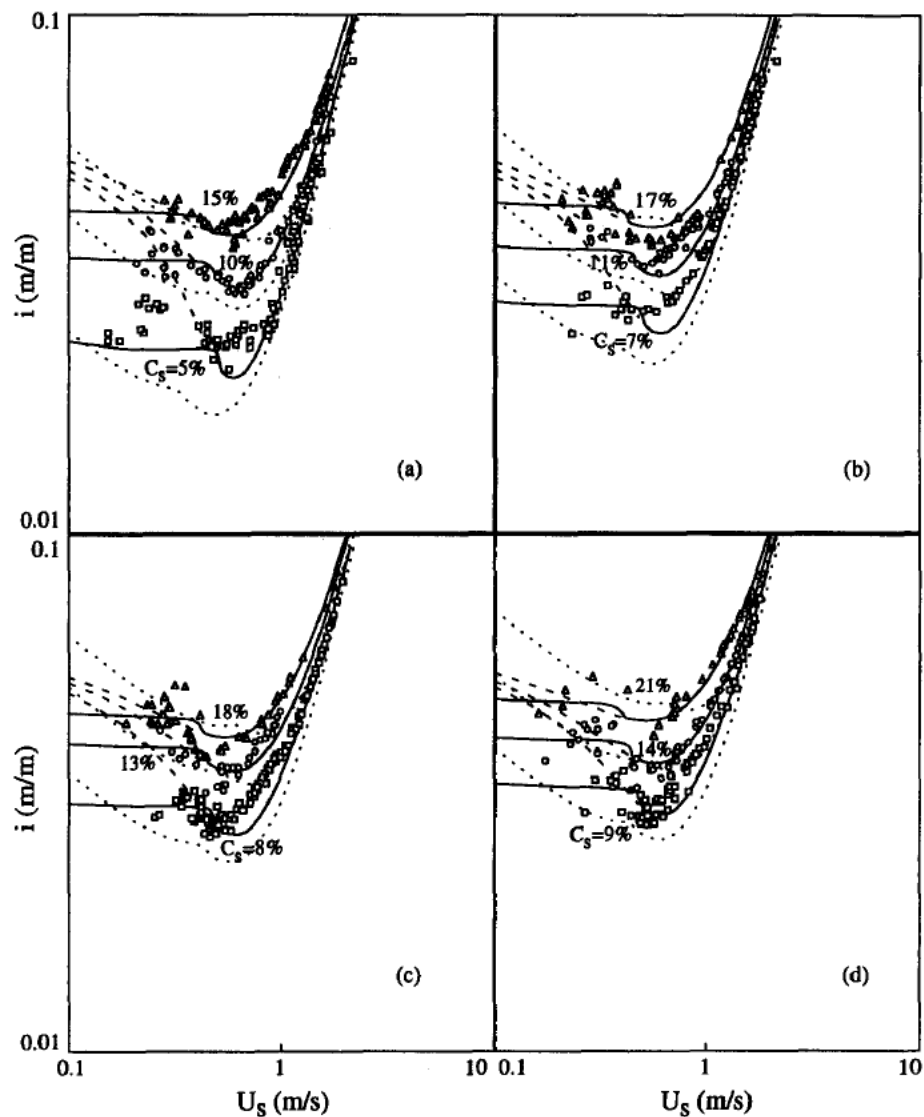


Figure 4-15: Effect of solid concentration on pressure gradient in water-Acetal flow in horizontal pipe (5).

$$D = 50 \text{ (mm)}, d_p = 3 \text{ (mm)}, \rho_s = 1240 \left(\frac{\text{kg}}{\text{m}^3} \right)$$

Vertical axis displays the pressure loss in a dimensionless form of meter of water per meter of pipe length. For a given slurry velocity, increasing the solid concentration will result in increased pressure loss. All curves

exhibit a unique shape where the slope of the curve changes suddenly at certain slurry velocities. This behaviour was also observed by other researchers such as Turian and Yuan (55). At constant solid concentration, pressure loss increases with slurry velocity which is expected. Because by increasing the velocity, shear forces at the interface with pipe and other layers will increase.

Pipe diameter and physical properties of the Doron and Barnea (5) experiment were used to run the code. Solid volumetric concentration was increased from 4% to 20% with 2% increment. For a given solid concentration, the slurry volumetric flow was varied starting from 0.1 (m/s) and increased with small increment until stratified flow couldn't be detected anymore. For each set of solid concentration and volumetric flowrate, system of non-linear equations was solved using the "Two-Guess" approach. Results are presented in Figures 4-16 to 4-19 for comparison with Doron and Barnea (5) work.

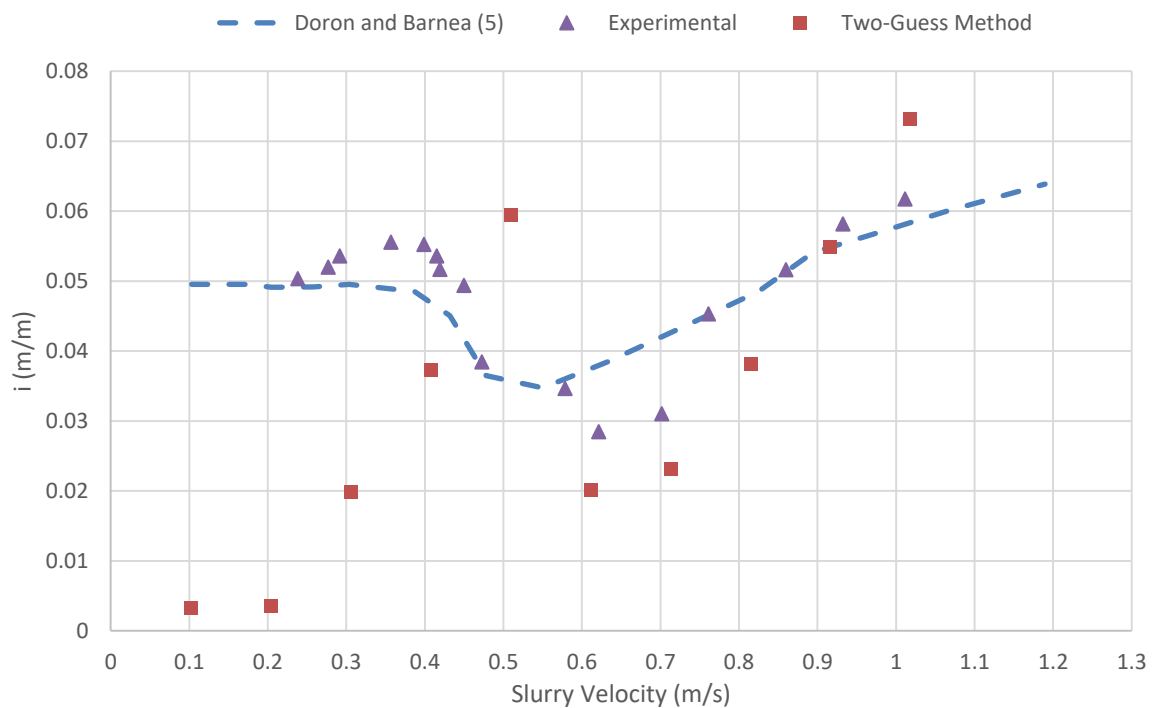


Figure 4-16: Pressure gradient vs slurry velocity for water-solid flow in horizontal pipe.

$$d_p = 3 \text{ (mm)}, D = 50 \text{ (mm)}, \rho_s = 1240 \left(\frac{\text{kg}}{\text{m}^3} \right), C_s = 8\%$$

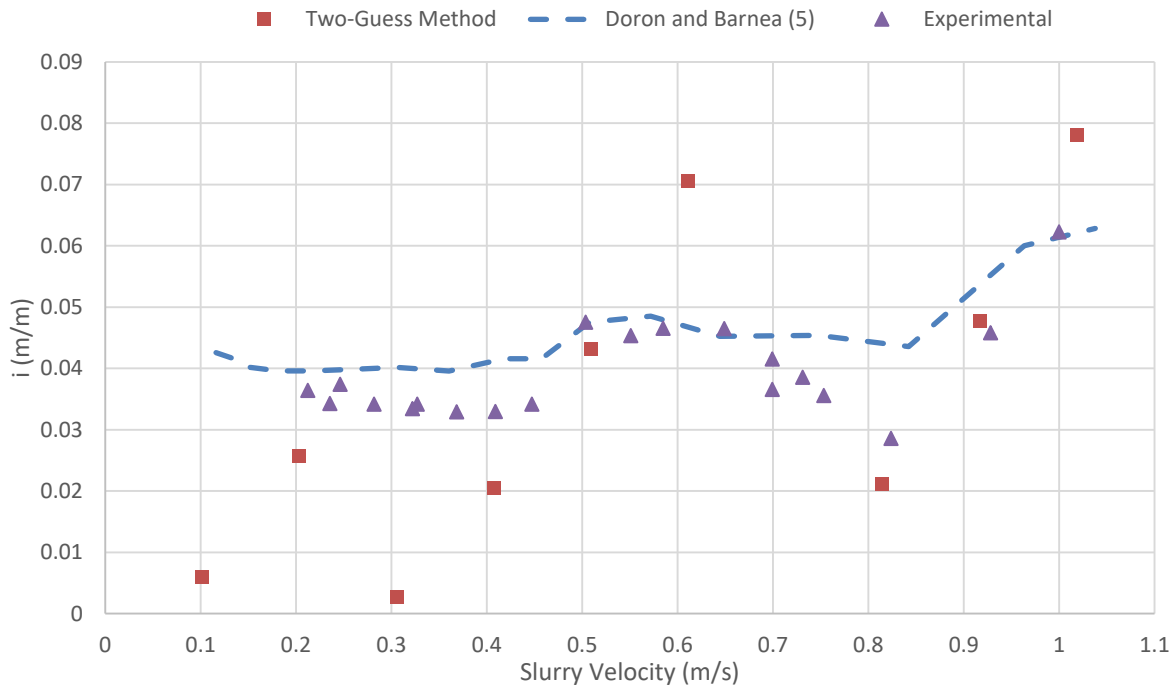


Figure 4-17: Pressure gradient vs slurry velocity for water-solid flow in horizontal pipe.

$$d_p = 3 \text{ (mm)}, D = 50 \text{ (mm)}, \rho_s = 1240 \left(\frac{\text{kg}}{\text{m}^3}\right), C_s = 10\%$$

Both Figures 4-16 and 4-17 exhibit the same characteristic that can be seen in Doron and Barnea (5) work. Pressure loss increases by slurry velocity but in and around certain velocities, there is a noticeable increase in gradient of pressure loss vs. slurry velocity. This trend can also be noticed in Doron and Barnea (5) experiments, shown in figure 4-15.

As explained by Doron and Barnea (5), at this break point where pressure gradient is at its minimum, stationary sand bed vanishes and flow regime is either with moving sand bed or fully suspended particles. Corresponding slurry velocity is called "Critical Velocity" as explained in chapter 2 of this research.

Even though calculated pressure gradient values for 8% and 10% solid concentration show satisfactory agreement with Doron and Barnea (5) work in Figure 4-15, results for 14% and 18% solid concentration are also plotted in Figures 4-18 and 4-19 below.

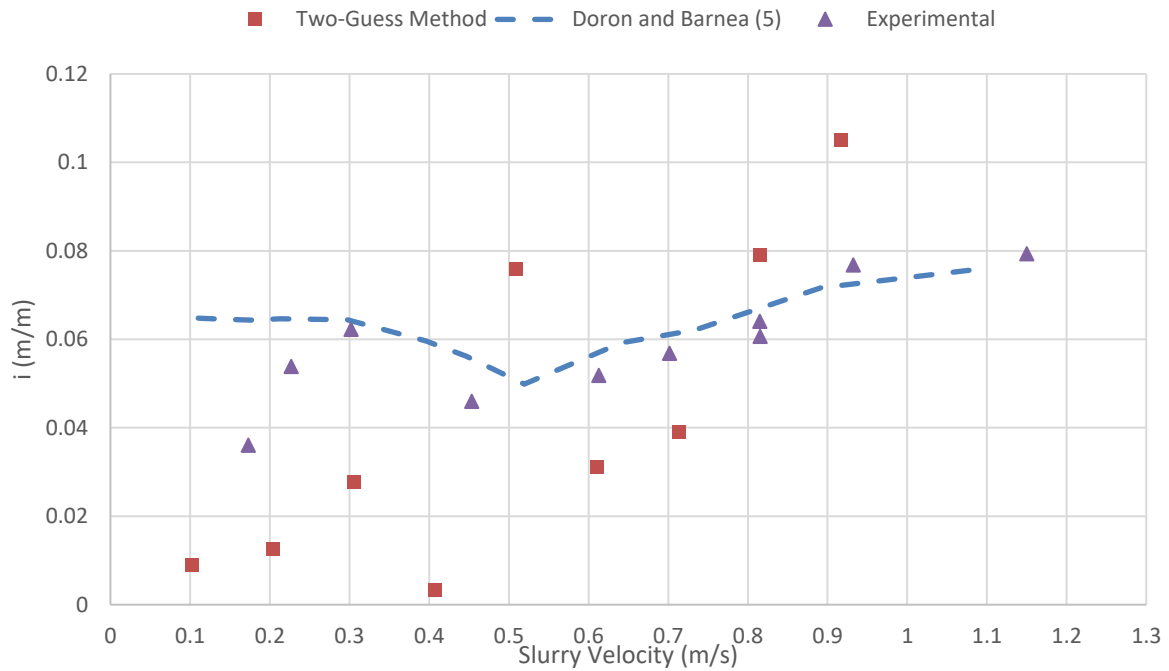


Figure 4-18: Pressure gradient vs slurry velocity for water-solid flow in horizontal pipe.

$$d_p = 3 \text{ (mm)}, D = 50 \text{ (mm)}, \rho_s = 1240 \left(\frac{\text{kg}}{\text{m}^3}\right), C_s = 14\%$$

By comparing pressure gradient values in Figures 4-18 and 4-19 with experimental results in Figure 4-15, it becomes evident that code is calculating higher pressure gradient at break point. The reason lies in the momentum equations where code should adjust momentum equations when switching between flow with and without stationary sand bed as explained in Section 4.2. As observed by Thomas (37), velocity in which sand bed starts to move and stationary bed starts to vanish is not a specific value but rather it happens in a range of velocities. Hence despite the logic detailed in the code, in reality, break point for i_{min} does not happen at a specific velocity. This could be one of the reasons that code results for i_{min} show some deviations from experiment for high solid concentrations. But despite not being able to accurately calculate pressure gradient at the break point for higher solid concentration cases, pressure gradient values in other slurry velocities are in good agreement with experimental results.

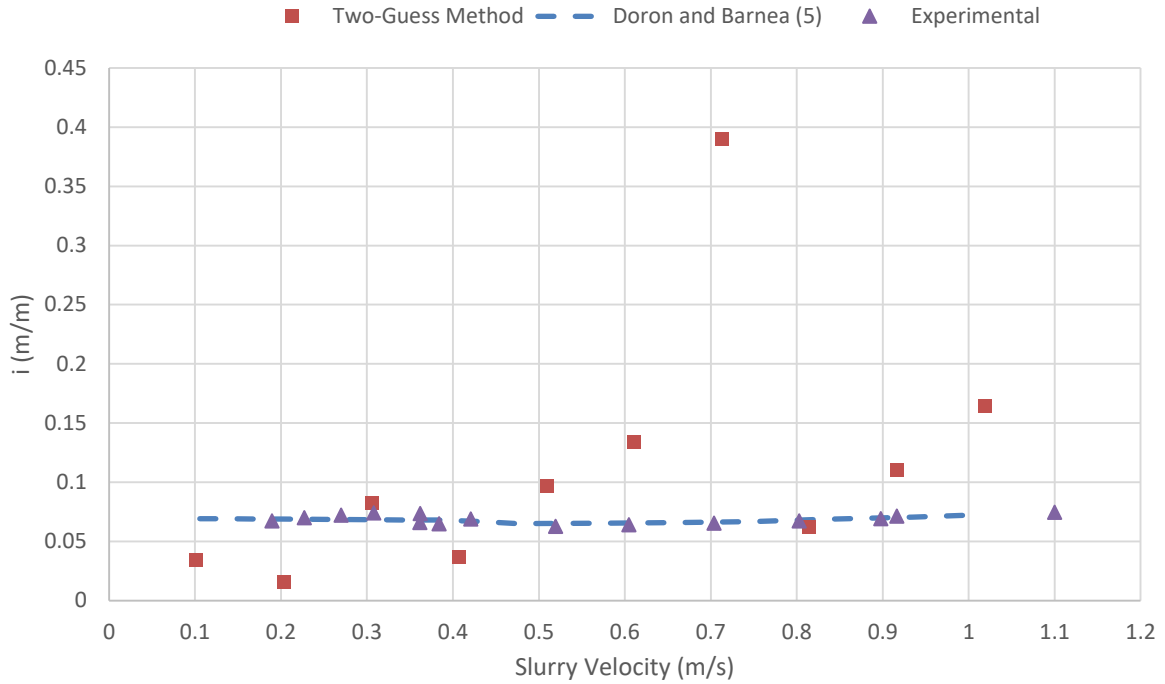


Figure 4-19: Pressure gradient vs slurry velocity for water-solid flow in horizontal pipe.
 $d_p = 3 \text{ (mm)}, D = 50 \text{ (mm)}, \rho_s = 1240 \left(\frac{\text{kg}}{\text{m}^3}\right), C_s = 18\%$

Figure 4-20 depicts the slurry velocities associated with the break points versus solid concentration, calculated by the code and experimental data gathered by Doron and Barnea (5). As explained before, velocity at break point where pressure gradient tends to be at its minimum is associated with the dissipation of stationary bed.

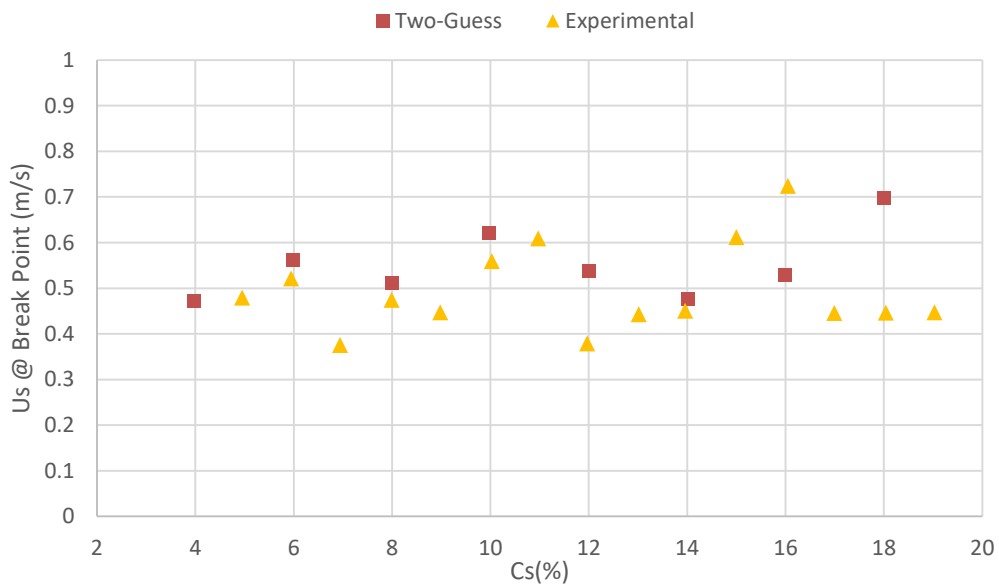


Figure 4-20: Effect of solid concentration on break point velocity for water-solid flow in horizontal pipe.
 $d_p = 3 \text{ (mm)}, D = 50 \text{ (mm)}, \rho_s = 1240 \left(\frac{\text{kg}}{\text{m}^3}\right)$

Some researchers considered this velocity threshold as Limit Deposit velocity and as long as slurry velocity is higher than this value, sand particles are moving. It can be seen in Figure 4-20 that break point velocity increases slightly with increase in sand concentration. It is worth noting that researchers have used different terminologies for deposit velocity. For example whilst Shook and Roco (91) used the term "Deposition Velocity" for the velocity at which particles settle to bottom of the pipe, Wood (92) used "Deposit Velocity" and Wilson (93) and Doron and Barnea (5) used the term "Limit Deposit Velocity" for the same velocity threshold. Even though Chapter 2 tries to clarify some of these terms and explains how those terms are being used in this research, nevertheless some discrepancies between terminologies used in this research and its references might be spotted.

4.5 Statistical Analysis of Model Performance

In order to study the accuracy of the developed code results versus three phase Taitel *et al.* (7) model and three layer Doron and Barnea (5) model, following statistical parameters are being used. Relative Error $\eta_{rel.}$ and Actual Error $\eta_{act.}$ are being calculated by Equations (4.8) and (4.9) respectively. X_i is measured or calculated value which is either holdup or pressure gradient and n is total number of test data.

$$\eta_{rel.} = \left(\frac{X_{calculated} - X_{experiment}}{X_{experiment}} \cdot 100 \right) \quad (4.8)$$

$$\eta_{act.} = X_{calculated} - X_{experiment} \quad (4.9)$$

Average relative error is:

$$\eta_1 = \frac{1}{n} \sum_{i=1}^n (\eta_{rel.})_i \quad (4.10)$$

Average actual error is:

$$\eta_2 = \frac{1}{n} \sum_{i=1}^n (\eta_{act.})_i \quad (4.11)$$

Absolute average relative error is:

$$\eta_3 = \frac{1}{n} \sum_{i=1}^n |(\eta_{rel.})_i| \quad (4.12)$$

Absolute average actual error is:

$$\eta_4 = \frac{1}{n} \sum_{i=1}^n |(\eta_{act.})_i| \quad (4.13)$$

Standard deviation from the average relative error is:

$$\eta_5 = \sqrt{\left(\sum_{i=1}^n (\eta_{rel.i} - \eta_1)^2 \right) / (n - 1)} \quad (4.14)$$

Standard deviation from the average actual error is:

$$\eta_6 = \sqrt{\left(\sum_{i=1}^n (\eta_{act.i} - \eta_2)^2 \right) / (n - 1)} \quad (4.15)$$

Section 4.3 of this report studied the code results for three phase liquid/liquid/gas flow against the Taitel *et al.* (7) model. Statistical parameters which are defined in Equations (4.10) to (4.15) for this comparison are calculated and shown in Table 4-1.

Table 4-1: Statistical parametrs- Two-Guess model vs. three phase Taitel et al. (7) model

Variable	η_1	η_2	η_3	η_4	η_5	η_6
$\frac{H_W}{D}$ as per Figure (4-4)	-15.85	-0.08	15.85	0.08	12.23	0.06
$\frac{H_L}{D}$ as per Figure (4-5)	-6.48	-0.05	6.48	0.05	6.14	0.05
$\frac{H_W}{D}$ as per Figure (4-9)	-0.87	0.0	8.10	0.02	12.09	0.04
$\frac{H_L}{D}$ as per Figure (4-10)	-16.89	-0.09	16.89	0.09	14.57	0.08

Average relative error of the Two-Guess model η_1 is negative in all the cases shown in Table 4-1. This indicates that hold up values which were calculated by Two-Guess model are generally less than values predicted by Taitel *et al.* (7) model. In fact, apart from water hold up in Figure (4-9) where code occasionally predicted higher values

than Taitel *et al.* (7) model, in all other figures in section 4-3, Two-Guess method resulted in less hold up. This is also reflected in Table (4-1) results, where average relative error η_1 and absolute average error η_3 have equal absolute values, with the exception of $\frac{H_W}{D}$ in Figure (4-9). Relatively low values of deviation parameters i.e. η_5 and η_6 , suggests that as low as 85% of the code results are less than Taitel *et al.* (7) model. As illustrated by Table 4-1, it can be concluded that accuracy of the Two-Guess model in comparison to Taitel *et al.* (7) model is in the region of $\pm 20\%$.

Table 4-2 shows the statistical performance of the Two-Guess method against experimental results used by Doron and Barnea (5) in their three layer sand-water model. Doron and Barnea (5) three layer model was studied in section 4.4 of this report with Figures (4-16) to (4-19) exhibits pressure gradient calculated by Two-Guess method vs. experimental data and Doron and Barnea (5) model. Table 4-2 only captures the statistical performance of the Two-Guess method against experimental data.

Whilst solid loading increases, the average error η_1 and total error η_2 parameters are increasing. At low solid loading i.e. $C_s = 8\%$, the average error of the model is 9% with almost 68% of the results are within 9% margin of the experimental data. But the average error of the model increases to 23% when solid loading increase to 18%. Calculated and experimental data for pressure gradient at $C_s = 18\%$ are shown in Figure (4-19). Even though most of the calculated values seem to be close to experimental data, at $U_s = 0.7 \left(\frac{m}{s}\right)$ code calculated a considerably higher pressure gradient compared to experimental data i.e. $i_{calculated} = 0.39$ vs $i_{experiment} = 0.065$.

Table 4-2: Statistical parameters- Two-Guess model vs. experimental data in Doron and Barnea (5) work

Variable	η_1	η_2	η_3	η_4	η_5	η_6
<i>i</i> as per Figure (4-16) $C_s = 8\%$	-9.09	-0.004	24.80	0.011	32.83	0.015
<i>i</i> as per Figure (4-17) $C_s = 10\%$	-11.70	-0.002	29.63	0.011	40.20	0.016
<i>i</i> as per Figure (4-18) $C_s = 14\%$	-17.83	-0.008	40.41	0.022	48.35	0.026
<i>i</i> as per Figure (4-19) $C_s = 18\%$	23.45	0.017	46.27	0.031	60.73	0.041

With solid loading of $C_s = 18\%$, pressure gradient reaches at break point at $U_s = 0.7 \left(\frac{m}{s}\right)$ and this has already been explained in Section 4.4. The reason that code calculated pressure gradient at break point is higher than experimental data lies behind the momentum equations where code

should adjust momentum equations when switching between flow with and without stationary sand bed as explained in Section 4.2. As illustrated by Table 4-2, it can be concluded that accuracy of the Two-Guess model in comparison to experimental data used in Doron and Barnea (5) three layer model, is between -10% and +24%.

Chapter 5

Results and Discussions

Following initial verification of the code using available experimental results for two and three phase flows, code is now being used to simulate the four-phase flow structure of sand/water/oil/gas which was the original intention of this research. Four-phase flow which is being studied here is based on experimental setup which was used by Dabirian *et al.* (13) for three phase sand/water/air. Obviously, the main difference is introducing the oil layer into fluid structure, which wasn't part of Dabirian *et al.* (13) experimental setup. The main reason for using Dabirian *et al.* (13) flow loop data is because they conducted their tests by achieving the stratified flow regime. As the current code formulation is only valid for stratified flow, by using their flow loop data in terms of slurry and gas flow rate and even after adding oil layer, it is likely that flow remains as stratified. Apart from Equation 4.6 which was proposed by Taitel *et al.* (7) for stability criteria of stratified three phase flow, no other formulation could be found to verify the stability of stratified four-phase flow. Moreover, it was reported by other researchers such as Açıkgöz *et al.* (90) that stratified regime seldom can be achieved in three phase flow. Hence it seems logical to use the Dabirian *et al.* (13) flow loop data, which is more likely to result in four-phase stratified flow. Moreover, they managed to observe different sand flow regimes by slightly changing the liquid and gas velocities, as shown in Table 5-1, while the overall stratified flow was maintained.

Table 5-1: Flow loop setup Dabirian et al (13)

Variable	Range	Units
<i>Pipe inner diam.</i>	0.097	<i>m</i>
<i>Particle specific gravity</i>	2.475	-
<i>Particle size</i>	45-90, 125-250, 425-600	μm
<i>Particle concentration</i>	250-10,000	<i>ppm</i>
<i>Superficial gas velocity</i>	4.5-15.5	$\frac{\text{m}}{\text{s}}$
<i>Superficial liquid velocity</i>	0.05, 0.1, 0.15	$\frac{\text{m}}{\text{s}}$

Superficial liquid velocity in Table 5-1 refers to a slurry mixture of sand and water velocity at the entry point test section (13). Physical properties of liquid and gas phases used in the code are listed in Table 5-2.

Table 5-2: Physical properties of liquid and gas phases

Physical Property	Value	Units
<i>Water viscosity</i>	0.89	<i>cP</i>

Water density	1000	kg/m^3
Oil viscosity	100*	cP
Oil specific gravity	0.8*	-
Air viscosity	0.01837	cP
Air specific gravity	$1.208 * 10^{-3}$	-

*: Taken from Taitel et al (7) work.

Oil phase should be added in such a way that stratified flow in Dabirian et al. (13) setup is likely to remain unchanged. Assuming slurry phase in Dabirian et al. (13) consists of 30% volumetric oil, Table 5-3 shows superficial velocities for liquid and gas phases, which will be used by the code.

Table 5-3: Modified superficial velocities

Variable	Range	Units
Superficial gas velocity	4.5-15.5	$\frac{\text{m}}{\text{s}}$
Superficial slurry velocity	0.035, 0.07, 0.084	$\frac{\text{m}}{\text{s}}$
Superficial oil velocity	0.015, 0.03, 0.036	$\frac{\text{m}}{\text{s}}$

30% volumetric oil flow rate is just an initial assumption in order to run the code. The main criterion is to ensure that the flow regime remains stratified. Otherwise, ratio between oil and water volumetric flow can be changed as long as it does not change the flow regime.

The highest gas and liquid superficial velocities in Table 5-3 are shown on Taitel et al. (7) flow regime map for three phase flow. Even though this operating point is very close to transition boundary between stratified and annular flow, it still falls within stratified flow region. Subsequently other points with lower gas and liquid superficial velocities will be well within the stratified flow boundary.

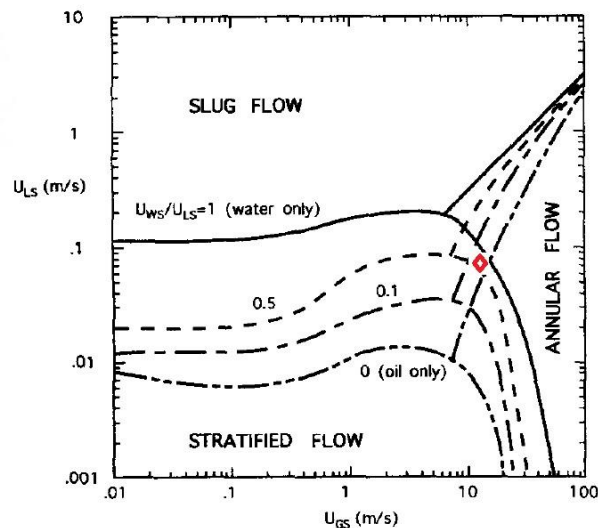


Figure 5-1: Operating point with highest gas and liquid superficial velocities (\diamond) is plotted on Taitel et al. (7) flow regime map for three phase flow

5.1 Effect of Particle Size on Flow Structure

The code formulation is being used to study the impact of sand particle size on flow structure for a set of given flow rates. For 1% volumetric concentration of sand in slurry flow, the Figures 5-2 and 5-3 below depict the effect of sand particle size increase on calculated height for each layer.

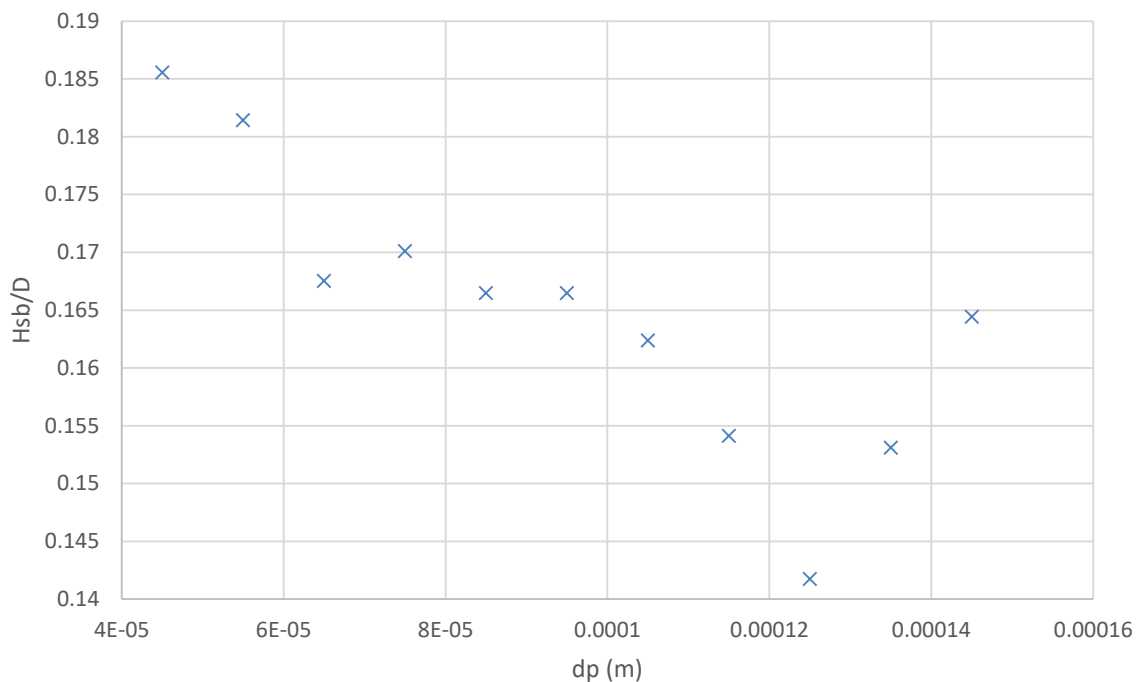


Figure 5-2: Effect of particle size on stationary sand bed height-
 $\rho_s = 2475 \left(\frac{kg}{m^3} \right), D = 0.097 (m), U_s = 0.035 (m/s)$

By comparing stationary sand bed height in figure 5-2 with moving sand bed in Figure 5-3, it appears that increasing moving bed height is in the expense of stationary bed height.

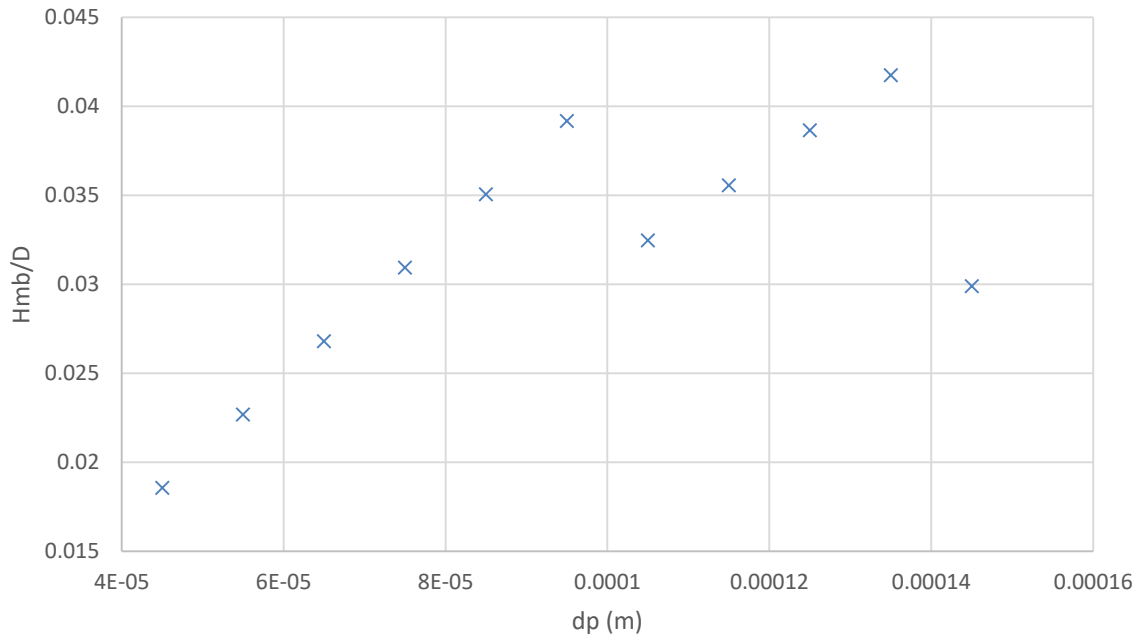


Figure 5-3: Effect of particle size on moving sand bed height-
 $\rho_s = 2475 \left(\frac{kg}{m^3} \right), D = 0.097 (m), U_s = 0.035 (m/s)$

Sudden reduction in moving bed height at higher d_p can be interpreted as the formation of sand dunes. Increased sand particle size will increase particle surface and consequently increase in torque applied on each particle by the effect of moving water layer. As long as local water layer velocity is greater than $U_{MB.minimum}$ which is detailed in Equation (4.7), particle is moving and subsequently moving bed height exists.

But at some point d_p is big enough where weight and drag forces are more significant than torque generated by the water layer. At this point, moving sand particles start to become stagnant which results in an increase in the height of stationary sand bed. In this situation, stationary and moving layers co-occur where their respective heights are in balance which means an increase in one results in a decrease in the other one.

Change in the height of other moving layers as a result of an increase in particle size is depicted in Figure 5-4.

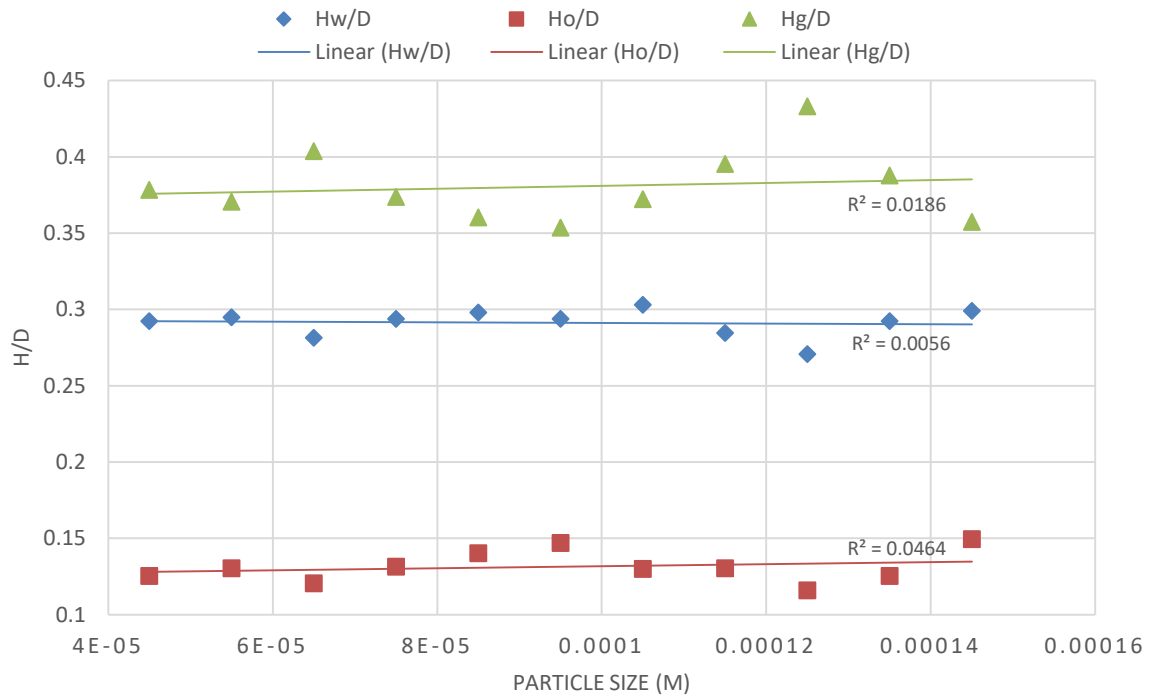


Figure 5-4: Effect of particle size on water, oil and gas layers-

$$\rho_s = 2475 \left(\frac{kg}{m^3} \right), D = 0.097 \text{ (m)}, U_s = 0.035 \text{ (m/s)}, U_g = 15.5 \text{ (m/s)}$$

The effect of change in the height of any of the layers shall be seen in other layers because the total summation of all heights shall equate to internal diameter. Figure 5-4 suggests that water, oil and gas layer heights remain almost constant whilst sand particle is gradually increasing up to 145 (μm). It is worth noticing that solid concentration is constant throughout this study.

Because oil layer is adjacent to the fast moving gas layer, its local velocity will be higher than water layer and consequently has lower holdup compared to water layer. This behaviour was observed in section 4.2 where code was validated against Taitel *et al.* (7) experimental results for three phase water/oil/air flow.

By reviewing Figures 5-2 and 5-3, it can also be concluded that sand particles are not dispersed in water layer. Code detected height for both stationary and moving sand bed layers, which is an indication of a high concentration of sand particles at the bottom of the pipe. This conclusion is in line with Dabirian *et al.* (13) experimental results where fully suspended regime was not observed.

To further study the effect of particle size on fluid structure, slurry and oil flow rates were increased as per Table 5-3 whilst gas flow rate remained unchanged. Figures 5-5 to 5-10 illustrate the effect of particle size on each phase at different flow rates.

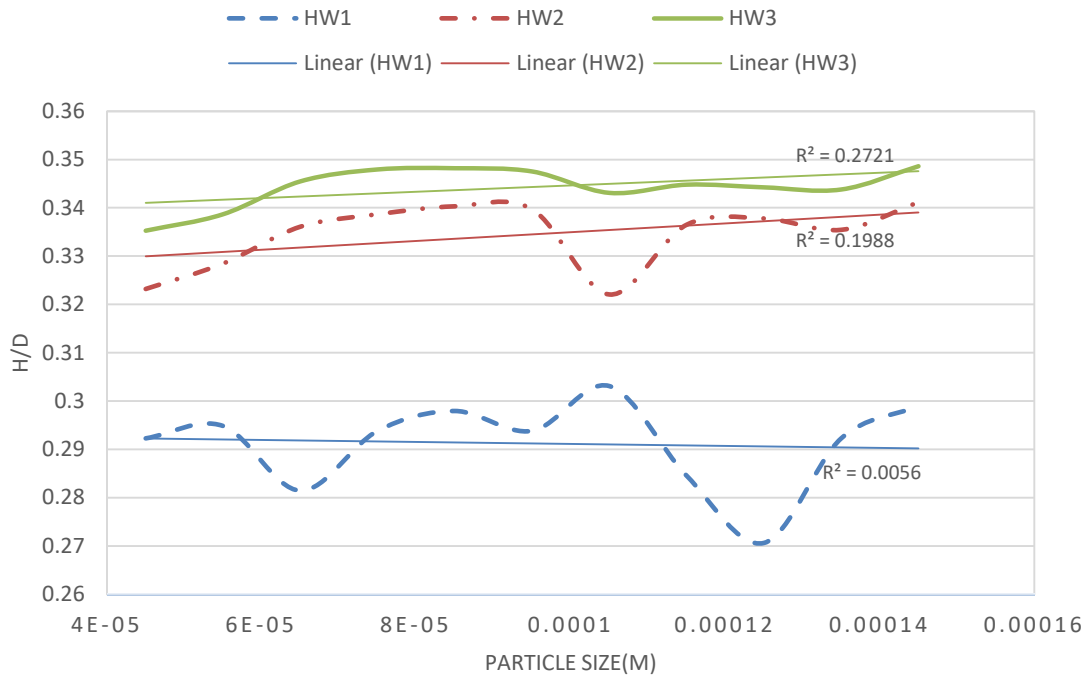


Figure 5-5: Effect of particle size and flow rate on height of water layer-
 $\rho_s = 2475 \left(\frac{kg}{m^3} \right), D = 0.097 \text{ (m)}, U_{HW1} = 0.035 \text{ (m/s)},$
 $U_{HW2} = 0.07 \text{ (m/s)}, U_{HW3} = 0.084 \text{ (m/s)},$

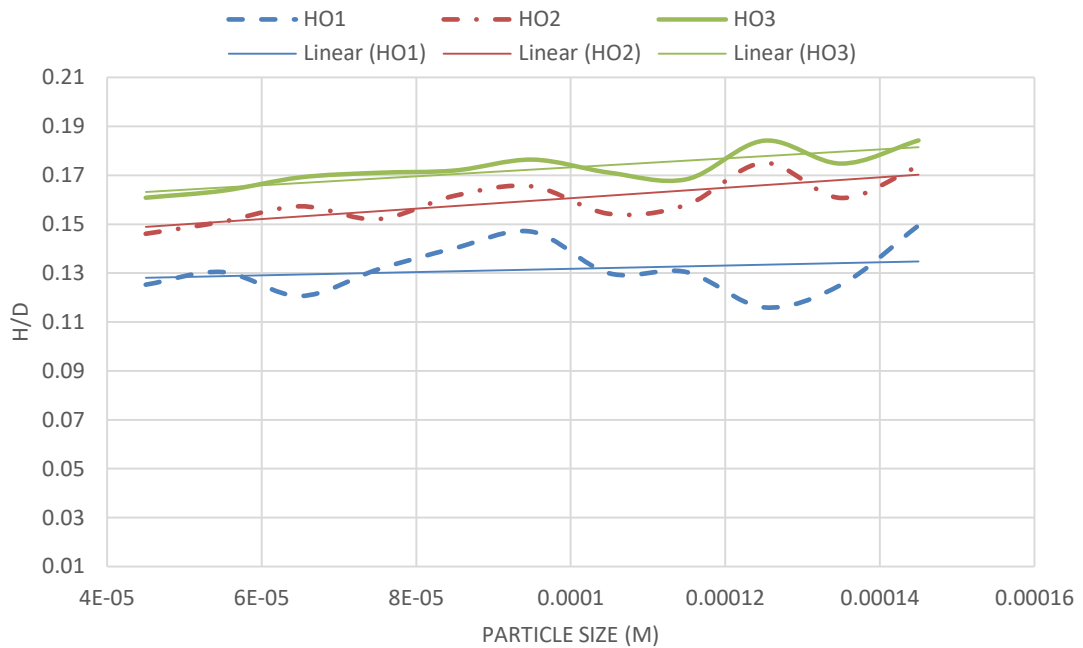


Figure 5-6: Effect of particle size and flow rate on height of oil layer-
 $\rho_s = 2475 \left(\frac{kg}{m^3} \right), D = 0.097 \text{ (m)}, U_{HO1} = 0.015 \text{ (m/s)},$
 $U_{HO2} = 0.03 \text{ (m/s)}, U_{HO3} = 0.036 \text{ (m/s)},$

Increase in flow rate has a more evident impact on height of the water layer than an increase in particle size. For lower slurry velocity, the average height of the water layer HW_1 seems to be almost constant when particle size increases. For HW_2 and HW_3 , and by increasing particle size, curves show a noticeable upward slope. Increasing the oil flow rate by increasing its superficial velocity from 0.015 (m/s) to 0.036 (m/s) result in an increase in oil holdup and consequently increase in the oil layer height. Even though curves are showing some fluctuations, the overall trend is that by increasing sand particle size, height of the oil layer also slightly increases. The reason for this behaviour can be because of the reduction in local velocities as a result of increased friction force. Increased sand particle will essentially result in a rougher contact surface between sand layer and water. This will cause the water layer to move with lower velocity and consequently resulted in the neighbouring oil layer to move slower. By reduction in local velocities, holdup for both oil and water layers increase which this can be seen in Figures 5-5 and 5-6.

One way to reverse the effect of sand particle size on local velocities is to increase the flow rate of fast moving gas phase. Increase in gas flow rate will indirectly increase the water velocity and result in a reduction in water and oil layer heights, whilst sand particle size increases. But the results shown in Figures 5-5 to 5-10 are all calculated at a constant gas flow of $Q_G = 0.1145 \text{ (m}^3/\text{s)}$. Hence the effect of particle size increase is evident in the figures.

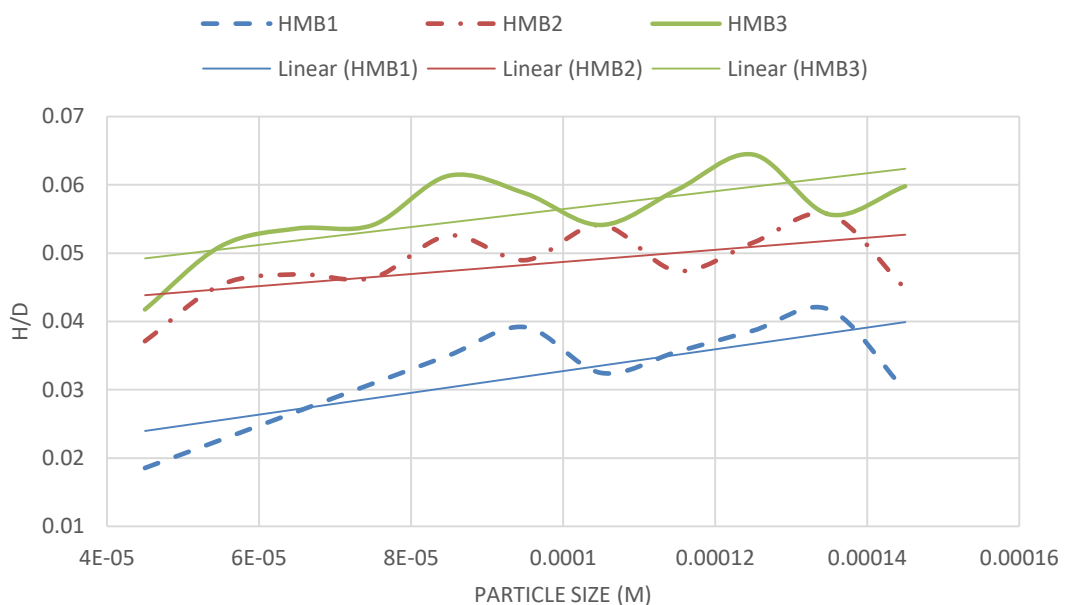


Figure 5-7: Effect of particle size and flow rate on height of moving bed layer-

$$\rho_s = 2475 \left(\frac{\text{kg}}{\text{m}^3} \right), D = 0.097 \text{ (m)}, U_{HW1} = 0.035 \text{ (m/s)},$$

$$U_{HW2} = 0.07 \text{ (m/s)}, U_{HW3} = 0.084 \text{ (m/s)},$$

Figure 5-7 exhibits an interesting behaviour for moving sand bed height when particle size and water flow rates are changing. At lower slurry flow rate HW_1 , moving sand bed height seems to have a linear relationship with particle size up to around 90 (μm). Then moving bed height reduces and built up again with particle size up to about 130 (μm) when it reduces again.

One hypothesis to explain this behaviour can be the formation of sand dunes which is direct result of increase in $U_{MB.minimum}$ value due to increase in particle size. At a given slurry flow rate, increase in particle size will increase the $U_{MB.minimum}$ value which is detailed in Equation 4.7. If slurry velocity is not big enough to justify formation of fully dispersed flow, then balance between moving and stationary sand layer heights will vary with the delta $\Delta = U_S - U_{MB.minimum}$.

Despite some fluctuations in H_{MB} value, increase in particle size shows that the height of moving bed increases to the point where slurry velocity is not big enough to keep all the parts in motion and H_{MB} starts to decline. This increasing trend in moving bed height is paired with a decline in height of stationary bed as depicted in Figure 5-8. When moving bed height starts to decline, stationary bed height starts to increase.

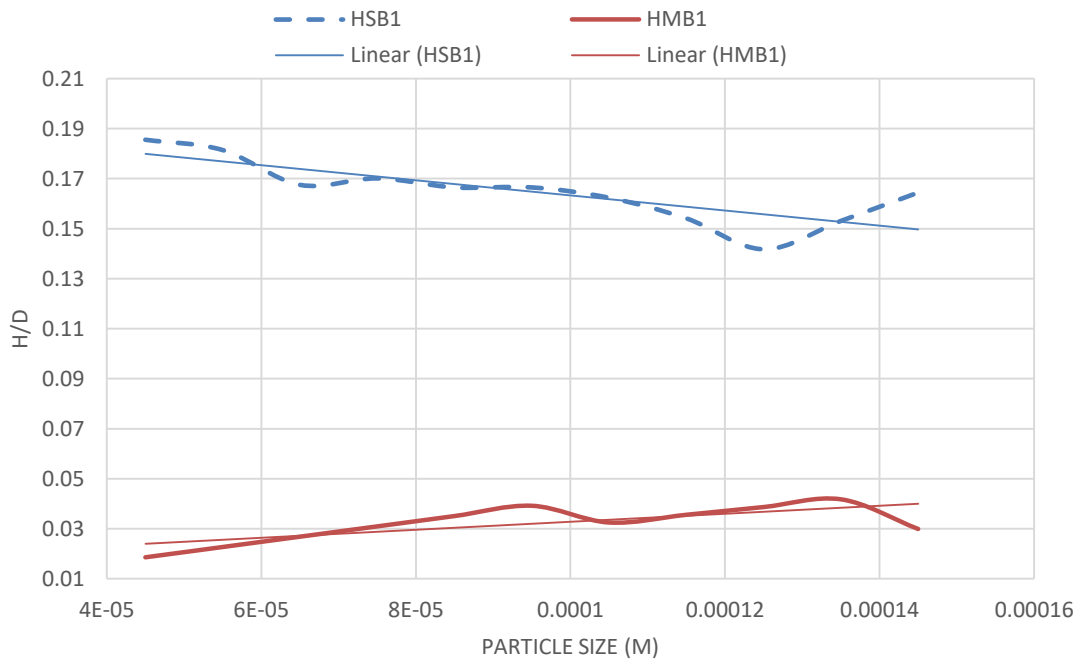


Figure 5-8: Effect of particle size on height of stationary and moving bed layers-
 $\rho_s = 2475 \left(\frac{\text{kg}}{\text{m}^3} \right), D = 0.097 \text{ (m)}, U_{HW1} = 0.035 \text{ (m/s)}$

The effect of particle size on average total sand bed height seems to be negligible when slurry flow rate and sand volume concentration remain unchanged. Figure 5-9 which shows sand bed height variation with particle size, illustrates that average total bed height is almost constant. Two main contributing factors i.e. water velocity U_w and sand concentration C_s are constant whilst particle size increases. Doron and Barnea (5) and Danielson (3) demonstrated that an increase in superficial water velocity will result in a reduction of sand holdup. But for a given slurry flow rate and concentration, an increase in particle size seems to have little effect on sand bed height. At first glance at Figure 5-9, it seems that total sand bed height is varying drastically by the increase in particle size. But to put this into perspective, it has to be noted that variation in total bed height is around $14 \times 10^{-4} (m)$ which considering average particle size of $95 (\mu m)$, variation in calculated total bed height equates to 14.7 particles in total. Hence it would be sensible to suggest that total bed height remains almost constant when particle size increases from $40 (\mu m)$ to $150 (\mu m)$. One explanation could be that when particle size is varying between $40 (\mu m)$ and $150 (\mu m)$ whilst slurry flow rate is constant, increase in moving bed height which is illustrated Figure 5-8, is balanced out by reduction in the stationary bed height. Hence total sand bed height which is summation of the stationary and moving bed heights remains constant. Similar observation has been reported by other researchers such as Danielson (3) and Doron and Barnea (5).

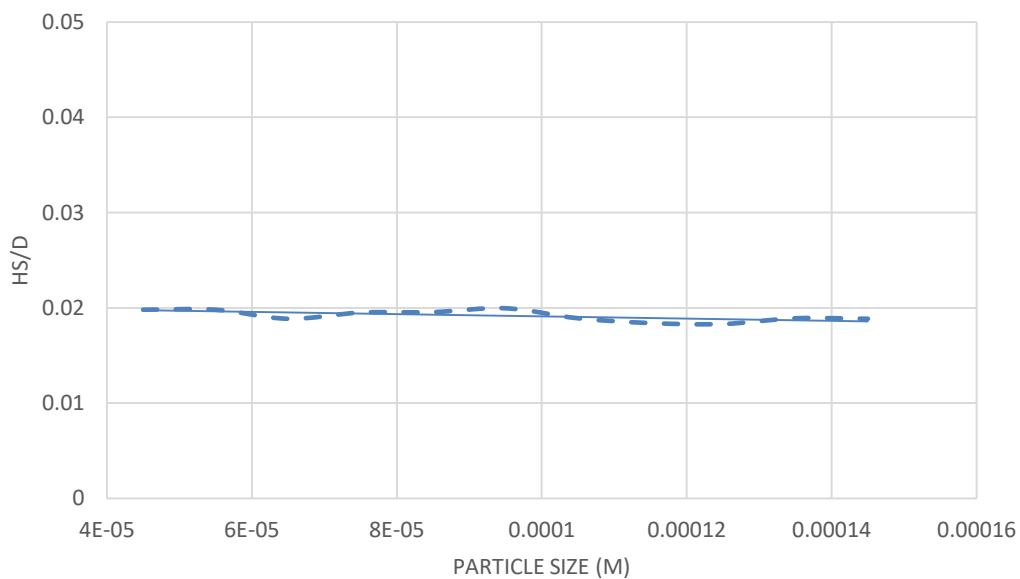


Figure 5-9: Effect of particle size on total sand layer height -
 $\rho_s = 2475 \left(\frac{kg}{m^3} \right), D = 0.097 (m), U_{HW1} = 0.035 (m/s)$

Figure 5-10 shows the effect of particle size on stationary bed height at different slurry flow rates.

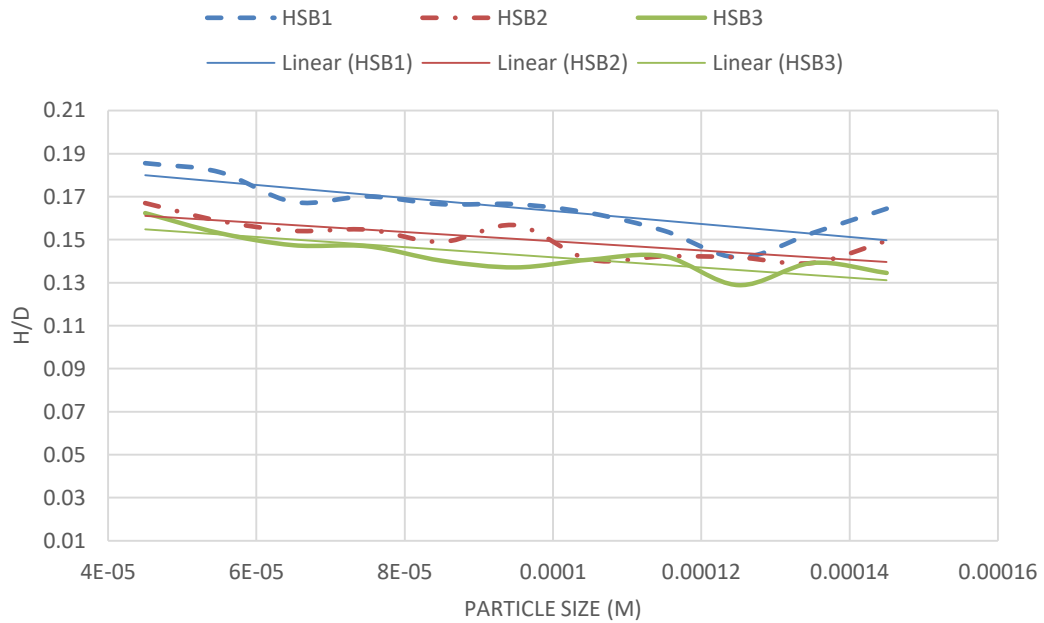


Figure 5-10: Effect of particle size and flow rate on height of stationary bed layer -

$$\rho_s = 2475 \left(\frac{kg}{m^3} \right), D = 0.097 \text{ (m)}, U_{HW1} = 0.035 \text{ (m/s)},$$

$$U_{HW2} = 0.07 \text{ (m/s)}, U_{HW3} = 0.084 \text{ (m/s)},$$

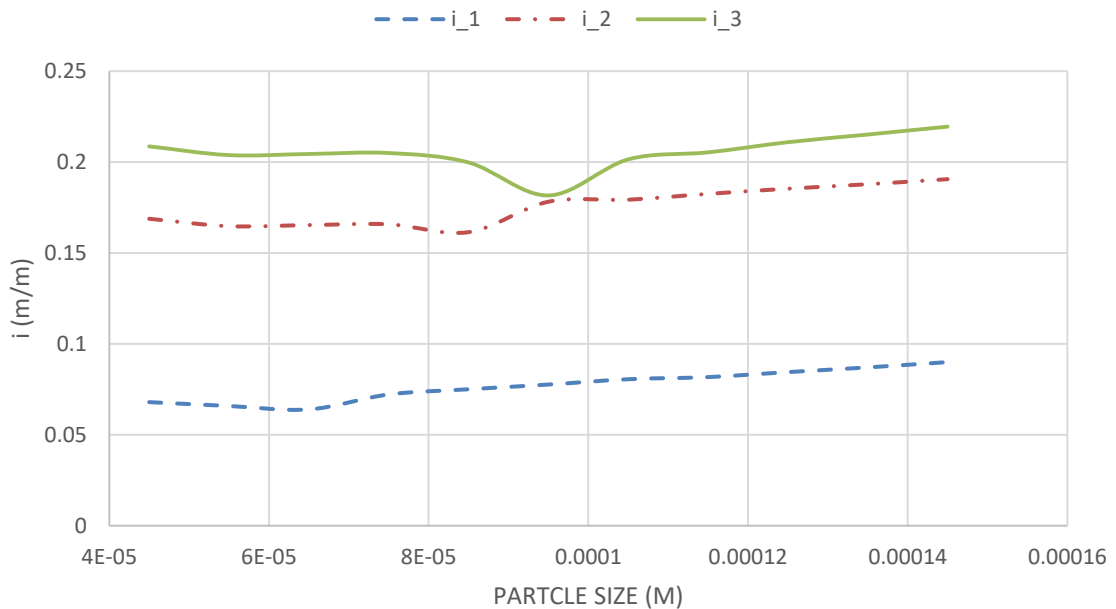


Figure 5-11: Effect of particle size and flow rate on pressure loss -

$$\rho_s = 2475 \left(\frac{kg}{m^3} \right), D = 0.097 \text{ (m)}, U_{HW1} = 0.035 \text{ (m/s)},$$

$$U_{HW2} = 0.07 \text{ (m/s)}, U_{HW3} = 0.084 \text{ (m/s)},$$

For a given particle size, increase in velocity results in reduction of stationary bed height, which is an expected outcome. In all these cases, code didn't detect fully suspended flow. Moving bed and stationary bed are identified by the code in all particle sizes and slurry velocities. This seems to be in line with the findings of Dabirian *et al.* (13,94).

Figure 5-11 illustrates the effect of particle size on pressure gradient in different slurry flow rates. All three graphs exhibit a similar trend. In a given flow rate, pressure gradient increase with increase in particle size. Increase in particle size will create rougher interface surface between water and moving or stationary sand bed layers and subsequently result in higher pressure loss in the moving layers.

5.2 Effect of Solid Concentration on Flow Structure

To study the effect of solid concentration on flow structure, for a given set of slurry, oil and gas flow rates, volumetric concentration of solid in slurry flow is increased gradually. Flow parameters are shown in Table 5-4. Solid volumetric concentration is changing from 1% to 30% in 1% increments. Particle size is constant throughout this simulation.

Table 5-4: Effect of solid concentration on flow structure- flow parameters

Variable	Value	Units
<i>Superficial gas velocity</i>	<i>15.5</i>	$\frac{m}{s}$
<i>Superficial slurry velocity</i>	<i>0.084</i>	$\frac{m}{s}$
<i>Superficial oil velocity</i>	<i>0.036</i>	$\frac{m}{s}$
<i>Solid volumetric concentration</i>	<i>1-30</i>	%
<i>Particle size</i>	<i>100</i>	μm

With reference to Equation (3.22), an increase in solid concentration will result in a reduction in water flow rate when the total slurry flow rate is constant. Therefore water flow rate is gradually decreasing in these runs.

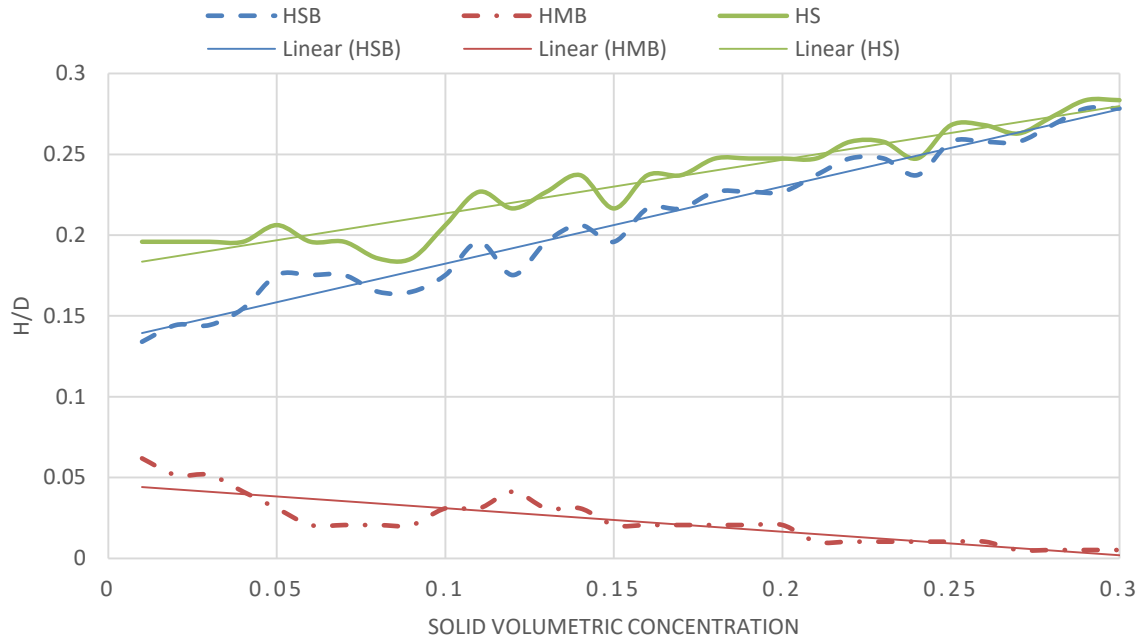


Figure 5-12: Effect of solid concentration on sand layer height -

$$\rho_s = 2475 \left(\frac{\text{kg}}{\text{m}^3} \right), D = 0.097 \text{ (m)}, U_w = 0.084 \left(\frac{\text{m}}{\text{s}} \right), d_p = 100 \text{ (\mu m)}$$

Figure 5-12 depicts that an increase in concentration, as it would be expected, results in the sand build-up. Reduction in water flow rate, causes the local velocity reduction which in turn results in a reduction in moving bed height. Moving bed height approaches zero and total sand bed height equates to stationary sand bed height in higher concentration.

As explained by Doron and Barnea (5) and was also shown in Section 4.4, critical sand velocity or $U_{MB.minimum}$ in Equation (4.7), does not change significantly with concentration. Therefore, increase in solid concentration does not change the sand moving mechanism as such because on one hand water flow rate is continually decreasing and on the other hand, sand particle size which has a greater effect on $U_{MB.minimum}$, mainly remains unchanged. It is also observed that at solid concentration below 4%, total sand height seems to be constant. Similar behaviour was observed in Figure 5-9 where volumetric solid concentration is 1%. It seems that at certain ranges of solid concentration, moving and stationary sand beds are in balance as long as other parameters which are influencing $U_{MB.minimum}$ are constant such as particle size and density of carrier liquid. In these ranges, sand particles switch between moving and stationary layers with negligible change in total sand height. But when solid loading increases beyond a certain threshold, the solid build-up will occur which will result in overall sand height increase.

Downward trend of H_{MB} in Figure 5-12 suggests that the whole sand layer will become stagnate if volumetric concentration increases beyond 30%.

Even though this is a plausible assumption, it has to be noted that the increase in sand layer height results in reduction of height of the other layers. Reduction in height of oil and gas layer, while flow rates remain constant will result in a reduction of flowing area which consequently causes local gas and oil velocities to increase. Increase in local velocities of gas and oil layers pushes the stratified flow regime towards either annular or intermittent flow as per flow regime map in Figure 5-1. Even if flow regime does not change and remains stratified, which is unlikely, an increase in oil layer velocity will result in an increase of water layer velocity. And as water layer velocity becomes greater than $U_{MB.minimum}$, which remains almost constant throughout this built-up, moving bed layer will form.

Hence as long as oil and gas flow rates remain constant, it seems unlikely that sand build up will cause complete blockage when volumetric concentration increases. Or in other words, it is unlikely that the moving sand bed layer vanishes completely throughout the build-up. It goes without saying that change in flow regime, will completely change the sand transport mechanism, as investigated by several researchers including Vocaldo and Charles (68), Parzonka *et al.* (69), Leporini *et al.* (95) and many more. Studying the flow structure when the flow regime is not stratified, is not the focus of this research. The effect of solid concentration on the pressure gradient is shown in Figure 5-13. Pressure loss in the entire flow area increases, whilst volumetric concentration increases. The general trend is in line with what has been observed in two and three phase flows by other researchers including Doron and Barnea (71).

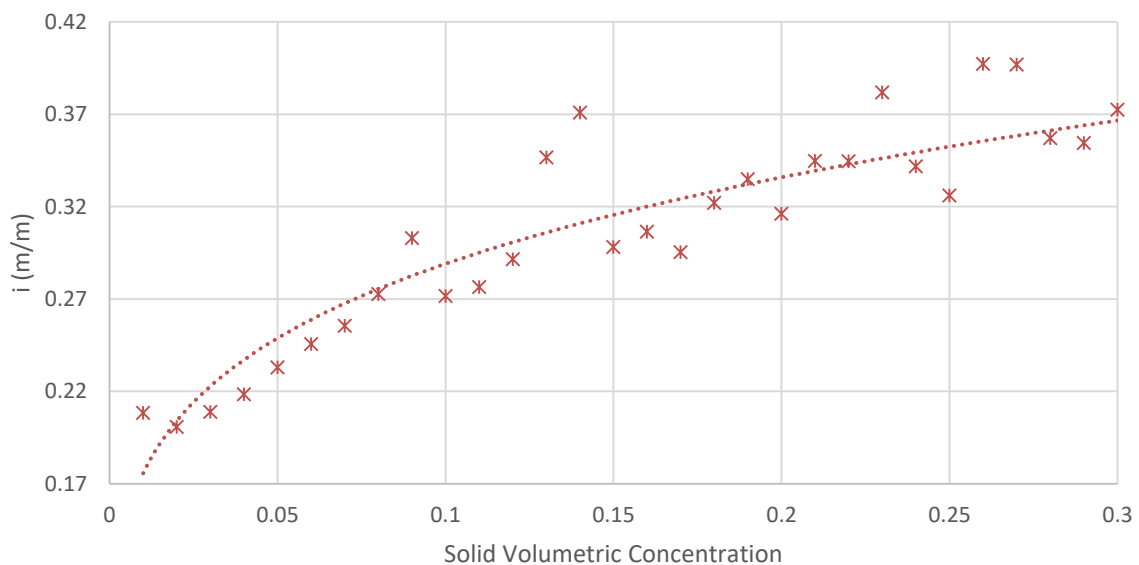


Figure 5-13: Effect of solid concentration on pressure loss -

$$\rho_s = 2475 \left(\frac{kg}{m^3} \right), D = 0.097 \text{ (m)}, U_w = 0.084 \text{ (m/s)}, d_p = 100 \text{ (\mu m)}$$

By studying the trend of pressure loss increase in Figure 5-13, it is observed that the gradient of the curve increases noticeably when concentration goes beyond 4%. It also appears to be a linear relationship between volumetric concentration and pressure loss up to 9% solid concentration.

When volumetric concentration value passes 10% mark, even though pressure loss is still increasing whilst concentration increases, some fluctuations are observed in the values calculated for pressure loss. This can be down to the accuracy of the solution algorithm. Ultimately, the solution method which is used in the code is not a direct numerical method. It is worth highlighting that the solution method used in this code is an iterative method that finds a valid physical answer by minimising the differences between pressure losses for each phase or layer.

Another point that is worth noting is that a significant reduction in water flow rate which is side effect of increasing solid volumetric concentration in slurry flow, can invalidate the formulations in the code.

As highlighted in Chapter 3, sand particles which are subject of this research are water wet particles. This means that only water layer is capable of carrying solid particles in the flow. This has been reflected in formulations where there is no coupling term between mass continuity equations of sand and oil. By significantly reducing the water flow rate, momentum continuity equations cannot converge to equal or near equal pressure loss because mass continuity equations will result in unrealistic velocities for each phase. The assumption to model water wet sand particle can be seen as one of the code limitations, even though it is based on experimental observations by Yang *et al.* (31). This can also be one of the reasons that pressure gradient values show some fluctuations when volumetric particle concentration increases beyond 10%. But what is evident from Figure 5-13 is that the pressure gradient is increasing while volumetric concentration increases.

It is of little value to plot water layer height in this case. The reason is that water flow rate is continuously reducing while particle concentration C_s is increasing. Hence two parameters i.e. C_s and water flow rate, are varying at the same time. This is not the case for oil and gas layers as their flow rates remain unchanged throughout the simulation.

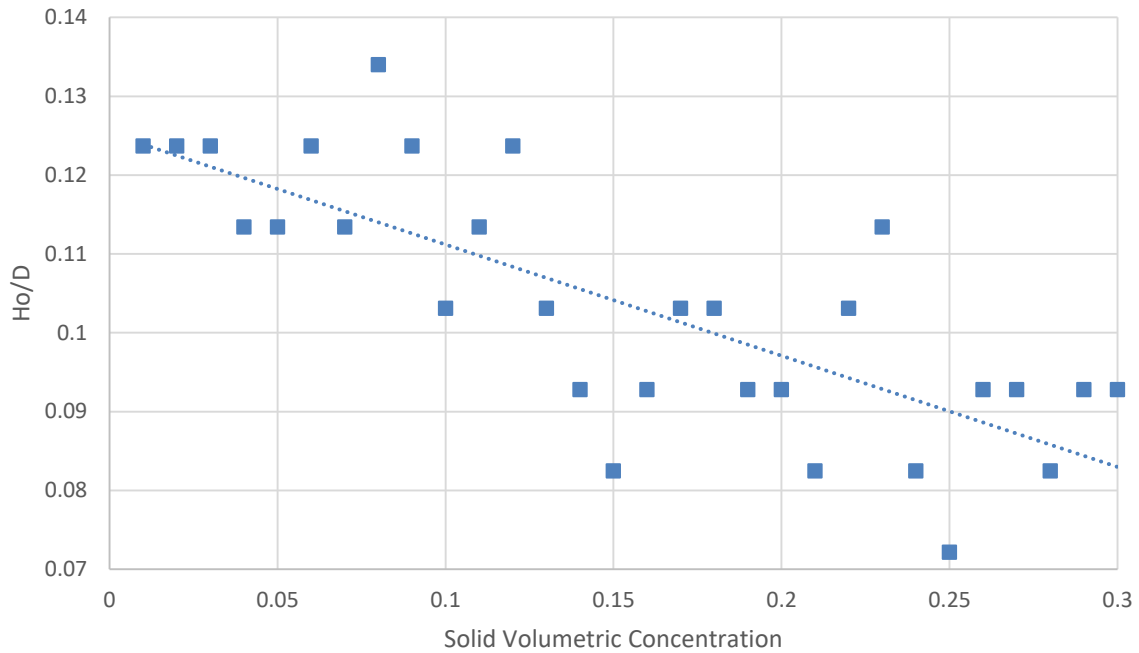


Figure 5-14: Effect of solid concentration on oil layer height -

$$\rho_s = 2475 \left(\frac{kg}{m^3} \right), D = 0.097 \text{ (m)}, U_o = 0.036 \text{ (m/s)}, d_p = 100 \text{ (\mu m)}$$

Variation in oil layer height while C_s increases is illustrated in Figure 5-14 which shows a downward trend. It was already explained that increase in concentration whilst slurry flow rate remains constant result in increasing sand bed height (Figure 5-12). Because the pipe cross section is occupied by sand particles which are also mainly stagnated, this will squeeze the other flowing phases which in turn will increase the local velocity of other phases. An increase in oil velocity will result in less holdup which is shown in Figure 5-14 as reduction in oil height. To put this into perspective, an increase in solid concentration by 30 times will result in 25% reduction in the oil layer height. It is worth noting that 30% solid concentration is exceptionally high solid loading in oil and gas industries.

The developed code formulation explained in Section 3.3 details the oil mass continuity equations which takes into account the oil flowing layer and oil particles in the gas phase. Even though the developed code is capable of calculating oil particles traveling in gas phase, when overall flow regime is stratified, oil particle mass in gas layer will be negligible. Therefore the whole mass of oil is flowing in the oil layer.

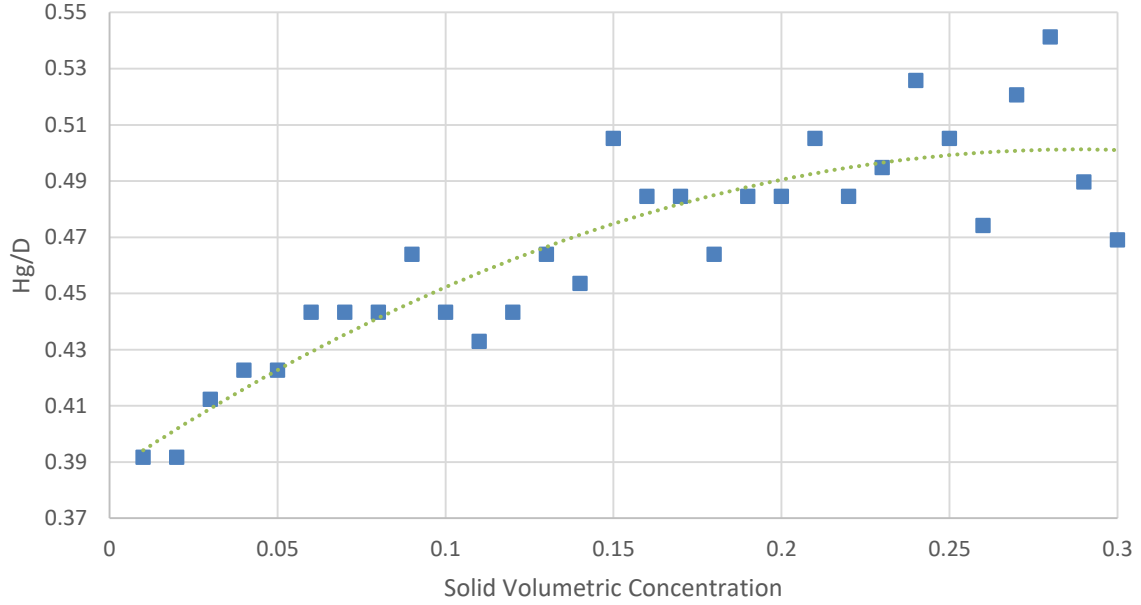


Figure 5-15: Effect of solid concentration on gas layer height -

$$\rho_s = 2475 \left(\frac{\text{kg}}{\text{m}^3} \right), D = 0.097 \text{ (m)}, U_G = 15.5 \text{ (m/s)}, d_p = 100 \text{ (\mu m)}$$

Gas layer holdup is depicted in Figure 5-15. Increase in volumetric concentration causes an increase in the gas layer height. This seems to be counter-intuitive assuming that sand layer height is continuously increasing which means other layers should be squeezed into smaller cross section of pipe. It has already been explained that an increase in solid concentration C_s whilst slurry flow rate is constant results in a reduction of water flow rate and consequently water layer height. It is also observed in Figure 5-14 that oil layer height decreases with increase in C_s which in fact is the result of increase in local velocity due to reduction in flowing area. Gas layer height is calculated by the code, using equation below:

$$H_G = D - (H_{SB} + H_{MB} + H_W + H_O) \quad (5.1)$$

Hence reduction in H_W and H_O result in increase of H_G even when total sand height is gradually increasing.

In this simulation, the concentration of fully suspended solids in water layer $C_{s,W}$ calculated is negligible. This was an expected result because flow rate combination which is used by Dabirian *et al.* (13) in their experiments, resulted in a fully stratified flow with fully segregated sand and water layers. To observe fully suspended solid phase, either particle size should be decreased while slurry flow rate remains constant or slurry flow rate should increase. The increasing slurry flow rate is studied in Section 5.4. However, increasing slurry flow rate can also push the

stratified flow regime towards either intermittent or annular flow regimes none of which is covered by the current formulations.

5.3 Effect of Solid Density

The developed code was used to run a series of simulation in order to study the effect of solid density on flow structure. Similar to previous simulation cases and to ensure the existence of the stratified regime, gas and slurry flow rates were selected from one of the test sets from Dabirian *et al.* (13) work. For a given volumetric concentration, solid density is increased gradually from 1800 ($\frac{kg}{m^3}$) to 2500 ($\frac{kg}{m^3}$) in 100 ($\frac{kg}{m^3}$) increments. Particle size and flow rates are kept constant whilst simulation is performed in four sets of solid concentration and water flow rate. Flow parameters for this simulation are listed in Table 5-5.

Table 5-5: Effect of solid density on flow structure- flow parameters

Variable	Value	Units
<i>Superficial gas velocity</i>	15.5	$\frac{m}{s}$
<i>Superficial slurry velocity</i>	0.084	$\frac{m}{s}$
<i>Superficial oil velocity</i>	0.036	$\frac{m}{s}$
<i>Solid density</i>	1800-2500	$\frac{kg}{m^3}$
<i>Solid volumetric concentration</i>	1,5,10,15	%
<i>Particle size</i>	100	μm

Figure 5-16 depicts variation in stationary bed with change in density at different concentrations. For densities less than 2100 ($\frac{kg}{m^3}$) code didn't detect any stationary bed. At densities of 2100 ($\frac{kg}{m^3}$) and above stationary bed is detected.

Once the stationary bed is formed, it seems that increase in density does not have any impact on the height. Stationary height appears to be constant at a given concentration, whilst particle density increases up to 2500 ($\frac{kg}{m^3}$). Increase in concentration results in stationary bed height increase. This behaviour has already been discussed in detail in Section 5-2. Stationary bed height for $C_s = 15\%$ is shown to be slightly less than bed height at $C_s = 10\%$. This slight difference is well within the accuracy margin of the code i.e. -10% to +24% which is detailed in section 4.5. Reference can also be made to Figure 5-12 which exhibits some fluctuations in H_{SB}/D whilst C_s is increasing.

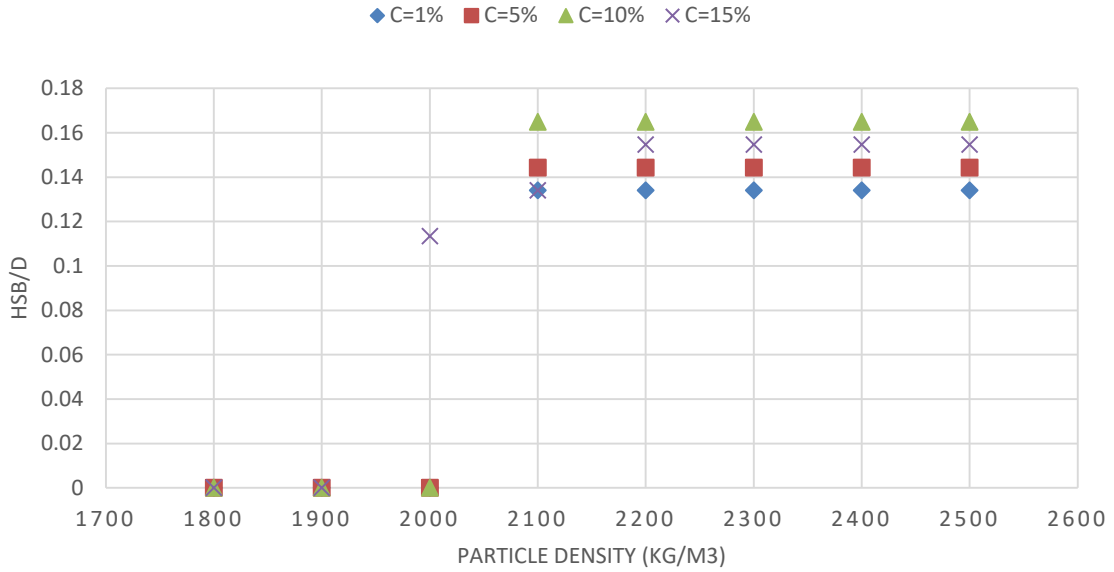


Figure 5-16: Effect of solid density on stationary bed height -
 $D = 0.097 \text{ (m)}, U_o = 0.036 \text{ (m/s)}, U_G = 15.5 \text{ (m/s)}, d_p = 100 \text{ (}\mu\text{m)}$

It is also worth mentioning that at $\rho_s < 2000 \text{ (kg/m}^3\text{)}$ code didn't detect stationary bed. As it was explained in Chapter 3, detection of stationary bed is entirely driven by Equation (3.45). When summation of the terms on left hand side of the Equation (3.45) results in higher numerical value than dry friction force F_{SB} , it means that shear forces which are applied to sand particles due to movement of moving bed layer and water medium are higher than dry friction force. Thus particles are moving. In these circumstances, the developed code should adjust the governing formulations to disregard equations related to stationary bed and essentially repeats the calculation process without stationary bed formulations, assuming that all the particles are at moving layer.

It is evident from Equation (4-7) that $U_{MB.Minimum}$ is direct function of ρ_s .

$$\rho_s \uparrow \Rightarrow U_{MB.Minimum} \uparrow \quad (5.2)$$

Increase in density will result in heavier particles, which means higher water velocity is required to overcome the gravitational forces and result in enough torque to roll the particle. Hence in higher particle density, there is more chance of stationary bed formation and this is what figure 5-16 is depicting.

Figure 5-17 shows the moving bed height, for the same simulation conditions as Figure 5-16. When $\rho_s < 2000 \text{ (kg/m}^3\text{)}$ whilst stationary bed couldn't be detected, code was able to calculate moving bed height. Increase in volumetric concentration results in reduction in moving bed height. This behaviour has already been discussed in Section 5.2. In reality, not all the particles will be neatly moving at moving bed layer. But in fact a portion of particles will be fully dispersed in water layer whilst concentration of particles at bottom of the pipe will be at its peak. But as explained in Chapter 3, one of the simplifying assumptions in this research is that a fully dispersed flow regime will be homogenous.

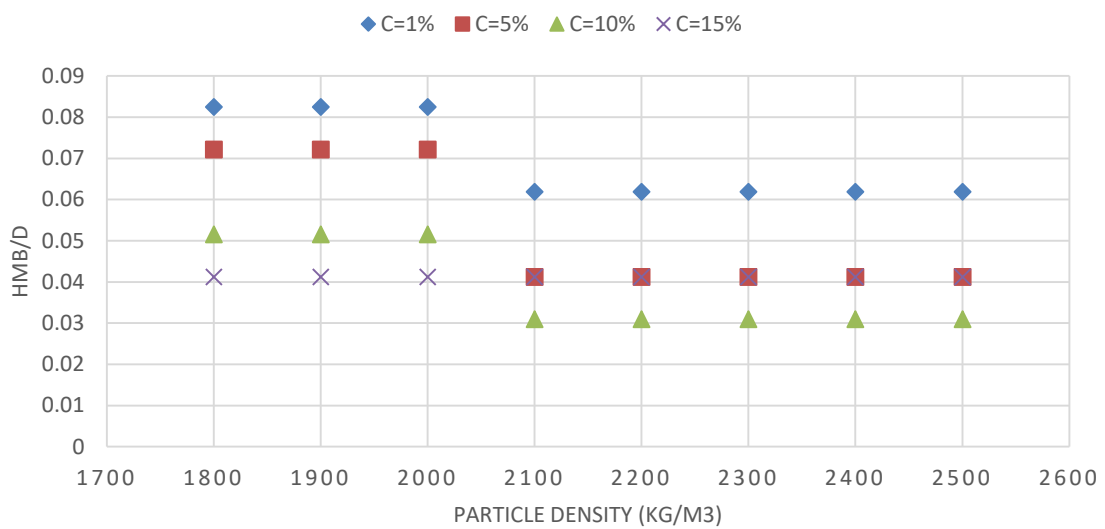


Figure 5-17: Effect of solid density on moving bed height -
 $D = 0.097 \text{ (m)}$, $U_o = 0.036 \text{ (m/s)}$, $U_G = 15.5 \text{ (m/s)}$, $d_p = 100 \text{ (}\mu\text{m)}$

Once stationary bed height was detected by the code at $\rho_s > 2000 \text{ (kg/m}^3\text{)}$, there will be a slight reduction in H_{MB} . This is also due to the fact that by the formation of a stationary bed, friction factor between moving bed layer and underneath layer will increase which results in more particle to stop moving by moving bed layer. Similar behaviour was observed in figure 5-12.

Total sand bed height which is summation of stationary and moving bed layers is shown in Figure 5-18. Formation of stationary bed at $\rho_s > 2000 \text{ (kg/m}^3\text{)}$ results in a sudden increase in total sand bed height. Increase in sand bed height should have an impact on the geometry of other layers. Figure 5-19 shows the change in water layer height whilst particle density is increasing. Even though it seems that the formation of stationary sand bed causes a reduction in water layer height, to put it

into context, reduction in water layer height is less than 20% which is well within the accuracy margin of the code i.e. -10% to +24%.

Formation of the stationary sand bed should squeeze other layers and result in the reduction of layers' height. But simulation results suggest that oil and gas layer remain unchanged for a given concentration, while particle density is increasing. Only the water layer which is immediately adjacent to the sand layer sees the effect of sand layer build up. It is worth highlighting that particle density is increased by 38% in this simulation. More increase in density could result in a more considerable sand layer build up and consequently change the geometry of the other two layers.

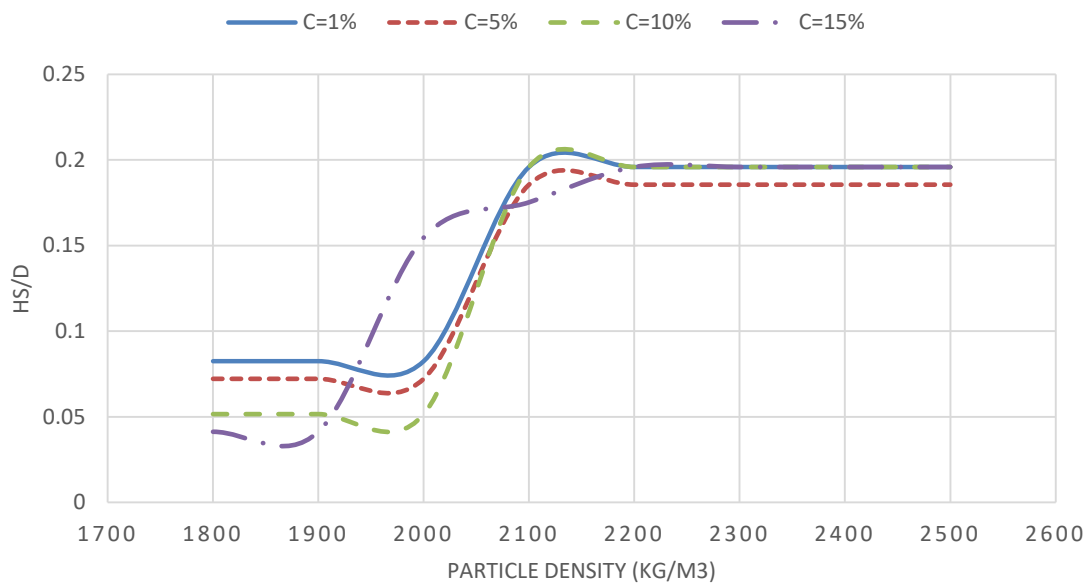


Figure 5-18: Effect of solid density on total sand bed height -
 $D = 0.097 (m), U_o = 0.036 (m/s), U_G = 15.5 (m/s), d_p = 100 (\mu m)$

But in order to keep the simulation conditions as close as possible to Dabirian *et al.* (13) work, increase in density is stopped at 2500 (kg/m^3). The oil and gas layers remained constant for all solid particle densities.

It is reasonable to assume that the formation of stationary sand bed as a result of particle density increase should result in pressure loss increase. Figure 5-20 shows the very same behaviour.

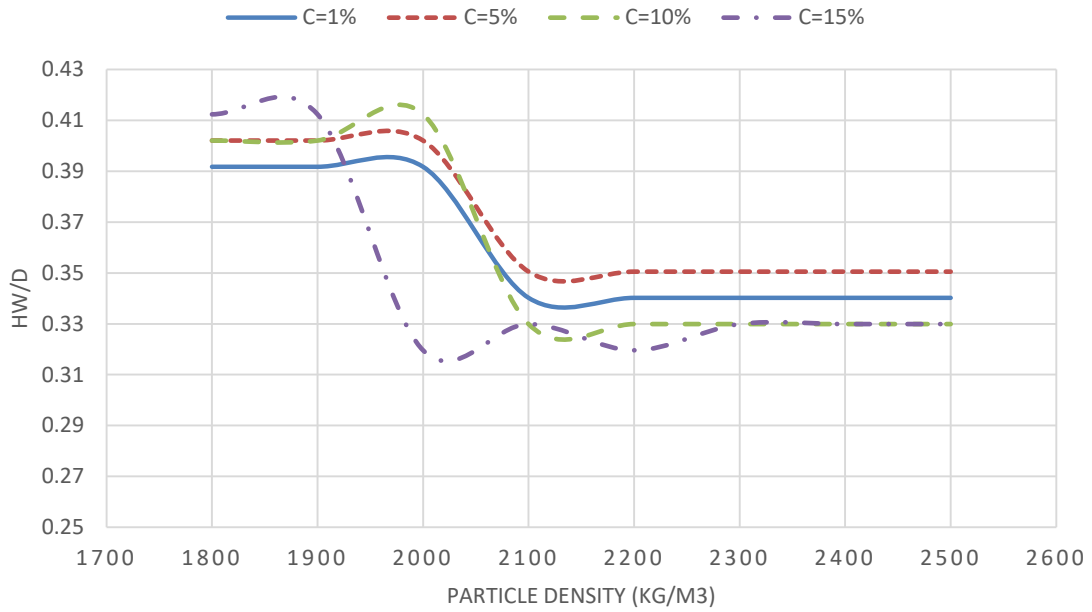


Figure 5-19: Effect of solid density on water layer height -
 $D = 0.097 \text{ (m)}, U_o = 0.036 \text{ (m/s)}, U_G = 15.5 \text{ (m/s)}, d_p = 100 \text{ (}\mu\text{m)}$

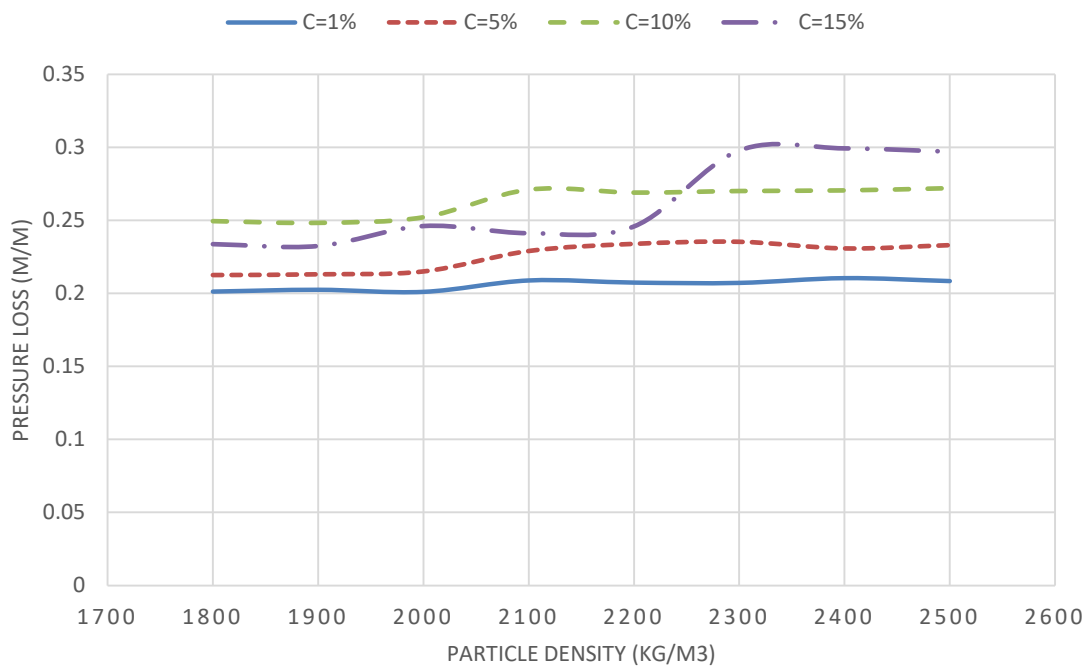


Figure 5-20: Effect of solid density on pressure loss -
 $D = 0.097 \text{ (m)}, U_o = 0.036 \text{ (m/s)}, U_G = 15.5 \text{ (m/s)}, d_p = 100 \text{ (}\mu\text{m)}$

Noticeable increase in pressure loss occurs around $\rho_s = 2000 \text{ (kg/m}^3\text{)}$, which seems to be the threshold for the formation of stationary bed.

Increase in pressure loss is more vivid at higher volumetric concentration. This is in line with the observations in Section 5-2. At $C_s = 1\%$, a minor step in pressure loss curve can be noticed at $\rho_s = 2000 \text{ (kg/m}^3\text{)}$, but overall, the curve seems to be flat. Raw data suggests that the increase in pressure loss for $C_s = 1\%$ is around 4%. This can even be seen as a numerical error. So it is reasonable to suggest that at $C_s = 1\%$, increase in particle density from $1800 \text{ (kg/m}^3\text{)}$ to $2500 \text{ (kg/m}^3\text{)}$ does not have an impact on pressure loss. This is despite the fact that stationary bed is formed at $\rho_s > 2000 \text{ (kg/m}^3\text{)}$. As a general conclusion, for a given set of volumetric concentration, particle diameter and flow rates, when an increase in particle density results in the formation of stationary bed, the pressure loss increases. Once stationary bed established, further increase in density does not show any noticeable increase in pressure loss. It is worth mentioning that this conclusion is based on density variation from $1800 \text{ (kg/m}^3\text{)}$ to $2500 \text{ (kg/m}^3\text{)}$ and does not include a wider particle density spectrum.

5.4 Effect of Slurry Velocity on Flow Structure

In this section, the influence of variation in slurry flow rate on the structure of four-phase flow is studied. Variation in slurry flow rate will be in accordance with flow variables detailed in Table 5-3, with the exception that superficial slurry velocity continuously increases from 0.035 (m/s) to 0.084 (m/s) whilst other flow parameters are constant as per Table 5-6.

Table 5-6: Effect of slurry flow rate on flow structure- flow parameters

Variable	Value	Units
<i>Superficial gas velocity</i>	15.5	$\frac{m}{s}$
<i>Superficial slurry velocity</i>	0.035-0.084	$\frac{m}{s}$
<i>Superficial oil velocity</i>	0.03	$\frac{m}{s}$
<i>Solid density</i>	2475	$\frac{kg}{m^3}$
<i>Solid volumetric concentration</i>	1	%
<i>Particle size</i>	100	μm

Particle volumetric concentration in this simulation remains constant as $C_s = 1\%$. Oil and gas flow rates are also constant. In order to keep the flow regime stratified as shown in figure 5-1, slurry superficial velocity is limited to 0.084 (m/s) . Because slurry flow rate is slightly less than

Dabirian *et al.* (13) work, it is expected that a fully dispersed particle regime will not be observed. It is explained in table 5-3 that flow parameters of Dabirian *et al.* (13) work have been modified in order to add the oil phase. Hence slurry flow rate in table 5-6 is 30% lower than original experiment which was conducted by Dabirian *et al.* (13).

As explained before, the main reason that parameters of Dabirian *et al.* (13) work were used to model the flow in this research is because those parameters resulted in a stabilised stratified flow. Maintaining a stratified flow regime for three phase liquid/liquid/gas flow proved to be a challenge as reported by many researchers (7,85,90). Consequently, little work was done to study the stability criteria of stratified three phase liquid/liquid/gas flow and same can be said for stratified four-phase solid/liquid/liquid/gas flow which is the subject of this research. Even though the code uses a criterion in Equation (4.6) to check the existence of stratified flow, it is worth highlighting that Equation (4.6) which is proposed by Taitel *et al.* (7) is not an accurate measure of flow regime transition for four-phase or even three phase flows. The main drawback of Equation 4.6 can be seen as its disregard for velocity difference between water phase U_w and oil phase U_o . It can be argued that the effect of any variation in water layer velocity U_w is indirectly being considered in oil layer velocity U_o via coupling terms in momentum continuity equation for each layer. This assumption might be true for three phase liquid/liquid/gas when water is flowing between smooth pipe surface and oil layer. But in four-phase flow, water layer is in contact with a rough surface of sand bed layer which is continuously changing. And surface disturbance of sand layer can cause disturbance in the water layer which in turn will result in a disturbance in the oil layer surface. In these circumstances, oil layer velocity U_o might remain unchanged whilst waves are forming on oil layer surface which can initiate the flow regime transition from stratified to intermittent flow. In a nutshell, further works to be done to establish a more accurate flow regime transition for four-phase flow.

Figure 5-21 illustrates the effect of slurry flow rate on water layer height. Curve exhibits a linear relationship between water layer height H_w and slurry superficial velocity U_{SS} , when $0.035 \text{ (m/s)} \leq U_{SS} \leq 0.084 \text{ (m/s)}$.

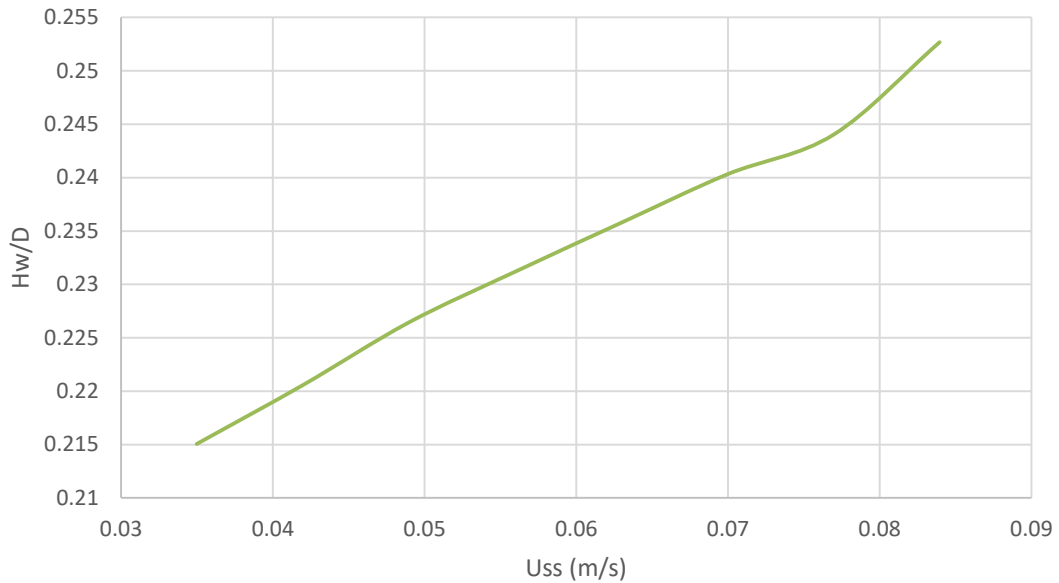


Figure 5-21: Effect of slurry flow rate on water layer -
 $D = 0.097$ (m), $U_o = 0.03$ (m/s), $U_G = 15.5$ (m/s), $d_p = 100$ (μm)

Trend of the curve in Figure 5-21 shows similarities with Taitel *et al.* (7) works for three phase liquid/liquid/gas flow which was studied in Section 4.3. In lower flow rates, liquid build up shows linear relationship with superficial liquid velocity and then gradually trend changes to exponential at higher superficial velocities. This was explained in more detail in Section 4.3. In this study, because simulation stopped at $U_{SS} = 0.084$ (m/s), exponential part of the curve could not be observed. Besides, at higher slurry flow rates, flow regime will probably change to intermittent which is out of the scope of formulations in this research.

Variation of sand bed heights H_{SB} and H_{MB} with slurry flow rate is shown in figure 5-22. Increase in slurry flow rate which means an increase in superficial water velocity $U_{s,W}$ results in an increase in moving bed height for a given particle diameter.

Forces acting on a single particle is a function of water velocity U_W (4,5,11). Therefore any variation which results in water velocity increase also increases Viscous F_D and Lifting F_L forces impose on single particle which eventually rolls the particle. More details can be found in Sections 2.2.2 and 2.3.1 of this report

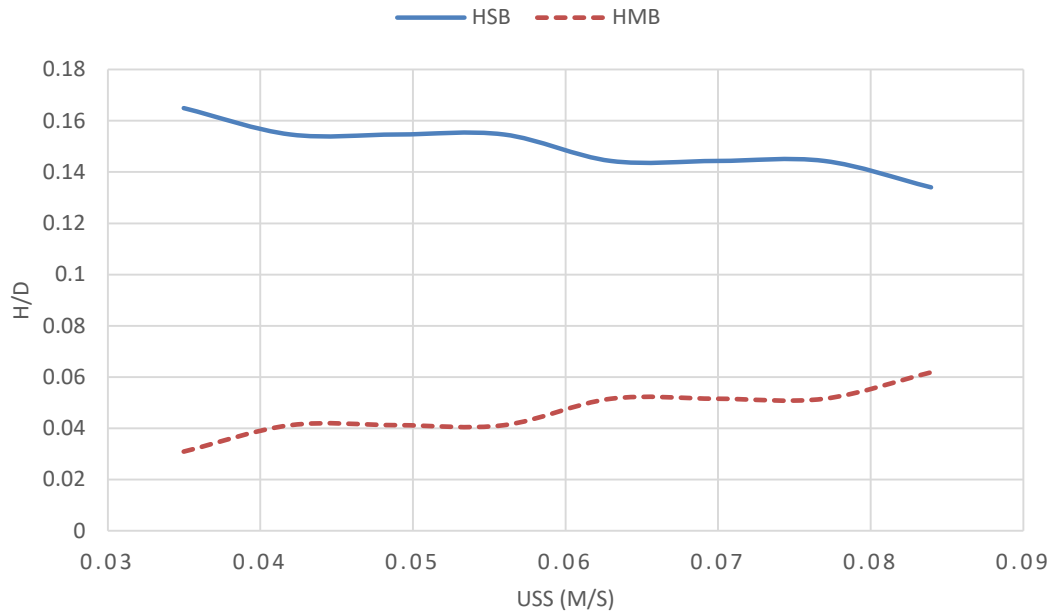


Figure 5-22: Effect of slurry flow rate on sand layer -
 $D = 0.097 \text{ (m)}, U_o = 0.03 \text{ (m/s)}, U_G = 15.5 \text{ (m/s)}, d_p = 100 \text{ (\mu m)}$

First, height of moving bed H_{MB} is limited to couple of particle diameter which are located next to the water layer. Particles which are trapped between moving bed layer and pipe wall need higher forces compared to particles in moving layer in order to start moving. This is predominately because of the weight force of particles at top layers (84). For smaller particle size, Van der Waals force also plays important role as shown by Rabinovich and Kalman(52,65). With the exception of Van der Waals force, apparent weight force is included in the formulations in this code as detailed in Section 3.5. With reference to Figure 3-2, term F_{SB} gradually reduces when the height of moving bed increases. Because apparent weight force which is exerted on particles in stationary bed reduces when more and more particles in top layers start to move as a result of an increase in slurry flow rate. Hence the height of moving bed increases while at the same time stationary bed height reduces as shown in Figure 5-22. It is worth noting that throughout the simulation, code detects both stationary and moving bed at the same time. Theoretically speaking, if U_{SS} can be increased continuously and assuming that flow regime remains as stratified, then H_{SB} approaches zero while H_{MB} approaches its maximum value before all particles start to fully suspend in water layer due to an increase in turbulent and lift forces(50).

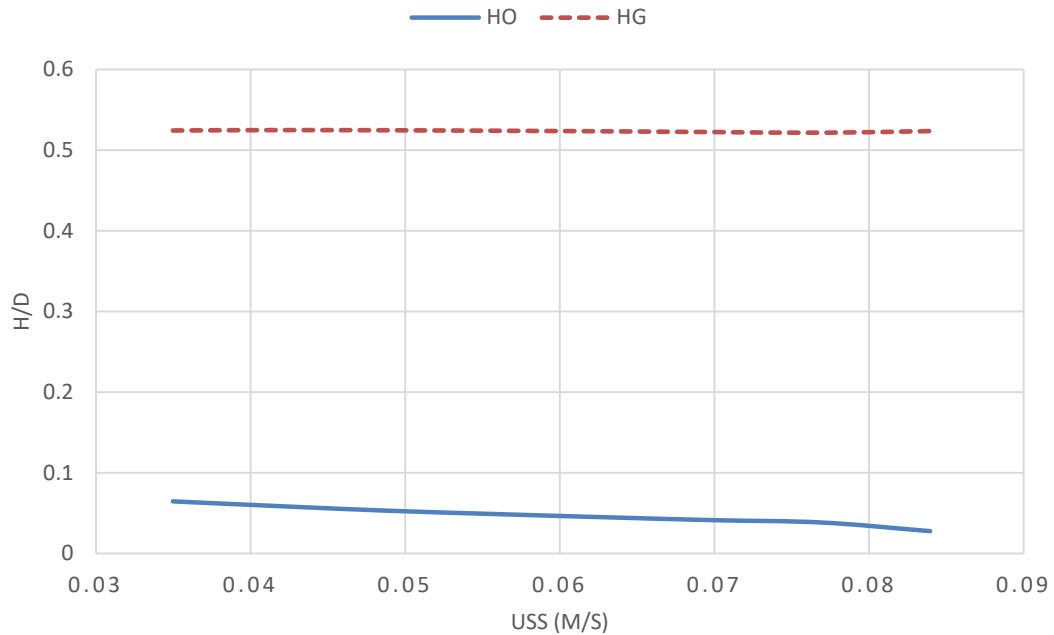


Figure 5-23: Effect of slurry flow rate on oil and gas layers -
 $D = 0.097$ (m), $U_o = 0.03$ (m/s), $U_g = 15.5$ (m/s), $d_p = 100$ (μm)

Figure 5-23 shows variation in oil and gas layer heights when slurry flow rate increases. Oil and gas flow rates remain constant throughout the simulation as detailed in Table 5-6. Reduction in oil layer height H_o is noticeable. Oil flow rate remains constant throughout the simulation. So when slurry flow rate increases, water layer velocity increases. Consequently oil velocity increases because oil layer is adjacent to water layer. This results in reduction of oil holdup and oil layer height.

On the other hand, gas layer height H_g remains almost constant. Even though gas flow rate is constant, increase in water velocity for flow parameters detailed in Table 5-6, does not significantly change the gas layer velocity. Hence gas holdup and gas layer height remains relatively constant.

If simulation could be continued beyond $U_{ss} > 0.084$ (m/s) while maintaining the flow regime as stratified, gas layer height would probably starts to decrease. This is due to the fact that a bigger portion of the pipe will be occupied by water which then will squeeze the gas layer into a smaller section.

As explained in Chapter 3, the formulation in the model treats the layers as being completely distinctive. For example, moving bed layer, when it exists, is completely separated from the water layer and does not have any overlap. Therefore, any increase in moving bed height results in a reduction in other layers' height because the summation of height of all

layers should be equal to pipe internal diameter, which is constant. But in reality, water layer and moving bed layer have overlap otherwise moving bed layer cannot exist. This is one of the shortfalls in the current formulation which requires further studies to rectify.

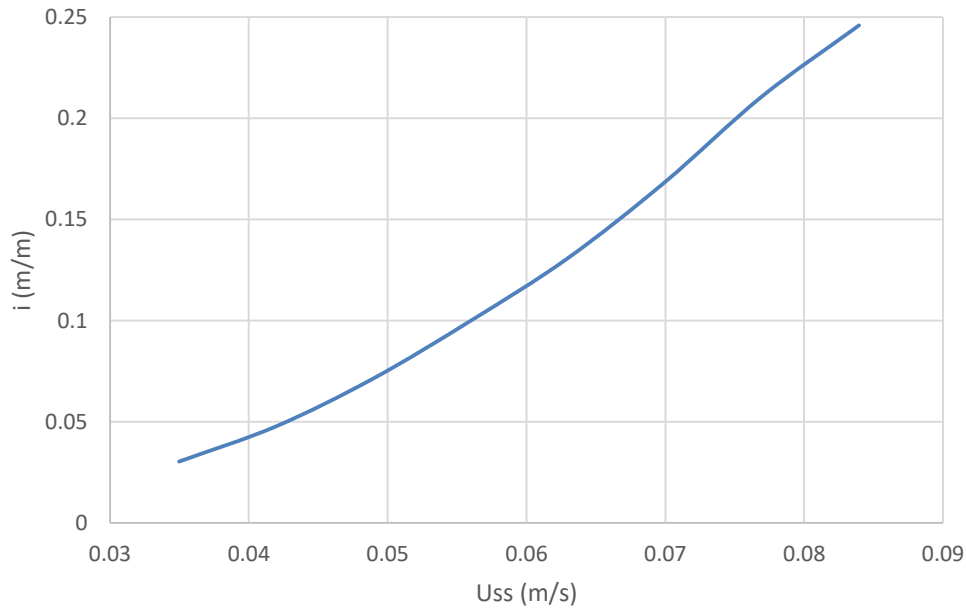


Figure 5-24: Effect of slurry flow rate on pressure loss -
 $D = 0.097$ (m), $U_o = 0.03$ (m/s), $U_G = 15.5$ (m/s), $d_p = 100$ (μm)

The variation of non-dimensional pressure gradient with slurry flow rate is depicted in Figure 5-24. It is expected that an increase in flow rate of any of the phases will result in higher pressure loss. In a single phase system, frictional pressure loss can be expressed as a quadratic function of liquid velocity. The curve in Figure 5-24 seems to exhibit a similar trend when slurry velocity varies between 0.035 (m/s) $\leq U_{ss} \leq 0.084$ (m/s). As demonstrated in Figure 5-22, both stationary and moving beds are present. Hence pressure loss curve shows an uninterrupted and continuous upward trend. It can be seen in previous simulation cases that sudden formation or disappearance of either moving or stationary beds has a noticeable influence on pressure gradient curve. But when these layers are in steady state equilibrium conditions, similar to Figure 5-22, then pressure gradient curve also shows a smooth and continuous behaviour. Similar characteristic of pressure gradient curve was also discussed in further details by Doron and Barnea (5) and Takaoka *et al.* (96).

5.5 Effect of Oil Velocity on Flow Structure

The effect of variation in oil velocity on flow structure is studied in this section. Oil flow rate is increased in defined steps whilst slurry and gas flow rates remain unchanged. The primary condition which should be met throughout this run is to make sure that flow regime stays as stratified so governing equations which are detailed in Chapter 3 are still applicable.

Variation in oil flow rate will be in line with the data in table 5-3. Oil velocity is continuously increasing from 0.015 (m/s) to 0.036 (m/s) while other flow parameters remain unchanged as shown in Table 5-7.

Table 5-7: Effect of oil flow rate on flow structure- flow parameters

Variable	Value	Units
<i>Superficial gas velocity</i>	15.5	$\frac{m}{s}$
<i>Superficial slurry velocity</i>	0.07	$\frac{m}{s}$
<i>Superficial oil velocity</i>	0.015-0.036	$\frac{m}{s}$
<i>Solid density</i>	2475	$\frac{kg}{m^3}$
<i>Solid volumetric concentration</i>	1	%
<i>Particle size</i>	100	μm

In order to make the results comparable with the findings in Section 5.4, gas flow rate, particle size and particle volumetric concentration are equal to flow parameters in Table 5-6.

In the case of three phase liquid/liquid/gas which was thoroughly discussed in Section 4.3 of this report, it was observed that an increase in oil velocity which is a consequence of flow rate increase, the velocity of the adjacent layers increases. This behaviour can be explained by the increase of shear stress element τ_i^k in momentum continuity Equations (3.41-3.43). Therefore it is expected that an increase of oil velocity in four-phase stratified flow results in an increase of water layer velocity. And the increase of water layer velocity has already been studied in Section 5.4 of this report.

Obviously any increase in oil layer velocity as a result of oil flow rate increase can also be seen as oil holdup increase. And while slurry and gas flowrates remain unchanged, the increase in oil layer height results in a reduction in gas and water layer height.

Figure 5-24 depicts the effect of oil layer velocity on the water layer height. Increase in oil flow rate results in a reduction of water layer height which was an expected outcome.

To quantify the variations, when oil velocity U_{SO} increases from 0.015 (m/s) to 0.036 (m/s) which equates to 140% increase, dimensionless water layer height $\frac{H_W}{D}$ reduces by around 10% from 0.293 to 0.262. If inherent numerical errors are taken in account, this variation in the water layer can be assumed as negligible.

Theoretically, increase in oil velocity should cause the water layer to flow faster and consequently for water holdup to reduce. Even though figure 5-24 confirms this trend, probably oil velocity should be increased beyond 0.036 (m/s) in order to observe the more significant reduction in water layer. But worth remembering that stratified flow should be maintained throughout the simulation process and increase in oil velocity will destabilise the stratified flow regime and push the flow regime towards intermittent flow. In fact, the flow regime stability condition which is built-in in the code as per Equation (4-6), could not be satisfied for oil velocities beyond 0.0375 (m/s).

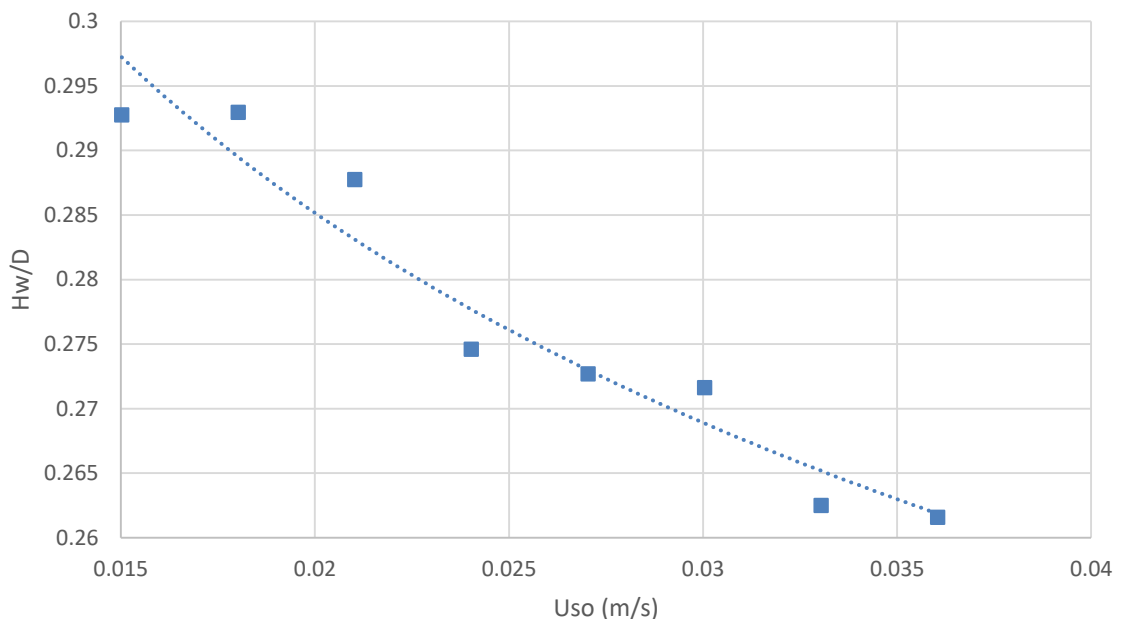


Figure 5-25: Effect of oil flow rate on water layer height - $D = 0.097$ (m), $U_S = 0.07$ (m/s), $U_G = 15.5$ (m/s), $d_p = 100$ (μm)

Despite the fact that reduction of water layer height in Figure 5-25 might be seen as inadequate to verify the hypothesis, the overall trend is in agreement with governing physics and also in line with the results of three phase flow which are detailed in chapter 4. Because the increase in water velocity is not significant enough, the developed code didn't detect

any noticeable change in stationary and moving sand bed heights and both heights remain almost constant throughout the simulation.

For completeness, heights of stationary and sand beds are shown in Figure 5-26. With the exception of some minor fluctuation in stationary bed height H_{SB} at lower oil velocities, both stationary and moving bed heights are very much unchanged. Relationship between sand layer height and water velocity which is governed by minimum moving bed velocity $U_{MB.Minimum}$ is detailed in Section 4.2. It seems that change in water velocity in this simulation is not significant enough to change the $U_{MB.Minimum}$ and consequently change the equilibrium balance between moving bed and stationary beds. Therefore code didn't detect any change in the height of these two layers.

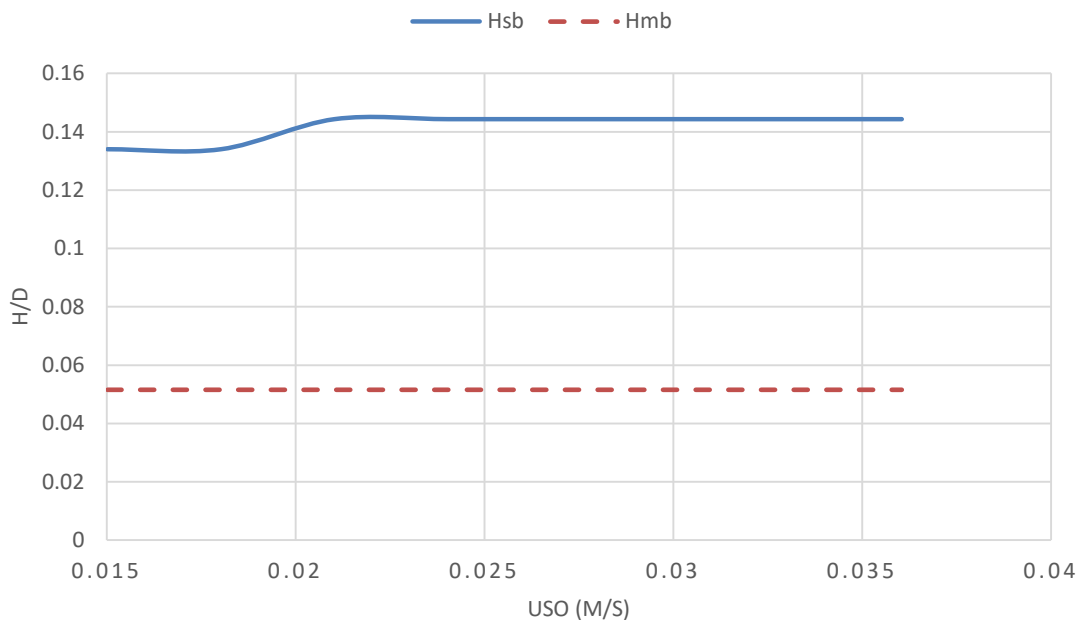


Figure 5-26: Effect of oil flow rate on sand layer height -
 $D = 0.097 \text{ (m)}, U_S = 0.07 \text{ (m/s)}, U_G = 15.5 \text{ (m/s)}, d_p = 100 \text{ (}\mu\text{m)}$

Effect of oil layer velocity U_O on sand layer height H_S is indirect and via water layer velocity U_W . An increase in oil layer velocity causes the water layer to flow faster. When water layer which is the carrier of sand particles flows faster, moving bed layer velocity U_{MB} increases and consequently the height of both moving bed and stationary bed start to change in order to maintain the mass and momentum equations detailed in Chapter 3. This indirect relationship between flowing layers was studied in Section 4.3 where the effect of gas layer velocity variations was studied on water layer height which was not adjacent to the gas layer in three phase water/oil/gas flow. In this simulation, because the

change in water layer height and consequently its velocity is negligible, sand layers do not notice any change in carrier flow velocity and therefore the governing terms in momentum Equations (3.44) and (3.45) do not change.

It is expected that an increase in oil flow rate will result in oil layer height to increase and the graph which is depicted in Figure 5-26 confirms this. Change in oil superficial velocity may seem to be significant i.e. around 140% increase, but increase in oil layer height is 10% which may be seen trivial.

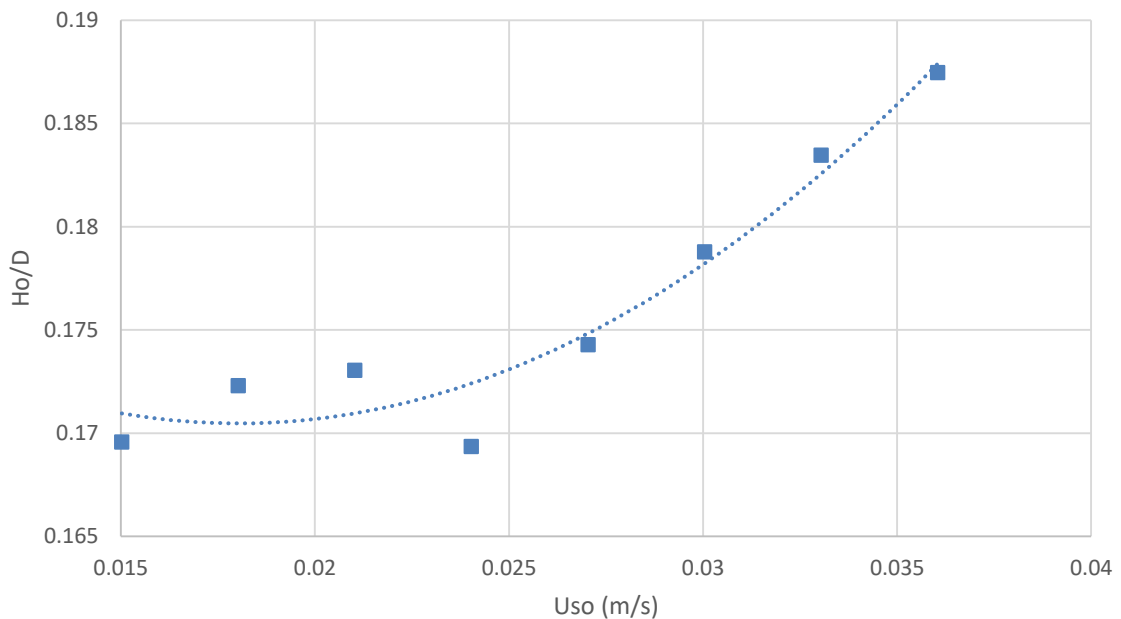


Figure 5-27: Effect of oil flow rate on oil layer height -
 $D = 0.097 \text{ (m)}, U_S = 0.07 \text{ (m/s)}, U_G = 15.5 \text{ (m/s)}, d_p = 100 \text{ (}\mu\text{m)}$

It was noticed in previous simulations that an increase in local velocity results in a reduction in phase holdup. This is the reason that the increase in oil layer height is not as significant as it was expected because local velocity increase causes a reduction in holdup and consequently dampens the oil height increase.

In order to visualise the variation in local velocities, Figure 5-28 is depicting the changes in flowing areas for water, oil and gas phases. Oil layer area A_o increases slightly which is in line with the slight increase in oil layer height which is shown in Figure 5-27. Increase in oil layer area and reduction on water layer area A_w balance each other out. This will result in the gas layer area A_g to remain reasonably constant, considering geometries of the solid layers remain unchanged. As a general observation, the increase in the oil flow rate seems to have more impact on the water layer than the gas layer. This can be a result of higher

surface tensions between oil/water layers in comparison to gas/oil layer. A similar phenomenon was observed in Section 4.3 with regard to three phase liquid/liquid/gas flow.

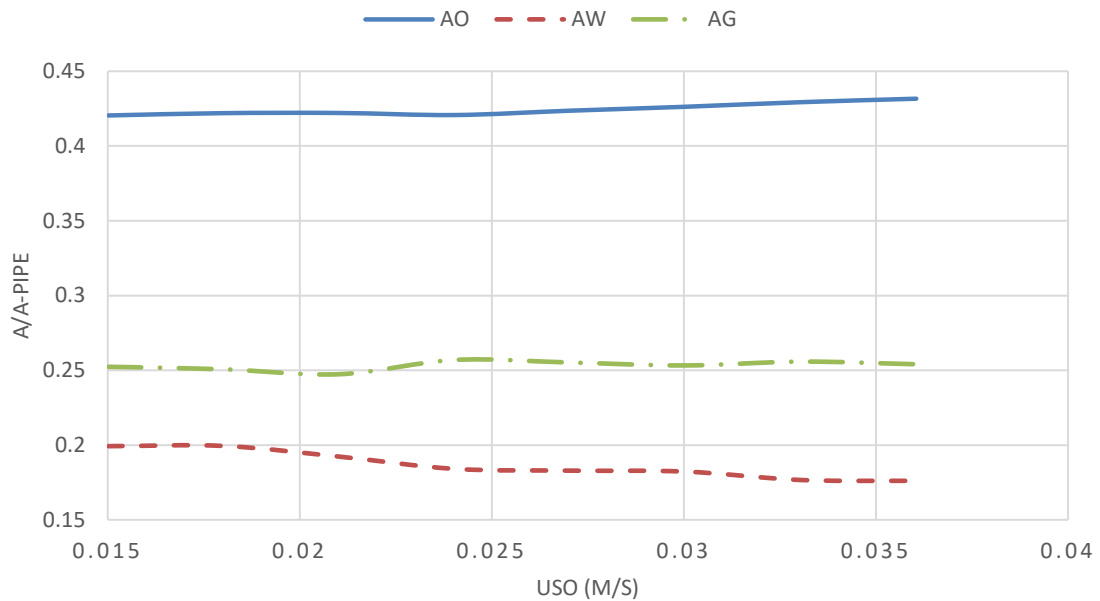


Figure 5-28: Effect of oil flow rate on flowing areas -
 $D = 0.097 \text{ (m)}$, $U_S = 0.07 \text{ (m/s)}$, $U_G = 15.5 \text{ (m/s)}$, $d_p = 100 \text{ (}\mu\text{m)}$

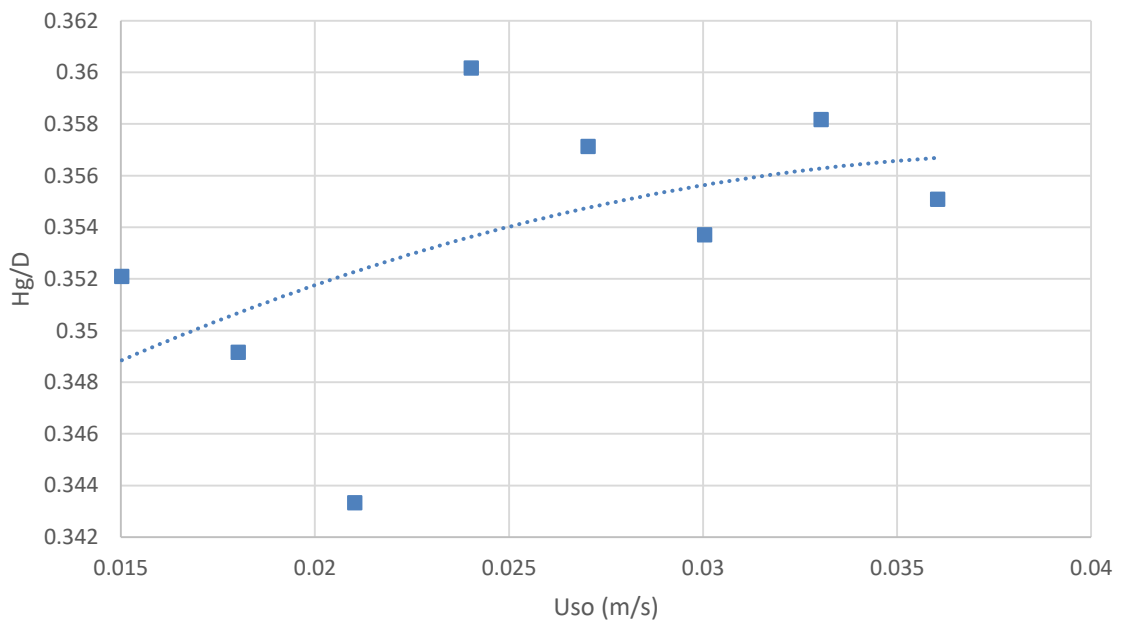


Figure 5-29: Effect of oil flow rate on gas layer height -
 $D = 0.097 \text{ (m)}$, $U_S = 0.07 \text{ (m/s)}$, $U_G = 15.5 \text{ (m/s)}$, $d_p = 100 \text{ (}\mu\text{m)}$

Variation in gas layer height H_G as a result of the increase in oil flow rate is shown in Figure 5-29. As explained before, gas layer height is

calculated by summation of all other layer heights and then deducting it from inside pipe diameter as shown in Equation (5.1). The trend in Figure 5-29 shows a very slight increase in gas layer height whilst the oil flow rate is increasing. This is in line with cross section area variations which is shown in Figure 5-28.

It is fair to conclude that the increase in oil flow rate as detailed in Table 5-7 has a more noticeable impact on water layer geometries than any other layer. Stationary and moving solid layers remain unchanged despite the fact that cross sectional area of the water layer slightly decreased which means local water velocity increases. But as explained in Figures 5-26 and 5-26, this increase in local velocity is not adequate to change the geometries of solid layers. To put into the context, Figure 5-30 shows variation in local velocities of water, oil and gas phases as a result of increase in oil flow rate. It is evident that the local velocity of the water layer U_W has negligible increase, i.e. around 13% increase, which is not enough to create more lifting and rolling forces to increase the moving sand bed height H_{MB} . Even though it is negligible, i.e. around 1%, gas phase local velocity U_G decreases because the gas layer height increases as shown in Figure 5-29.

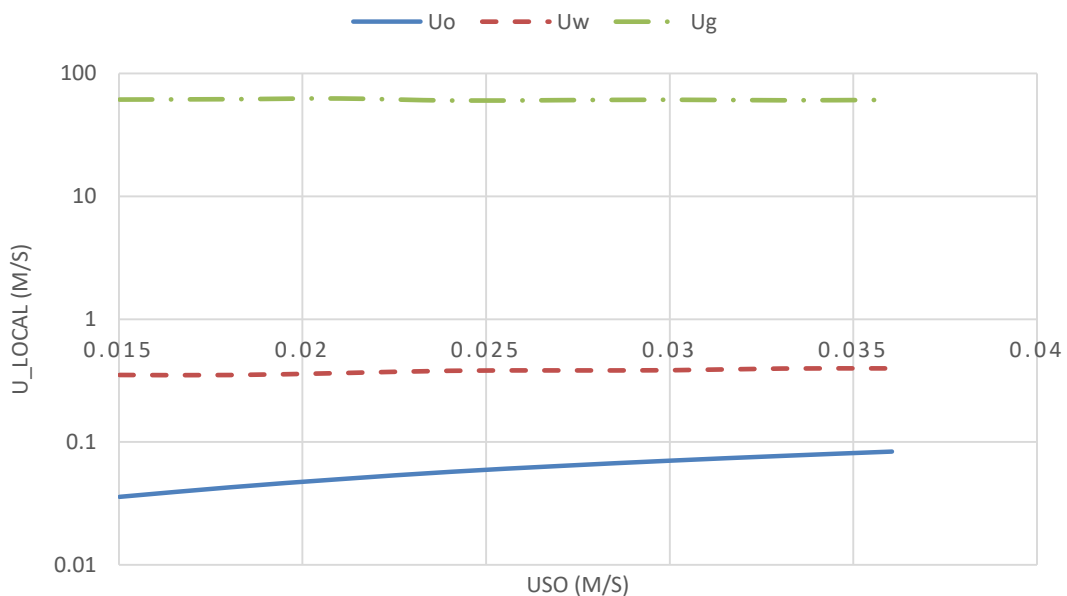


Figure 5-30: Effect of oil flow rate on local velocities -
 $D = 0.097 (m)$, $U_S = 0.07 (m/s)$, $U_G = 15.5 (m/s)$, $d_p = 100 (\mu m)$

Chapter 6

Conclusion

A comprehensive literature survey of available sand transport models in two and three phase flow was completed in this study. Following the literature survey, a set of formulations has been developed in this study to model the governing physics of horizontal stratified four-phase flow. To the best of our knowledge, this is the first four-phase stratified flow model which is developed based on Mechanistic approach. In order to represent the untreated oil production, four-phase flow which is represented in this study comprises of solid, water, oil and gas.

The developed formulations consist of mass and momentum continuity equations which are represented by system of 12 non-linear equations. Closure terms which are primarily in the form of friction factor f_i , sand concentration distribution C_s and Reynolds number Re_i are also represented by non-linear equations.

A solution method called "Two-Guess" has been developed in this research which is based on equalising the pressure gradient of flowing phases. Unlike methods developed by other researchers for two and three phase flow, "Two-Guess" method negates the need for any priori to solve the system of non-linear equations. Main concept behind this solution method is that the flow regime is stable, and results are acceptable only if the pressure gradient of moving layers are equal.

A code was developed in MATLAB to execute the iterative "Two-Guess" method to solve the system of non-linear equations. The developed code also contains the algorithm to detect whether solid particles are in layered or fully dispersed state.

The developed code then was verified against three phase liquid/liquid/gas and three layer solid/liquid models where results were found to be satisfactory. In the case of three phase water/oil/gas model, the developed code was ran for two oil viscosity values of 1 (cP) and 100 (cP). Variation in the height of each layer versus slurry flow rate was studied. The code results showed acceptable comparison to published experimental data.

Comparison with three layer solid/liquid model was done by running the code while sand volumetric concentration was increased from 4% to 20% with 2% increment. For a given solid concentration, then slurry volumetric flow was varied from 0.1 (m/s) with small increment until stratified flow couldn't be detected anymore. Then for each set of solid

concentration and volumetric flow rate, system of non-linear equations was solved using the "Two-Guess" method and results were compared with experimental data which were found in reference publications. The developed code results showed satisfactory comparison with experimental data.

The developed code then was employed to model the four-phase horizontal stratified sand/water/oil/gas flow. Flow parameters were chosen in such a way that flow most likely remained stratified. Test setup for three phase solid/water/air from one of the reference publications was used as basis to simulate the stratified flow. Total slurry flow rate assumed to be 30% volumetric oil and 70% volumetric water. So total liquid flow rate remained unchanged compared to original test setup as an assurance that stratified flow regime less likely to transit to other regimes. A parametrical analysis was completed to study the effect of several flow parameters on flow structure. The parameters which were captured in this study comprises of particle size, solid concentration, solid density, slurry velocity and oil velocity.

At constant solid concentration and slurry flow rate, increase in solid size d_p results in reduction in stationary bed height H_{SB} and increase in moving bed height H_{MB} . Increased sand particle size will increase particle surface and consequently increase in torque applied on each particle by the effect of moving water layer. As long as local water layer velocity is greater than $U_{MB.minimum}$, particle is moving and subsequently moving bed height exists. But at some point d_p is big enough where weight and drag forces are more significant than torque generated by the water layer. At this point, moving sand particles start to become stagnant which results in an increase in the height of stationary sand bed. In this situation, stationary and moving layers co-occur where their respective heights are in balance which means an increase in one results in a decrease in the other one. It was observed that oil and gas layer heights remain almost constant whilst sand particle is gradually increasing up to 145 (μm).

To further study the effect of particle size on fluid structure, slurry and oil flow rates were increased whilst gas flow rate remained unchanged. Increase in flow rate has a more evident impact on height of the water layer than an increase in particle size. Increasing the flow rate resulted in an increase in oil holdup and consequently increase in the oil layer height. Increased sand particle essentially resulted in a rougher contact surface between sand layer and water. This will cause the water layer to move with lower velocity and consequently resulted in the neighbouring oil layer to move slower and phase holdup to increase. In terms of pressure gradient, it increases with increase in particle size.

To study the effect of solid concentration on flow structure, for a given set of slurry, oil and gas flow rates, volumetric concentration of solid in slurry flow was increased gradually. It was demonstrated that increase in concentration results in the sand build-up. Reduction in water flow rate, causes the local velocity reduction which in turn results in a reduction in moving bed height. Critical sand velocity or $U_{MB.minimum}$ did not change significantly with concentration. Therefore, increase in solid concentration does not change the sand moving mechanism as such because on one hand water flow rate is continually decreasing and on the other hand, sand particle size which has a greater effect on $U_{MB.minimum}$, mainly remains unchanged.

It is also observed that at solid concentration C_s below 4%, total sand height is constant. It was shown that at certain ranges of solid concentration, moving and stationary sand beds are in balance as long as other parameters which are influencing $U_{MB.minimum}$ are constant such as particle size and density of carrier liquid. In these ranges, sand particles switch between moving and stationary layers with negligible change in total sand height. Pressure loss showed a linear increasing trend whilst solid concentration is increasing.

Oil layer height showed a downward trend while C_s increases. Because total sand layer height increases by increasing solid concentration C_s , given a constant pipe cross section, other layers will be squeezed which in turn will increase the local velocity of other phases. The effect of gas velocity on solid and water layers is very much similar to oil layer velocity i.e. has an indirect impact on water velocity and consequently solid layer geometry.

To study the effect of solid density on flow structure, series of flow scenarios were simulated with constant particle and flow rates whilst solid density was increased gradually from $1800 \left(\frac{kg}{m^3}\right)$ to $2500 \left(\frac{kg}{m^3}\right)$ in $100 \left(\frac{kg}{m^3}\right)$ increments. For a given flow conditions, increase in density showed some effect on transition from stationary to moving bed and on water layer height but hasn't had noticeable impact on height of oil and gas layers. For solid density $\rho_s < 2000 \left(\frac{kg}{m^3}\right)$, stationary bed disappeared and solid particles were observed in the moving layer, entirely. It is due to reduction of dry friction force which is consequence of density reduction.

Gradual Increase in density resulted in heavier particles, which means higher water velocity is required to overcome the gravitational forces and

result in enough torque to roll the particle. Hence it is more likely to have stationary bed in higher particle density. Formation of stationary bed at $\rho_s > 2000 \text{ (kg/m}^3\text{)}$ resulted in a sudden increase in total sand bed height. Formation of the stationary sand bed should squeeze other layers and result in the reduction of layers' height. But simulation results suggest that oil and gas layer remain unchanged for a given concentration, while particle density is increasing. Only the water layer which is immediately adjacent to the sand layer sees the effect of sand layer build up.

Noticeable increase in pressure loss observed around $\rho_s = 2000 \text{ (kg/m}^3\text{)}$, which seems to be the threshold for the formation of stationary bed. Increase in pressure loss is more vivid at higher volumetric concentration. At $C_s = 1\%$, a minor step in pressure loss curve can be noticed at $\rho_s = 2000 \text{ (kg/m}^3\text{)}$, but overall, the curve seems to be flat. As a general conclusion, for a given set of volumetric concentration, particle diameter and flow rates, when an increase in particle density results in the formation of stationary bed, the pressure loss increases. Once stationary bed established, further increase in density does not show any noticeable increase in pressure loss.

Influence of variation in slurry flow rate on the structure of four-phase flow was studied by running the developed code for set of given flow characteristics whilst superficial slurry velocity was continuously increased from 0.035 (m/s) to 0.084 (m/s) . Increase in slurry flow rate showed a linear relationship with water layer height for $0.035 \text{ (m/s)} \leq U_{SS} \leq 0.084 \text{ (m/s)}$. Increase in slurry flow rate which means an increase in superficial water velocity $U_{s,W}$ resulted in an increase in moving bed height for a given particle diameter while at the same time stationary bed height reduces.

Slurry flow increase resulted in noticeable reduction in oil layer height H_o whilst gas layer height H_G remained almost constant. As expected, increase in water layer height H_W as a result of slurry flow rate increase showed more vivid effect on adjacent oil layer than gas layer. The slurry flow rate increase resulted in higher pressure loss. The relationship between pressure loss and slurry flow rate exhibited a trend similar to single phase flow for $0.035 \text{ (m/s)} \leq U_{SS} \leq 0.084 \text{ (m/s)}$.

To simulate the effect of oil flow rate on flow structure, the developed code was used for set of variable oil velocities from 0.015 (m/s) to 0.036 (m/s) while other flow parameters remained unchanged. Increase in oil layer velocity caused water layer to flow faster and resulted in reduction of water layer height. Sand bed heights remained almost constant because increase in local water velocity wasn't significant to change the

balance between moving and stationary sand beds. As expected, the oil layer height showed upward trend with increase in oil flow rate. The gas layer height H_G showed a very slight increase as a result of the increase in oil flow rate is shown. Overall, it was noticed that increase in oil flow rate had a more noticeable impact on water layer geometries than any other layer.

As overall conclusion, the novel technique which was developed in this research to solve the non-linear governing equations for four-phase stratified flow proved to be reliable and resulted in satisfactory results. Unlike the other numerical methods which were used by others and necessitate using a priori to start the solution process, "Two-Guess" method developed in this research does not need any priori and can, in fact, be extended to work with more than two estimated values. Results generated by the code based on the four-phase model, which was developed in this research are showing logical trends which can reasonably be explained by governing physics. Referring to the research objectives which are listed in section 1.3, all the defined objectives have been met and resulted in the following novel contributions:

- As detailed in chapter 3, governing equations have been developed for the first time, to model a four-phase stratified flow in a layered arrangement.
- Chapter 4 contains the novel Two-Guess solution algorithm which was developed to solve the system of non-linear equations without any priori. The developed algorithm can detect different solid phase configurations in stratified flow including layered and fully dispersed solid phase.
- A computer code was written in MATLAB to solve the four-phase stratified flow model.
- Chapter 5 contains the results of a parametrical study which was carried out to evaluate the effects of physical properties on liquid holdup and pressure gradient of four-phase stratified flow.

6.1 Proposal for Future Works

The areas which have been identified as immediate development opportunities are listed below. This list is not exhaustive and can be altered by whoever continues this research in the future.

- *Enhancing the MATLAB code to shorten the running time:* the developed solution algorithm is an iterative method whose compilation time is heavily influenced by several factors mainly internal diameter of the pipe " D " and solid particle size " d_p ". The bigger the pipe size and the smaller the particle, the more time the code needs to complete the calculation loop. For example, for $D = 0.97$ (m) and $d_p = 50$ (μm) compilation took 6 hrs 32 minutes.

Following some investigations, it was noticed that one of the reasons for such a long running time is because code is calling more than 25 different MATLAB functions in every single iteration step. Some of these functions are developed as part of this research and others are built-in MATLAB functions which are often used as part of algorithm to solve the non-linear equations. In order to improve the performance of the code and consequently shorten the running time, it is suggested to review and restructure the code in order to take benefit of "Nested Functions" techniques.

Allocation of matrix variables which are being used in each iteration to store the calculated results only, can also be reviewed. Improvement can be made by reducing the number of temporary matrix variables.

- *Adjusting the formulations to add the pipe inclination angle:* Momentum continuity formulations can be modified in order to include the pipe inclination angle. Even though this seems to be an easy alteration, the main challenge would be to rewrite the force balance equations on solid particle which is the basis for " U_{MB} " calculation and " F_{SB} ", " $F_{friction.MB.SB}$ " and " $F_{friction.MB}$ " formulations
- *Develop a flow stability criterion for stratified four-phase flow:* The developed model is using stability criterion for three phase liquid/liquid/gas flow to verify the existence of stratified four-phase solid/liquid/liquid/gas flow. It would be recommended to develop a method to verify the stability of four-phase flow by taking into account presence of solid and water layers. The Kelvin-Helmholtz instability theory for oil layer surface, can be influenced by changes in water and or solid heights. Hence it would be suggested to consider other more advanced stability methods developed by other researchers.
- *Develop Mechanistic sand transport formulations for other flow regimes:* The formulations introduced in this research are only valid for stratified flow. Stratified flow was chosen because studies by other researchers has shown that stratified flow is still the more dominant flow in flow regime map for three phase liquid/liquid/gas flow.

But like any other Mechanistic model, for the model to be as comprehensive as possible, other flow regimes regardless of how rare those are should be incorporated in the formulations. It would be suggested to start with slug or intermittent four-phase flow because phases can still be reasonably separated in slug regime.

- *Adding energy continuity equations to model formulation:* The developed model is one-dimensional steady state isothermal model based on momentum and mass continuity equations. The aim was to calculate the hold up for each phase and pressure loss for the entire flow structure. Due to effect of temperature on physical properties of liquid and gas phases, it would be suggested to add energy continuity equations in order to make the model closer to reality. By adding energy continuity equations, coupling terms should be rewritten. Physical properties of liquid and gas phases should be calculated in each iteration based on phase temperature.
- *Developing a test loop for four-phase flow to verify the results of this code:* A comprehensive literature survey was done during this research which proved that experimental results for four-phase flow are scarce. No empirical data for four-phase flow could be found in open publications. Literature survey suggested that most comprehensive experimental data set were generated at Multiphase Flow Laboratory at SINTEF Petroleum Research Facilities in Norway, but those data were only referenced in some publications and were not accessible to use for verification of the model which was developed in this research. There are several multiphase test loop available in the UK namely WASP (water, air, sand, petroleum) in Imperial College London and CRAN in Cranfield University. Even though some of these test loops, e.g. WASP, seem to be capable of measuring the flow parameters of four-phase flow, no comprehensive test on four-phase flow has ever been carried out in those facilities. Thus, it seems to be very beneficial to either modify and equip these existing loops to perform experiments on four-phase sand/water/oil/gas flow or develop a new flow loop which is capable of doing such tests.
- *Developing flow regime map for four-phase flow:* Even though this seems to be a long term goal which requires a fully equipped flow loop for four-phase flow and numerous tests, like two and three phase flow, it will be extremely beneficial to develop a flow regime map for four-phase flow. This map can also be used to study the flow regime transition in four-phase flow.

References:

- (1) Durand R. *Basic relationships of the transportation of solids in pipes-Experimental research*. The Minnesota International Hydraulics Convention; 1953; Minneapolis, MN: University of Minnesota; 1953. p. 89-103.
- (2) Newitt DM, Richardson JF, Abbot M and Turtle RB. *Hydraulic conveying of solids in horizontal pipes*; London, Department of Chemical Engineers, Imperial College of Science and Technology; 1955; Vol. 33: p. 93-113.
- (3) Danielson TJ. *Sand transport modeling in multiphase pipelines*. Houston, Texas, U.S.A.: Offshore Technology Conference; 2007J2: OTC-18691-MS.
- (4) Han Q, Hunt JD. *Particle pushing: critical flow rate required to put particles into motion*. Journal of Crystal Growth. 1995; 152(3):221-227.
- (5) Doron P, Barnea D. *A 3-Layer model for solid-liquid flow in horizontal pipes*. International Journal of Multiphase Flow. 1993; 19(6):1029-1043.
- (6) Yang ZL, Ladam Y, Laux H, Danielson T, Leporcher E and Martins AL. *Dynamic simulation of sand transport in pipeline*. 5th North American Conference on Multiphase Technology, May 31, 2006 - June 2; 2006; Banff, Canada: BHR Group Limited; 2006. p. 405-419.
- (7) Taitel Y, Barnea D, Brill JP. *Stratified 3-phase flow in pipes*. International Journal of Multiphase Flow. 1995; 21(1):53-60.
- (8) Shippen M, Bailey WJ. *Steady-state multiphase flow-past, present, and future, with a perspective on flow assurance*. Energy & Fuels. 2012; 26(7):4145-4157.
- (9) Bratland O. *PipeFlow*. 2nd ed. Online-E book: drbratland.com; 2013.
- (10) Soepyan FB, Cremaschi S, Sarica C, Subramani HJ, Kouba GE. *Solids transport models comparison and fine-tuning for horizontal, low concentration flow in single-phase carrier fluid*. AIChE Journal. 2014; 60(1):76-122.
- (11) Doron P, Granica D, Barnea D. *Slurry flow in horizontal pipes—experimental and modeling*. International Journal of Multiphase Flow. 1987; 13(4):535-547.
- (12) Doron P, Simkhis M, Barnea D. *Flow of solid-liquid mixtures in inclined pipes*. International Journal of Multiphase Flow. 1997; 23(2):313-323.
- (13) Dabirian R, Mohan R, Shoham O, Kouba G. *Critical sand deposition velocity for gas-liquid stratified flow in horizontal pipes*. Journal of Natural Gas Science and Engineering. 2016; 33:527-537.
- (14) Prosperetti, A, Tryggvason, G. *Computational methods for multiphase flow*. 2nd ed. Cambridge UK: Cambridge University Press; 2009.

- (15) Le Roux JP. *Entrainment threshold of sand- to granule-sized sediments under waves*. *Sedimentary Geology*. 2015; 322:63-66.
- (16) Khosronejad A, Kozarek JL, Diplas P, Hill C, Jha R, Chatanantavet P, et al. *Simulation-based optimization of in-stream structures design: rock vanes*. *Environmental Fluid Mechanics*. 2018; 18(3):695-738.
- (17) Kou X, Wereley ST, Heng PWS, Chan LW, Carvajal MT. *Powder dispersion mechanisms within a dry powder inhaler using microscale particle image velocimetry*. *International Journal of Pharmaceutics*. 2016; 514(2):445-455.
- (18) Richardson JF, Zaki WN. *Sedimentation and fluidisation: Part I*. *Chemical Engineering Research and Design*. 1997; 75:82-100.
- (19) Lockhart RW, Martinelli RC. *Proposed correlation of data for isothermal two-phase, two-component flow in pipes*. *Chemical Engineering Progress*. 1949; 45(1):39-48.
- (20) Flanigan O. *Effect of uphill flow on pressure drop in design of two-phase gathering systems*. *Oil & Gas Journal*. March (1958); 56(10):132.
- (21) Beggs H, Brill J. *Study of 2-phase flow in inclined pipes*. *Journal of Petroleum Technology*. 1973; 25(MAY):607-617.
- (22) Wasp EJ, Aude TC, Seiter RH. *Paper 13 - Hetero-homogeneous solids/liquid flow in the turbulent regime*. Reproduced In: ZANDI I, editor. *Advances in Solid-Liquid Flow in Pipes and its Application*. : Pergamon; 1971. p. 199-210.
- (23) Wicks M. *Paper 7 - Transport of solids at low concentration in horizontal pipes*. Reproduced In: ZANDI I, editor. *Advances in Solid-Liquid Flow in Pipes and its Application*. : Pergamon; 1971. p. 101-124.
- (24) Taitel Y, Dukler AE. *A model for prediction of flow regime transitions in horizontal and near horizontal gas-liquid flow*. *AIChE Journal*. 1976; 22:47-55.
- (25) Dukler AE, Wicks M, Cleveland RG. *Frictional pressure drop in two-phase flow: B. An approach through similarity analysis*. *AIChE Journal*. 1964; 10(1):44-51.
- (26) Eaton BA, Knowles CR, Silberberg IH. *The prediction of flow patterns, liquid holdup and pressure losses occurring during continuous two-phase flow in horizontal pipelines*. *Journal of Petroleum Technology*. 1967; 19(06):815-828.
- (27) Guzhov AL, Mamayev VA and Odishariya GE. *A study of transportation in gas liquid systems*. In: IG V H, editor. 10th Int. Gas Union Conf.; 6-10 June 1967; Hamburg: IG V; 1967. p. C19-C67.
- (28) Brill JP, Arirachakaran SJ. *State-Of-The-Art in Multiphase Flow*. *Journal of Petroleum Technology*. 1992; 44(5):538-541.
- (29) Taitel Y. *Advances in two-phase flow mechanistic modeling*. Tulsa, Oklahoma: Society of Petroleum Engineers; 1994J2: SPE-27959-MS.

- (30) Taitel Y, Dukler AE. *Model for slug frequency during gas-liquid flow in horizontal and near horizontal pipes*. International Journal of Multiphase Flow. 1977; 3(6):585-596.
- (31) Yang ZL, Ladam Y, Laux H, Danielson T, Goldszal A, Martins AL. Simulation of sand transport in a stratified gas-liquid two-phase pipeflow. Edinburgh, UK: BHR Group; 2007J2: BHR-2007-F1.
- (32) Bendiksen KH, Maines D, Moe R, Nuland S. *The dynamic two-fluid model OLGA: theory and application*. SPE Production Engineering. 1991; 6(02):171-180.
- (33) Zhang H, Wang Q, Sarica C, Brill J. *A unified mechanistic model for slug liquid holdup and transition between slug and dispersed bubble flows*. International Journal of Multiphase Flow. 2003; 29(1):97-107.
- (34) Danielson TJ, Bansal KM, Hansen R, Leporcher E. *LEDA: The Next Multiphase Flow Performance Simulator*. Barcelona, Spain: BHR Group; 2005J2: BHR-2005-H4.
- (35) Barnea D. *Transition from annular flow and from dispersed bubble flow—unified models for the whole range of pipe inclinations*. International Journal of Multiphase Flow. 1986; 12(5):733-744.
- (36) Barnea D. *A unified model for predicting flow-pattern transitions for the whole range of pipe inclinations*. International Journal of Multiphase Flow. 1987; 13(1):1-12.
- (37) Thomas AD. *Predicting the deposit velocity for horizontal turbulent pipe flow of slurries*. International Journal of Multiphase Flow. 1979; 5(2):113-129.
- (38) Harrington GL, Davis AJ, McIntosh CJ. *Balmoral FPV: three years on*. Houston, Texas: Offshore Technology Conference; 1990J2: OTC-6248-MS.
- (39) Hill A, Arevalo B, Almutahar F, McLaury B. *Critical liquid velocities for low concentration sand transport*. ASME-JSME-KSME 2011 Joint Fluids Engineering Conference, AJK 2011. 2011; 1.
- (40) Hewitt GF. *Views of the Future. A Report on Discussions at the Third International Workshop on Multiphase Flow*. Third International Workshop on Multiphase Flow; June 1992; London: Multiphase Sci. Technology.; 1992. p. 59-77.
- (41) Ibarra R, Mohan RS, Shoham O. *Critical sand deposition velocity in horizontal stratified flow*. Society of Petroleum Engineers; 2014J2: SPE-168209-MS.
- (42) Barnea D. *A unified model for predicting flow-pattern transitions for the whole range of pipe inclinations*. International Journal of Multiphase Flow. 1987; 13(1):1-12.
- (43) Xiao JJ, Shonham O, Brill JP. *A comprehensive mechanistic model for two-phase flow in pipelines*. New Orleans, Louisiana: Society of Petroleum Engineers; 1990J2: SPE-20631-MS.

- (44) Volcado JJ and Charles ME. *Prediction of pressure gradient for the horizontal turbulent flow of slurries*. 2nd international conference on the hydraulic transport of solids in pipes; September 1972; Coventry, UK: BHRA; 1972. p. 1-12-Paper C1.
- (45) Goedde E. *The critical velocity of heterogeneous hydraulic transport*. 5th Int. Conf. on Hydraulic Transport of Solids in Pipes; Paper B4. Hanover; 1978. p. 81-98.
- (46) Parzonka W, Kenchington JM, Charles ME. *Hydrotransport of solids in horizontal pipes: effects of solids concentration and particle size on the deposit velocity*. *Canadian Journal of Chemical Engineering*. 1981; 59(3):291-296.
- (47) Ramadan A, Skalle P, Johansen ST. *A mechanistic model to determine the critical flow velocity required to initiate the movement of spherical bed particles in inclined channels*. *Chemical Engineering Science*. 2003; 58(10):2153-2163.
- (48) Stevenson P, Thorpe RB, Davidson JF. *Incipient motion of a small particle in the viscous boundary layer at a pipe wall*. *Chemical Engineering Science*. 2002; 57(21):4505-4520.
- (49) Doron P, Barnea D. *Flow pattern maps for solid-liquid flow in pipes*. *International Journal of Multiphase Flow*. 1996; 22(2):273-283.
- (50) Oroskar AR, Turian RM. *Critical velocity in pipeline flow of slurries*. *AIChE Journal*. 1980; 26(4):550-558.
- (51) Gruesbeck C, Salathiel WM, Echols EE. *Design of gravel packs in deviated wellbores*. *Journal of Petroleum Technology*. 1979; 31(1):109-115.
- (52) Rabinovich E, Kalman H. *Incipient motion of individual particles in horizontal particle-fluid systems: A. Experimental analysis*. *Powder Technology*. 2009; 192(3):318-325.
- (53) Grass Anthony J., Ayoub Ragaei N.M. *Bed load transport of fine sand by laminar and turbulent flow*. 24; doi:10.1061/9780872623736.096.
- (54) Zandi I, Govatos G. *Heterogeneous flow of solids in pipelines*. *Journal of the Hydraulics Division*. 1967; Issue 3:145-159.
- (55) Turian RM, Yuan T. *Flow of slurries in pipelines*. *AIChE Journal*. 1977; 23(3):232-243.
- (56) Durand R. *The hydraulic transportation of coal and other materials in pipes*. *Proceedings of colloquium on the hydraulic transport of coal*, National coal board London; 1959. p. 39-51.
- (57) Bonnington AG, Bain ST. *The hydraulic transport of solids by pipeline*. Oxford: Pergamon Press Ltd.; 1970.
- (58) Shook CA. *Liquid-solid flow research*. *Chemical Engineering Research and Design*. 1987; 65(6):498-500.

- (59) Babcock HA. *Heterogeneous flow of heterogeneous solids*. In: Zandi I, editor. *Advances in solid-liquid flow in pipes and its application*. Oxford: Pergamon press inc.; 1971:125-148.
- (60) Thomas DG. *Transport characteristics of suspensions: II. minimum transport velocity for flocculated suspensions in horizontal pipes*. *AIChE J.* 1961; 7(3):423-430.
- (61) Dahl AM, Ladam Y, Unander TE and Onsrud G. [SINTEF report no. 32.1932.00/02/04]. SINTEF-IFE Sand transport 2001-2003-Phase II & III Experiments. Norway: SINTEF; 2004.
- (62) Dahl AM, Ladam Y and Onsrud G. [SINTEF report no. 32.1032.00/01/03]. SINTEF-IFE Sand transport 2001-2003-Phase I Experiments. Norway: SINTEF; 2003.
- (63) Salama MM. *Sand production management*. *Journal of Energy Resources Technology*. 1999; 122(1):29-33.
- (64) Televantos Y, Shook C, Carleton A, Streat M. *Flow of slurries of coarse particles at high solids concentrations*. *Canadian Journal of Chemical Engineering*. 1979; 57(3):255-262.
- (65) Rabinovich E, Kalman H. *Pickup velocity from particle deposits*. *Powder Technology*. 2009; 194(1-2):51-57.
- (66) Wu F, Chou Y. *Rolling and lifting probabilities for sediment entrainment*. *Journal of Hydraulic Engineering*. 2003; 129(2):110-119.
- (67) Ramadan A, Skalle P, Johansen ST. *A mechanistic model to determine the critical flow velocity required to initiate the movement of spherical bed particles in inclined channels*. *Chemical Engineering Science*. 2003; 58(10):2153-2163.
- (68) J.J Vocaldo MEC. *Prediction of pressure gradient for the horizontal turbulent flow of slurries*. *Prediction of pressure gradient for the horizontal turbulent flow of slurries*. Proceedings of the 2nd International Conference on the Hydraulic Transport of Solids in Pipes; 1972; Paper C1, Coventry, UK. Coventry, UK: paper C1; 1972. p. 1-12.
- (69) Parzonka W, Kenchington J, Charles ME. *Hydrotransport of solids in horizontal pipes: effects of solids concentration and particle size on the deposit velocity*. *Can.J.Chem.Eng.* 1981; 59:291-296.
- (70) Ayazi Shamlou P, Koutsakos E. *Solids suspension and distribution in liquids under turbulent agitation*. *Chemical Engineering Science*. 1989; 44(3):529-542.
- (71) Doron P, Barnea D. *Pressure drop and limit deposit velocity for solid-liquid flow in pipes*. *Chemical Engineering Science*. 1995; 50(10):1595-1604.
- (72) Ladam Y and Dahl AM. [SINTEF report no. 27.5596.00/01/05]. Sand transport experiments in liquid flow in inclined test section and water wetted sand transport in horizontal oil flow in a medium scale flow loop. Norway: SINTEF; 2005.

- (73) Ishii M, Hibiki T. *Thermo-fluid dynamics of two-phase flow*. 2nd ed. New York, NY: Springer; 2011.
- (74) Nicklin DJ. *Two-phase bubble flow*. Chemical Engineering Science. 1962; 17(9):693-702.
- (75) Pan L, Hanratty TJ. *Correlation of entrainment for annular flow in horizontal pipes*. International Journal of Multiphase Flow. 2002; 28(3):385-408.
- (76) Gillies RG, Hill KB, McKibben MJ, Shook CA. *Solids transport by laminar Newtonian flows*. Powder Technology. 1999; 104(3):269-277.
- (77) Lee A, Sun J, Jepson WP. Study of flow regime transitions of oil water-gas mixtures in horizontal pipelines. Singapore: International Society of Offshore and Polar Engineers; 1993J2: ISOPE-I-93-121.
- (78) Hsu F, Turian RM, Ma T. *Flow of noncolloidal slurries in pipelines*. AIChE Journal. 1989; 35(3):429-442.
- (79) Andritsos N, Hanratty TJ. *Interfacial instabilities for horizontal gas-liquid flows in pipelines*. International Journal of Multiphase Flow. 1987; 13(5):583-603.
- (80) Kowalski JE. *Wall and interfacial shear stress in stratified flow in a horizontal pipe*. AIChE Journal. 1987; 33(2):274-281.
- (81) Khor SH, Mendes-Tatsis M, Hewitt GF. *One-dimensional modelling of phase holdups in three-phase stratified flow*. International Journal of Multiphase Flow. 1997; 23(5):885-897.
- (82) Al-lababidi S, Yan W, Yeung H. *Sand transportations and deposition characteristics in multiphase flows in pipelines*. Journal of Energy Resources Technology. 2012; 134(3):034501-034501-13.
- (83) Taylor G. *The dispersion of matter in turbulent flow through a pipe*. Proceedings of the Royal Society of London. Series A, Mathematical and Physical Sciences. 1954; 223(1155):446-468.
- (84) Bagnold RA. *Transport of solids by natural water flow: Evidence for a worldwide correlation*. Proceedings of the Royal Society of London, Series A: Mathematical and Physical Sciences. 1986; 405(1829):369-374.
- (85) Barnea D, Taitel Y. *Stratified three phase flow in pipes - Stability and transition*. Chemical Engineering Communications. 1996; 141:443-460.
- (86) Angelson S, Kvernfold O, Linglem M and Oslen S. *Long distance transport of unprocessed hydrocarbon: sand settling in multiphase flowlines*. In: BHRA, editor. Proc. 4th Int. Conf. on Multiphase Flow Nice, 1989. France.: BHRA; 1989. p. Paper D2.

- (87) Barnea D. *On the effect of viscosity on stability of stratified gas—liquid flow—application to flow pattern transition at various pipe inclinations*. Chemical Engineering Science. 1991; 46(8):2123-2131.
- (88) Petalas N, Aziz K. *A mechanistic model for multiphase flow in pipes*. Journal of Canadian Petroleum Technology. 2000; 39(6):43-55.
- (89) Gregory GA, Nicholson MK, Aziz K. *Correlation of liquid volume fraction in slug for horizontal gas-liquid slug flow*. International Journal of Multiphase Flow. 1978; 4(1):33-39.
- (90) Açikgöz M, França F, Lahey Jr RT. *An experimental study of three-phase flow regimes*. International Journal of Multiphase Flow. 1992; 18(3):327-336.
- (91) Shook CA, Roco MC. *Slurry Flow: Principles and Practice*. Boston: Digital Press; 1991.
- (92) Wood DJ. *Pressure gradient requirements for re-establishment of slurry flow*. Hydrotransport. 1979; 1:217-228.
- (93) Wilson KC. *Solid-liquid pipeline flow - from menagerie to mechanistic modelling*; 4th International Symposium on Dredging Technology; Singapore: BHRA Fluid Engineering; 1983. p. 19-12.
- (94) Dabirian R, Mohan RS, Shoham O. *Mechanistic modeling of critical sand deposition velocity in gas-liquid stratified flow*. Journal of Petroleum Science and Engineering. 2017; 156:721-731.
- (95) Leporini M, Marchetti B, Corvaro F, di Giovine G, Polonara F, Terenzi A. *Sand transport in multiphase flow mixtures in a horizontal pipeline: An experimental investigation*. Petroleum. 2019; 5(2):161-170.
- (96) Takaoka T, Hisamitsu N, Ise T and Takeishi Y. *Blockage of slurry pipeline*. In Proc. 7th Conf. on the Hydraulic Transport of Solids in Pipes; 1980; Sendai, Japan; 1980. p. 71-88.